

# **Integration of renewable energy with urban design**

Based on the examples of the solar photovoltaics and micro wind turbines

By

Heshuang Zeng

Master of Engineering in Urban Planning and Design  
Tsinghua University (2009)  
Bachelor of Architecture  
Tsinghua University (2007)

Submitted to the Department of Urban Studies and Planning  
in partial fulfillment of the requirements for the degree of

Master in City Planning

at the

MASSACHUSETTS INSTITUTE OF TECHNOLOGY

September 2011

© 2011 Heshuang Zeng. All Rights Reserved

The author here by grants to MIT the permission to reproduce and  
to distribute publicly paper and electronic copies of the thesis  
document in whole or in part.

Author \_\_\_\_\_  
Department of Urban Studies and Planning  
(Aug 8<sup>th</sup>, 2011)

Certified by \_\_\_\_\_  
Dennis Frenchman, Leventhal Professor of Urban Design and Planning  
Department of Urban Studies and Planning  
Thesis Supervisor

Accepted by \_\_\_\_\_  
Professor Joseph Ferreira  
Chair, MCP Committee  
Department of Urban Studies and Planning



# **Integration of renewable energy with urban design**

Based on the examples of the solar photovoltaics and micro wind turbines

By  
Heshuang Zeng

Submitted to the Department of Urban Studies and Planning  
On Aug 11<sup>st</sup>, 2011 in partial fulfillment of the requirements for the degree of  
Master in City Planning

## **Abstract**

To deal with the challenge of climate change and energy security, renewable energy has been widely regarded as an increasingly important solution leading to a more sustainable future. Given the fact that more than half of all energy is consumed in cities today, designers and academics have sought to integrate renewable energy technologies at small scale into the urban environment.

This thesis explores effective ways of combining renewable energy with urban development through analyzing the relationship between urban form and renewable energy production. It focuses on two renewable technologies: solar photovoltaics (PV) and micro-wind turbines, both to produce electricity, at the urban scale. The study starts with a detailed review of the characteristics of both technologies. It then analyzes the energy potential simulation methodologies and examines relevant urban-form indicators qualitatively and quantitatively. A comparison of renewable energy potential in four different neighborhoods in Jinan, China then follows to distill the key urban-form factors. With the simulation results in Jinan, the thesis then studies the implications of the key urban form factors and provides design principles that could improve renewable energy potential in future urban development.

The research shows that urban form has quite significant impact on potential neighborhood renewable energy output under a given climate condition. PV would make a much larger contribution to total renewable potential than wind energy in cities with climates similar to Jinan's. Low-rise neighborhoods with high roof coverage provide the best conditions for solar PV integration; whereas the windward open area best accommodates the wind power generation. For future developments, urban renewable energy potential could be increased through existing or innovative urban forms, such as the low-rise courtyard prototype for solar integration and a combination of low-rise blocks and high rise towers that accommodates both sun and wind.



## Acknowledgement

First of all, I express my thanks to the “Making the Clean Energy City in China” research project, sponsored by China Energy foundation, for providing me such a great opportunity in working on this exciting topic. The integrated research framework of the project offers me a better understanding on the role of renewable energy integration in sustainable development. The previous work to create an Energy Pro-forma© done by my team members helped me tremendously in launching my study of the renewable-energy-and-form relationship. The team members that I want to thank in this project are Jiyang Zhang, Yang Jiang, Nah Yoon Shin, Jue Wang, Shani Sharif and Genevieve Rose Sherman.

I also have to thank the partners of our project: Tsinghua University for research collaboration, Shangdong University for providing the survey data and Beijing Normal University for building the GIS database used to analyze the neighborhood urban form in my research

I must also thank my thesis advisor, Prof. Dennis Frenchman. He has been an extremely kind and helpful supervisor and mentor to me at MIT over the past two years, a professor who is always there for his students. I have learned a lot from him in the field of urban design and development, and also how to be a good and passionate person. I really appreciate the incredible opportunity he offered me to conduct research with clean energy city project. During the thesis writing, he gave me helpful suggestions, especially new insights on the innovativeness of urban form.

I also send my great gratitude to my reader Prof. Jessika Trancik. Her class on energy systems inspired me to choose this topic for my mater thesis. Her patient guidance has deepened my understanding of renewable energy technologies, and her innovative perspective on the nexus between energy and cities encouraged me to continue in this field in my future career. I greatly thank her for her long-standing support and responsive supervision.

Another thank you is owed to Prof. Chris Zegras, the second reader of my thesis. As co-professor of the “Making the Clean Energy City in China” project, Chris helped me link my studies with on-the-ground cases in Jinan as well as our team’s existing energy pro forma. His suggestions on my draft thesis helped me during the revision process.

Thanks Kevin Feeney and Tyler Corson-Rikert for proofreading my thesis.

A last thank you goes to my dear family and friends. Sometimes, people are too close to say thank you to each other. But I want to use the tiny space here to say a soft thanks to the people I deeply love. I cannot be who I am without support from all of you.



# **Content**

<b>ABSTRACT</b>	<b>3</b>
<b>ACKNOWLEDGEMENT</b>	<b>5</b>
<b>CONTENT</b>	<b>7</b>
<b>CHAPTER 1: INTRODUCTION</b>	<b>9</b>
1.1 Research Background	9
1.2 Research Scope	10
1.3 The Hypothesis of this research	12
1.4 The key findings	14
1.5 The thesis structure	15
<b>CHAPTER 2: UNDERSTANDING RENEWABLE ENERGY TECHNOLOGIES: KEY FEATURES</b>	<b>17</b>
2.1 Solar Photovoltaic	17
2.2 Urban micro wind turbines	23
2.3 Cost and carbon intensity	27
2.4 The Future of Solar PV and micro urban wind turbines	31
2.5 Conclusion	33
<b>CHAPTER 3: RENEWABLE ENERGY POTENTIAL: SIMULATION METHODOLOGIES AND FORM-RELATED DETERMINANTS</b>	<b>35</b>
3.1 Solar PV	35
3.2 Urban Wind Turbines	47
3.3 Discussions and Conclusion	58
<b>CHAPTER 4: THE RENEWABLE ENERGY POTENTIAL OF THE FOUR NEIGHBORHOODS IN JINAN</b>	<b>60</b>
4.1 The four neighborhoods in Jinan	60

4.2 Simulating the renewable energy potential of the four Jinan neighborhoods	66
4.3 The renewable energy potential and the form determinants	72
<b>CHAPTER 5: THE URBAN DESIGN IMPLICATIONS FOR RENEWABLE ENERGY INTEGRATION</b>	<b>78</b>
5.1 Surface area and its physical form implication	78
5.2 Roof Design	84
5.3 Shading concerns	87
5.4 Wind energy in the city – integrating with open space	90
5.5 Combining solar and wind energy in urban development	92
5.6 Summary	93
<b>CHAPTER 6: CONCLUSION</b>	<b>95</b>
6.1 The role of the renewable energy integration	95
6.2 The relationship between urban form and renewable energy potential	96
6.3 The contribution to the “Making the Clean Energy City” in China project	99
6.4 Directions for future work	102
<b>BIBLIOGRAPHY</b>	<b>105</b>
<b>APPENDIX I: THE SITE PLANS AND SOLAR ENERGY POTENTIAL SIMULATED RESULTS OF 100 BUILDING CLUSTER MODELS</b>	<b>110</b>
<b>APPENDIX II: RENEWABLE ENERGY POTENTIAL SIMULATION METHODOLOGY</b>	<b>114</b>
<b>APPENDIX III: THE DETAILED SIMULATED RESULTS OF SOLAR ENERGY POTENTIAL IN FOUR GEOMETRIC PROTOTYPES OF THE NEIGHBORHOODS IN CHAPTER 5</b>	<b>127</b>
<b>APPENDIX IV: THE METRIC OF RENEWABLE POTENTIAL SIMULATION IN THE ENERGY PRO-FORMA</b>	<b>128</b>



## **Chapter 1: Introduction**

The climate change challenge and increasing urban energy demand makes the integration of the renewable energy at the neighborhood level more and more important. This thesis explores the renewable-energy-and-form relationship to help guide future urban development. This chapter introduces the research background, scope, hypothesis, methodology and framework of the thesis.

### **1.1 Research Background**

Renewable energy integration at the urban scale could be a meaningful solution to the climate challenge facing cities. A variety of evidence shows that global climate change is caused by the increased burning of fossil fuels (IPCC, 2007). To reduce future greenhouse gas emissions (GHG) from fossil fuels and mitigate climate change risk, adopting clean and renewable energy quickly, effectively and extensively has become an important solution to the climate change issue. (Hoffert, Caldeira et al. 1998).

Facing increasing GHG emissions in cities, urban planning and design will also have to consider renewable energy technologies with the design of the urban fabric sooner or later. Residential GHG consumption constitutes 21.5% of total carbon equivalent emissions in the United States in 2009 (U.S. EPA, 2011). And its contribution will experience a significant increase in the future (EIA, 2010). The growth in the share of residential emissions will be even more radical in developing countries due to continuing urbanization and improvements in people's living standards. For example, GHG emissions in the "building and appliances sector" is projected to have the fastest growth rate in the next twenty years in China (Jiahua, Pan, et al 2007; McKinsey Company 2009).

Renewable energy integration at a small scale could provide a valuable clean energy supply in cities and help address increasing residential energy use and emissions. These additional urban renewable energy systems serve as small,

distributed sources, diversifying the energy supply. Compared with large-scale renewable power plants located far away from cities, renewable systems in cities can be integrated with built structures without using additional land, and directly connect with the grid. Since urban renewable energy is produced where it is used, it also eliminates the transmission loss. For this reason, the power generated onsite is more valuable due to transmission loss-saving. As demonstrated in studies in the UK, one unit of onsite renewable electricity is around three times the value of energy produced from remote sources (Allen, Hammond et al. 2008).

What is more, renewable energy integration could have social consequences, encouraging residents and businesses to conserve energy, since its production and performance can be gauged and understood on a neighborhood scale. Many studies have shown that making cause and effect visible to communities can influence their behavior towards more sustainable, less consumptive patterns (Lazarus 2009). Therefore, renewable energy integration is an important and quite feasible strategy in urban sustainable development in response to increasingly serious climate change effects and growing urban energy demand.

## **1.2 Research Scope**

Current research relevant to the renewable energy technologies and urban development are mostly focus at the building and transport scale - mainly because such studies have been done by engineers, but not holistically at the scale of the neighborhood. This is a conceptual gap at urban level, the scale on which cities are built, and interconnected. The thesis is a step towards filling this gap. It aims to explore the impact of urban form on the renewable energy generation potential at building cluster scale.

By urban form, I mean the typologies of buildings and their spatial arrangement at development scale. It not only refers to the shape and the function of individual buildings, but also covers the related street layout, mobility systems, and structure of open space in that neighborhood.

The scale that this thesis is focused on is the “urban development level” or “building cluster scale”. A building cluster is a basic spatial component in cities, which captures a fundamental set of relationships between buildings, spaces, movement systems, and activities that underlie patterns of energy use in the urban environment (Frenchman, Zegras et al. 2010). It usually covers an area with identifiable building and urban spatial patterns, whose boundaries are within walking distance from each other.

Renewable energy, by definition, covers “those energy flows that occur naturally and repeatedly in the environment – from the wind, the movement of the ocean, from the sun, the earth, and also from biomass”, and renewable energy technologies (RETs) refer to “technologies such as onshore wind generation, hydro, photovoltaics, passive solar, biomass and energy crops, energy from waste, and landfill and sewage gas”(Office of the Deputy Prime Minister 2004) Renewable energy sources account for nearly 20% of the global energy supply (REN21, 2010). Among them, the sun and wind are probably the most available renewable energy sources that can be captured and used at small scale. This thesis will only focus on these two renewable energies. Other renewable energy sources like geothermal and biogas could be implemented at the urban level as well, but they are excluded from the scope of this study.

Among the energy systems related to the sun and the wind, this thesis will concentrate on the two most mentioned and fastest-growing technologies: solar photovoltaic and micro wind turbines, both for electricity generation in unit of KWh. Other relevant technologies, such as solar thermal, are not included in this discussion. However, they would share similarities in terms of design principles.

This study is built on and will contribute to an MIT research project -”Making the Clean Energy City” in China, sponsored by the Energy Foundation. This research project aims to explore the relationship between urban form and energy

use. The project has used Jinan City in China as a test venue to generate data on form-energy relationships, as well as a location for designing new clean energy neighborhoods using the knowledge gained. In the simulations, I will use the four neighborhoods in Jinan, drawing from this project as well.

The Clean Energy City research team is developing a neighborhood-scale energy evaluation tool “the Energy Pro-forma ©” through empirical studies in Jinan. Currently, the pro-forma consists of three modules: transportation, embodied and operational energy use. This thesis will add an important new component to the pro-forma: a measure of the renewable energy production potential of a neighborhood form (design). The Pro-forma will therefore be translated from a tool that evaluates energy consumption of a neighborhood form, to one that also accounts for the potential of a neighborhood form to produce renewable energy -- a more integrated and comprehensive way to assess and design clean energy cities.

This research focuses on making use of solar PV and micro turbines in the urban context of Jinan city, China. The study itself is location-specific, due to the consistency with the research project as well as to control for climate conditions that might have great effect on renewable energy output. However, the form implications drawn from this study could be adopted to other places around the world.

### **1.3 The Hypothesis of this research**

Currently, renewable technology is considered to be an “add-on” to existing urban forms. However, a greater understanding of the relationship between neighborhood form and renewable energy potential could provide a new paradigm for neighborhood design with broad consequences for more comprehensive sustainable development, and a more sustainable style of urban life.

The key questions I try to answer are: What is the relationship between renewable energy production/production potential and urban design and development form? How could urban design better accommodate renewable energy integration to improve energy output potential?

In general, the way we design our places of living directly influences building energy consumption. For example, passive solar rooms in houses can make use of the daily temperature difference to store solar heat for later use, and thus save energy. At the neighborhood level, design could adjust the arrangement of buildings to create a wind corridor and improve natural ventilation, in order to save cooling energy use.

There is a similar relationship between urban form and renewable energy production potential. Renewable energy systems are a new “layer” upon the urban form. Firstly, renewable energy output is determined by installed capacity, which is subject to the area that buildings can provide for its integration; secondly, in order to maximize energy production, the urban form, such as the building height and spacing, needs to accommodate renewable resources, sun and wind, in the right way. This study analyzes these unique characteristics of the renewable layer to meaningfully inform the neighborhood scale.

The first hypothesis underlying the thesis is: Different renewable energy technologies favor different urban forms in optimizing their energy potential at the urban scale

To test this hypothesis, I carefully study the key features of solar PV and urban micro wind turbines respectively, and also the relevant urban form factors in their energy production. I start from common energy production formulas, distill the underlying urban-form-related factors from the variables in the formulas, and evaluate their impacts for each technology, in both qualitative and quantitative ways. A form-incorporated renewable energy potential simulation methodology is

also developed through this analysis.

By “energy potential”, I use the annual energy production potential per built space as the criterion. Since the built area is a pure spatial indicator related to the size of the development, examining the energy potential by per built area incorporates the urban physical form characteristic. The “energy potential” in later discussions refers to this criterion; the unit is KWh/square meter/year.

A second hypothesis underlying the thesis is that: Different neighborhood forms have different total renewable energy potential at the same location. In Jinan, low-rise neighborhoods with high roof coverage would have higher energy potential than high-rise towers. On a broader scale, the urban design of a city affects its potential to incorporate renewable sources in a way that is predictable and quantifiable.

To test this hypothesis, I select four different neighborhoods in Jinan and apply renewable energy potential simulation to evaluate their renewable energy potential respectively. By comparing energy potential with the corresponding urban form across four empirical cases, the thesis tests the correlation between renewable energy potential and the urban form.

This thesis also attempts to derive design principles for better renewable integration at neighborhood scale. Since urban form is a combined result of various design criteria, with renewable energy integration being only one of them, my goal is to explore the design principles that could achieve an increase in renewable energy potential in a more holistic way, bringing net positive environmental and social impacts to cities.

## **1.4 The key findings**

Centered on the two hypotheses, this thesis carries out a series of quantitative and qualitative analysis on the relationship between urban form and renewable

energy. The key findings are summarized as follows:

- ◆ The relationship between urban form and the renewable energy potential is quite significant. Under climate conditions similar to Jinan, solar energy offers the primary component for renewable potential across all urban forms.
- ◆ In terms of solar energy, urban development with lower height and higher roof coverage carries the highest potential. The solar-friendly form is usually flat and close to the earth to allow harvesting solar energy via large building tops or roof-like structures. The low-rise perimeter block, or courtyard, carrying all the above-mentioned features, could be a recommended renewable and sustainable form prototype for PV integration in the future.
- ◆ In terms of wind energy, placing the turbine high and at the edge of windy open space is the key principle. Such places might include, for example, along the waterfront, within a “wind corridor”, and the windward urban edge of a project facing the prevailing wind.
- ◆ The hybrid “high-low rise” building combining the sun and wind advantages block demonstrates promise as an innovative development prototype. This form could accommodate solar integration via its low-rise courtyard podium, with the possibility of incorporating wind turbines through its high-rise towers inserted at the intervals of the fabric. Being applicable in various climate conditions, this prototype could help increase renewable energy potential and diversify the energy supply of the development.

## **1.5 The thesis structure**

The thesis is organized as follows:

Chapter 2 will explore the technologies in terms of technical features, types, constraints, cost and environmental impact, for the decision-making of designers and development.

To understand the correlation between form-related factors and the energy potential, Chapter 3 studies the renewable energy potential estimation formulas of solar PV and the wind turbines, and identifies the correlations between form-related indicators and different variables in the formula.

In order to further distill the most important form-related factors, Chapter 4 applies the renewable energy estimation methods to four different neighborhoods in Jinan. It then examines the relationship between renewable energy potential and different form factors. I find that solar energy is the primary contributor to renewable energy potential in the Jinan neighborhoods and the key factor affecting its potential is surface area, while roof tilt and floor area ratio have substantial impact as well.

Chapter 5 “translates” the impact of form-related factors into design principles that designers could use in real developments. The analysis in this section focuses on solar energy. Through simulations and the quantitative analysis, I find that, at the same building density, the most renewable-friendly neighborhood prototype is the low-rise courtyard form. Additional design implications and strategies regarding roof design, wind turbine planning and solar-wind integrated urban prototypes are discussed as well.

Chapter 6 concludes by discussing the interaction between urban form and renewable energy potential. It highlights again the design principles for renewable integration and also the meaning of this study in improving the energy pro-forma. It also points out the directions for future work.



## **Chapter 2: Understanding Renewable Energy Technologies:**

### **Key Features**

When urban designers consider the incorporation of renewable energy technologies, they will weigh over many aspects, such as the appearance of the facilities in buildings, the options/types of technologies and their pros and cons, and their sustainable contribution, environmental impact and cost. The final decision aims to balance all these considerations. This chapter is a review of these dimensions of renewable energy technologies. It aims to explore their technical, environmental and economic characteristics. It describes the technical, environmental and economic characteristics of solar photovoltaics and micro urban wind turbines and compares their cost and carbon intensity.

PV panels are material-based solar-responsive systems; and urban micro wind turbines can be regarded as a variety of complex architectures designed in response to aerodynamic conditions in cities. The characteristics of these technologies are often more important than the design principles in renewable integration. Only with sufficient understanding of the renewable energy technologies can decision-makers select the most appropriate approach in urban development.

### **2.1 Solar Photovoltaic**

Solar Photovoltaics converts sunlight to direct current electricity. It is the most popular renewable energy system at the building and neighborhood scale.

#### **2.1.1 Solar energy resource**

Solar energy is the most common and abundant energy resource in the world. Globally, the earth receives 174 petawatt (PW) of solar radiation at the upper

atmosphere, and about 1700 TW of solar power are theoretically available over land for PV use, before removing exclusion zones where solar insolation is low (Jacobson 2009). The earth's energy consumption is around 15 terawatt (REN21, 2010), so if human beings used 0.01% of the solar energy in nature, we would sustain our society without burning fossil fuels (Randolph and Masters 2008).

Theoretically, solar PV can be installed anywhere in the world can be installed with access to sunlight. PV can be regarded as the most flexible energy system.

### 2.1.2 Operating Principle

PV cells generate direct current electricity by utilizing particular characteristics of semi-conducting materials. Figure 2.1 illustrates the process of electricity generation in a PV system. The PV produces electricity like this: when the PV cell is exposed to the sunlight, the photons from the sunlight first come in contact with the absorbed semi-conducting material, which excites the electrons, and then current is generated through an external load.

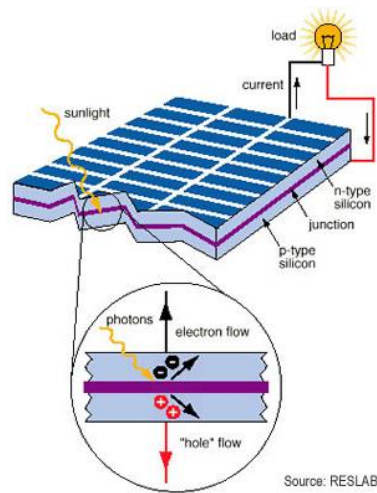



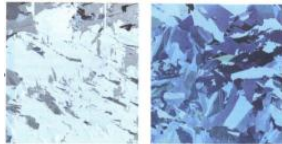



Figure 2.1 The electricity generation process from PV  
Source: [http://www.rids-nepal.org/index.php/Solar\\_Photo\\_Voltaic.html](http://www.rids-nepal.org/index.php/Solar_Photo_Voltaic.html)

The effectiveness of PV electricity generation is dependent on the physical property of the semi-conductive material itself - the propensity and density of the material matters.

### **2.1.3 Types of Photovoltaic**

By material, there are two types of photovoltaic: crystalline PV and thin film PV. The PV products in each category vary from one another based on manufacturing process, efficiency and appearance. Table 2.1 summarizes key features of various PV products.

Table 2.1 The features of various PV products

PV TYPE	Solar Cell Material	Cell efficiency	Module Efficiency (series production)	Form	Size	Thicknesss	Colour	APPEARANCE	
Crystalline PV	Monocrystalline Silicon	21.50%	16.90%	round or square (depending on how much the mono-crystal is sliced away)	10cm*10cm;12.5cm*12.5cm;or 15cm*15cm; $\Phi$ :12.5 or 15cm	0.2-0.3mm	dark blue to black(with Anti-reflective coat); grey (without AR)	uniform	
	Polycrystalline Silicon	16.50%	14.20%	square	10cm*10cm;12.5cm*12.5cm;or 15cm*15cm;15.6*15.6cm; and 21cm*21cm	0.24-0.3mm	Blue (with AR); Silver Grey (without AR)	forest pattern	
Thin Film PV	Amorphous silicon	10.50%	7.50%	retangular	0.79m*2.44m; special module; maxium 2*3m	1-3mm substrate material with approximately 1 $\mu$ m coating, with which approximately 0.3 amorphous silicon	reddish brown to blue or blue violet	uniform	
	Copper indium diselenide (CIS)	14.00%	11.00%	retangle	1.2m*0.6m	2-4mm substrate material, of which approximately 1 $\mu$ m CIS Layered	dark grey to Black	uniform	
	Cadmium telluride	10.00%	9.00%	retangular	1.2m*0.6m	3mm substrate material (non-hardened glass) with 0.005mm coating.	reflective dark green to black	uniform	

Data source : DGS, 2008

Image source: Monocrystalline Silicon and poly crystalline sillicon is from DGS , 2008;

Amorphous silcon is from <http://www.home-solar-power-hour.com/amorphous-silicon-solar-panels.html>

CIS: [https://caluvtech.com/products/Alternative\\_Energy/ACC/Solarpanels/Brunton/Solaris26/Solaris26.htm](https://caluvtech.com/products/Alternative_Energy/ACC/Solarpanels/Brunton/Solaris26/Solaris26.htm)

Cadmium telluride: <http://www.treehugger.com/files/2008/08/cheaper-solar-panels-first-solar.php>

- **Crystalline Photovoltaic**

Crystalline silicon is the most prevalent bulk material for solar cells (abbreviated as C-Si). There are two types of C-Si PV, mono-crystalline and polycrystalline.

The manufacture of crystalline PV starts with extraction, the de-oxidation and purification of poly-silicon, which is often carried out under temperatures above 1000 centigrade. Mono-crystalline is produced through a process called “Czochralski drawing<sup>1</sup>”. This solo-direction material-drawing process makes mono-crystalline PV more pure and uniform with solo cell color in appearance. Whereas for polycrystalline cells, their ingots are directly cast into cuboids from the original melt ploy-silicon. Due to the block casting with different orientation, polycrystalline has the surface in forest pattern.

The crystalline PV cells are mostly in the form of round or square wafers ranging between 10 cm by 10 cm to 15cm by 15cm in size. The PV cells are interconnected into modules, and modules to panels – the PV panels we see in the daily life. Mono-crystalline PV has energy efficiency of over 20% since it contains denser silicon atoms. The efficiency of polycrystalline is lower, about 16.5% (Table 2.1).

- **The Thin film Photovoltaic**

Thin film PV cells apply photoactive semiconductor materials such as amorphous silicon, copper indium diselenide (CIS) and cadmium telluride (CdTe) as thin layers onto low-cost substrate (in most of cases, glass). The high light absorption rate of these materials allows the layers to be thinner than 0.001mm, the width typically sufficient for converting sunlight into electricity.

The manufacture of thin film PV includes vaporous, deposition, sputter processes

---

<sup>1</sup> Czochralski drawing process works like this: A seed crystal with a defined orientation is dipped into the silicon melt and slowly drawn upwards out of the melt.

and electrolytic baths. The required decomposition temperature is around 200 to 600 centigrade, much lower than the temperature needed in crystalline PV production. So thin film PV uses less energy than crystalline PV during the production process.

The efficiency of thin film PV is lower than crystalline PV. Currently, the most efficient thin film is CIS, with a module efficiency of 10% (DGS 2008). But thin film is cheaper than crystalline PV. Based on the price data on Solar Buzz in May 2011, the lowest price of thin film PV is \$1.37/watt, while the cheapest multi-and mono-cSi cost \$1.8/watts and \$1.84/watts respectively<sup>2</sup>.

Thin film PV also has higher flexibility than crystal PV. Its manufacture process allows the size of the thin film cell to be customized according to design requirements. And 1-5  $\mu\text{m}$ -thick material could be laminated on various substrates, not only glass, but also fabric and soft material.

#### **2.1.4 The Constraints of solar PV technologies**

Constrained by solar characteristics, energy production of solar PV systems faces problems of instability and intermittency. The power of PV energy systems is highly dependent on temporary solar irradiance, so the change of solar irradiation intensity across seasons causes fluctuations of energy output over a year, which might not be consistent with demand. Even during the course of a single day, the sudden appearance of clouds will cause the electricity current from PV system to fluctuate. For this reason, solar PV energy systems cannot be used as a base-load power supply. It is often used as the peak load energy supply, supplemented by another energy system to ensure stable output.

To ensure stable electricity, the urban PV could either store electricity in the battery or connect with the power grid. In our later research, we assume all the

---

<sup>2</sup> <http://www.solarbuzz.com/facts-and-figures/retail-price-environment/module-prices>, 2010-05-26

PV energy systems are grid-connected.

## **2.2 Urban micro wind turbines**

Wind energy is regarded as the most promising clean renewable energy (Sims, Schock et al. 2007). Even though commercial wind farms on open fields have been deployed for several years, the utilization of the wind energy in cities is at an emerging stage. The size and capacity of urban wind turbines are much smaller than turbines in the open wind farm, with the blade diameter ranging from 2 meters to 9 meters and the capacity ranging from 1KW to 20KW.

### **2.2.1 Wind energy resources**

Wind is the second most abundant renewable resource in the world. According to Global Wind Energy Council<sup>3</sup>, in locations over land with mean wind speeds exceeding 6.9 m/s, the globally-available wind power at 80 meter height is about 72 TW, five times total global energy consumption(Jacobson 2009). Wind energy is not as easy to capture as solar because it keeps flowing, moving and changing. It is even harder to predict in cities due to complex physical conditions.

### **2.2.2 Operating Principle**

Wind electricity generation is a mechanical process. As shown in Figure 2.2, firstly, driven by the wind, moving blades turn the low-speed shaft, then the gearbox connected with the low-speed shaft shifts its rotation speed into a higher speed for the high-speed shaft. Following that, the secondary shaft goes directly into the generator and produces alternative current electricity.

---

<sup>3</sup> The world's wind resource. <http://www.gwec.net/index.php?id=148>

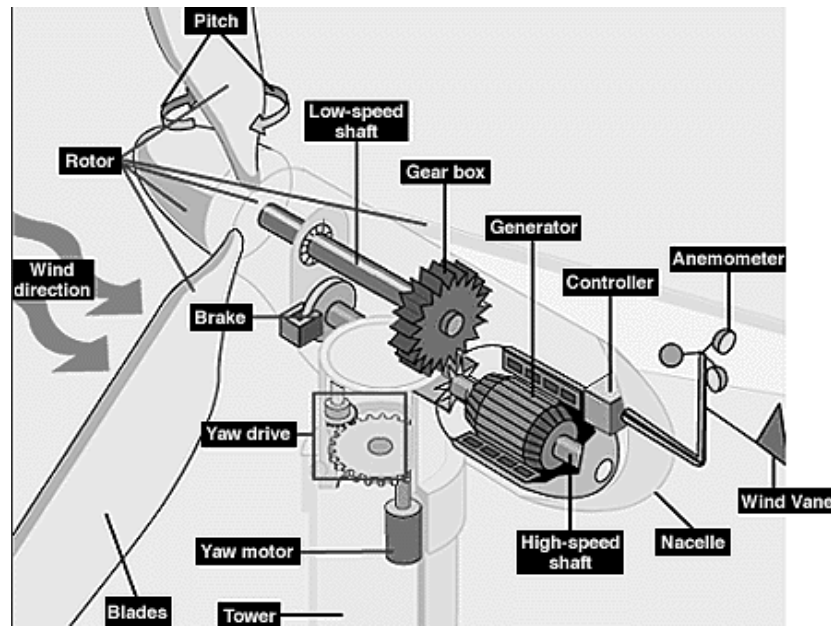


Figure 2.2: Inside of the wind turbines

Source:

[http://jisibhlphysics.wikispaces.com/file/view/EERE\\_illust\\_large\\_turbine.gif/66239994/EERE\\_illust\\_large\\_turbine.gif](http://jisibhlphysics.wikispaces.com/file/view/EERE_illust_large_turbine.gif/66239994/EERE_illust_large_turbine.gif)

### 2.2.3 Types of wind turbines

Wind turbines involve a variety of technical solutions in response to complicated surrounding aerodynamic environments. There are two types of wind turbines- vertical axis wind turbines (VAWT) and horizontal axis wind turbines (HAWT).

As we can see from Figure 2.3, the HAWTs have a very different appearance from VAWTs. Their gearbox and generators must be placed near the blades in the nacelle on top of the tower- and they often associate with stronger towers, too. In the case of vertical wind turbines, their gearbox and generator can be installed on the ground, so their forms are lighter and more aesthetically appealing.

Figure 2.4 shows five different wind turbines, the HAWTs on the left look similar, and VAWTs show more variety, including drag-type turbines like Savonius and lift-type turbines resembling an egg-beater-Darrieus and Giromill.



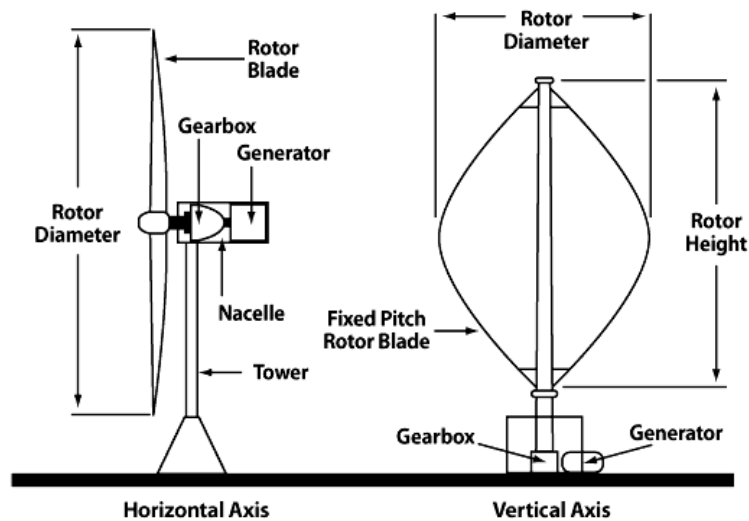


Figure 2.3: Horizontal-Axis and Vertical-Axis Wind turbines  
Source: American Wind Energy Association



Figure 2.4 Different types of wind turbines, from the left to right are Proven Turbines (HAWT), Skysteam 3.7 (HAWT), QR5KW triple helix blade (VAWT- Darrieus), Skyröta 5.0 two blade (VAWT-Giromill), Helical 3 KW wind generator(VAWT-Savonius)  
Source: [http://www.solener.com/novedad\\_e.html](http://www.solener.com/novedad_e.html) (the first right)  
[http://www.planetenergy.co.uk/windtubines\\_files/](http://www.planetenergy.co.uk/windtubines_files/) (the others)

HAWT and VAWT have their own advantages and drawbacks –the selection of the turbine style often depends on the specific situation. HAWT has been favored in history due to the maturity of the technology, higher rotation speed and cheaper price. VAWTs are relatively new but have great potential for they can better deal with turbulences or swirling steam, and also produce less noise. (Stankovic, Campbell et al. 2009).

## **2.2.4 The Constraints of the urban wind turbines**

The utilization of the wind energy is confined by significant constraints. It has the same problem of intermittency as solar energy. In addition, the minimum required wind speed, as well as noise, vibration and flicker shadows during operation would also cause negative impacts.

- **Intermittency and Uncertainty**

Similar to solar energy, wind energy has the problem of intermittency. Wind changes from time to time with seasons and weather. It is hard to guarantee a stable energy output, so it cannot be used as the base load energy system either.

Nevertheless, wind conditions are hard to predict without long-time monitoring or complex Computational fluid dynamics (CFD) modeling. According to a recent monitoring report done by Massachusetts Technology Collaborative, the real energy yield of 19 monitored small-wind projects in the US are all smaller than the estimation, 17 of them much smaller (Shawn 2008). The uncertainty of the available energy sources makes wind turbine integration harder than solar PV under the urban situation.

- **Minimum annual wind speed**

Only when the mean annual wind speed of a given location exceeds the minimum annual wind speed of the turbine, can the location be considered viable for wind energy integration. The Wind Energy Integration in the Urban Environment (WINEUR) project<sup>4</sup> pointed out in their 2007 report that, wind turbines are recommended to be installed in locations where wind speed is higher than 5.5m/s (Cace, Horst et al. 2007).

---

<sup>4</sup> It is a project supported by the European Commission, explored the development of small wind energies in cities

- **Noise, safety, resonance, flicker shadow and aesthetic concerns**

The noise of wind turbines comes from mechanical operation and aerodynamic interactions. The faster the blades rotate, the louder noise it produces. In the urban environment, noise should be kept below certain levels, thus some big wind turbines should be kept a certain distance away from the building.

Safety is another concern. Ensuring wind turbines are installed in a safe location in the city is crucial, for there is higher probability of injury in populated areas if a malfunction were to occur.

Resonance is another concern for building mounted wind turbines. Resonance will occur when the eigenfrequency of the building equals the frequency of the wind turbine, causing destructive vibration of the building. The eigenfrequency of the building is negatively correlated to the building's height. The taller the building is, the less likely that resonance will occur (Mertens 2006).

Flicker shadow occurs when the turbine's rotating blades cast shadows on stationary objects, such as nearby buildings. Although flicker shadow only happens several hours per year, depending on the site, it may cause great inconvenience for nearby residents.

Last but not least, the aesthetics of wind turbines is also a problem. Since wind turbines appear like machinery, some neighborhoods are reluctant to accept wind turbines in their open space because they view the turbines as detracting from the natural scenery.

### **2.3 Cost and carbon intensity**

Besides the technical features, the trade-offs between cost and carbon content play an important role in renewable integration, since renewable energies emit lower carbon than, but are also more costly than, conventional fossil-fuel energy.

This section uses “life cycle analysis greenhouse gas emissions (LCAGHG)” and “levelized cost of energy (LCOE)” as carbon intensity and cost criteria respectively, in examining the two technologies. Both LCAGHG and LCOE assess the performance of the technology over its lifetime<sup>5</sup>.

### **2.3.1 Life cycle analysis greenhouse gas emission (LCAGHG)**

LCAGHG calculates carbon intensity, which is the total carbon emission over total energy production, in the life span. The unit is “g CO<sub>2</sub>eq/KWh”, carbon emission equivalent per kilowatt-hour, i.e. the carbon intensity. Different from conventional energy systems, the solar PV and the wind turbines emit very little carbon during operation. Most of carbon emissions in their life cycle are from manufacturing and installation processes.

Daniel Weisser summarized and compared the LCAGHG of various energy systems. As shown Figure 2.5, the LCAGHG of solar PV ranged from 43 to 73 g CO<sub>2</sub> eq/KWh, much less than conventional energy systems such as coal, petroline and gasoline. 50-80% of carbon emissions come from the production process of PV cells. Among different types of solar PV systems, mono-crystalline PV emits the least GHGs, ranging between 43 and 62 g CO<sub>2</sub> eq/KWh, due to its higher system efficiency (Weisser 2007).

In contrast to integrated PV systems which often show similar efficiency to large-scale PV farms, urban micro turbines cannot achieve the same efficiency as onshore wind farms. Research shows that a small wind turbine of 1 KW requires about three times more life-cycle energy per unit power than a large wind turbine of 1 MW (Lenzen, 2002). Mithraratne estimated the LCAGHG of micro wind energy in New Zealand and found it to be between 130-220 g CO<sub>2</sub> eq/KW, much larger than the normal wind energy carbon intensity shown in

---

<sup>5</sup> The life spans of solar PV and wind turbines are similar, both between 20 and 30 years. However, the LCAGHG and LCOE will change a lot if the life span changes. For the estimation, I assume the life span of wind turbines is 25 years.

Figure 2.5. However, micro wind energy is still a cleaner energy compared to fossil fuel.

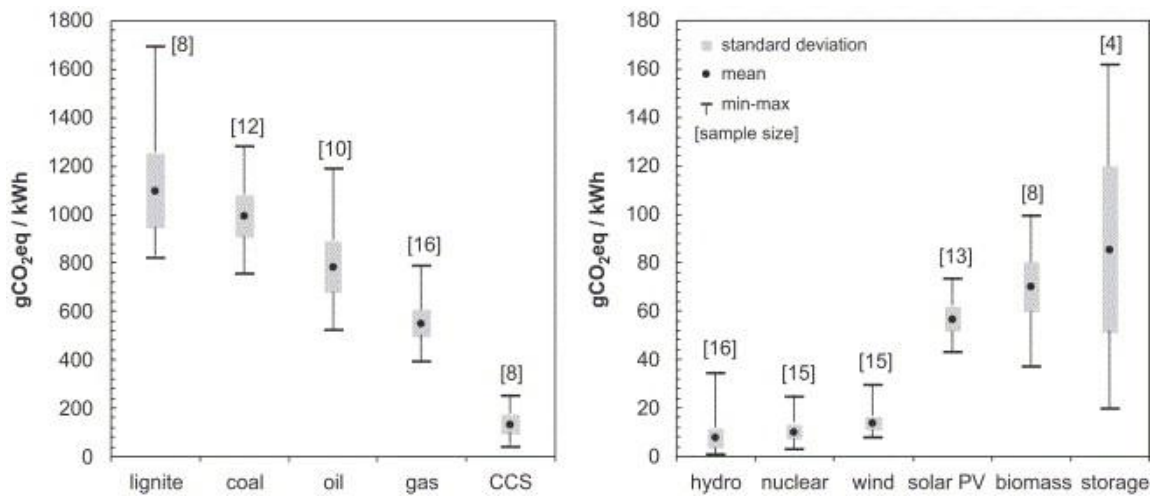


Figure 2.5 The carbon intensity of different energy systems  
Source: Weisser 2007

### 2.3.2 Levelized cost of energy (LCOE)

Levelized cost of energy (LCOE) studies the average cost per energy unit over the technology's lifetime. It is a cost estimating methodology adopted by National Renewable Energy Laboratory (NREL)<sup>6</sup>. Based on the range of various factors ([http://www.nrel.gov/analysis/tech\\_cap\\_factor.html](http://www.nrel.gov/analysis/tech_cap_factor.html)), and the data assembled in the Trancik Lab Database ([www.mit.edu/~trancik](http://www.mit.edu/~trancik)), the range of cost of energy systems is estimated and shown in Figure 2.13. The price of solar PV ranges from 18 to 60.83 ¢/KWh, which is about 5 to 10 times more expensive than coal and natural gas. For the normal wind energy, the cost is between 2.48 and 14.93 ¢/KWh. However, if the lower efficiency of performance factor was applied in LOCE estimation, the average levelized cost for urban micro energy spans from 42.9 to 139.5 ¢/KWh, even higher than the price of solar PV.

<sup>6</sup> LCOE gives a metric that allows the comparison of capital costs, capital rate, discount rate, operation and maintenance (O&M) cost and capacity factor over the life time of the system.

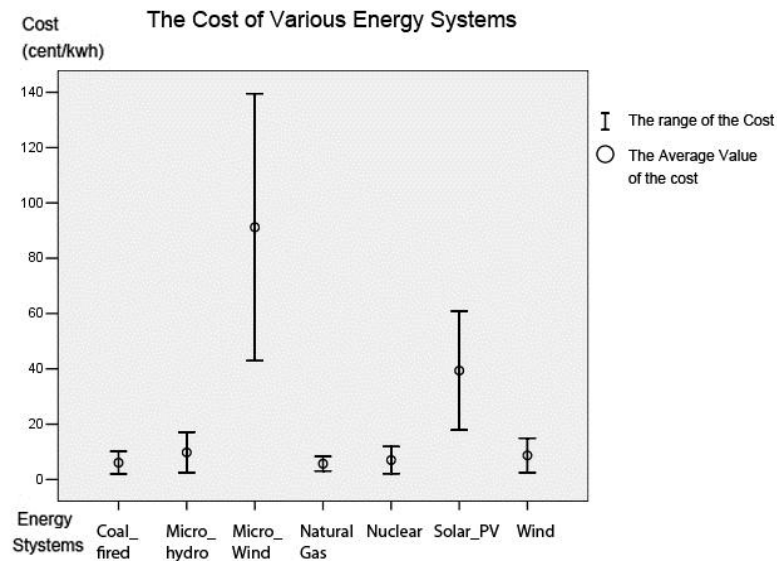


Figure 2.6 The cost of various energy system

Data Source: Trancik, 2011

*Note: The cost of micro wind energy is calculated through NREL's LCOE tool using the capacity range of urban wind turbines which is 2% -6.4%*

### 2.3.3 Cost-carbon trade-offs of PV and micro wind turbines

While wind energy is less costly and less carbon intensive than solar PV, micro wind turbines do not share the same advantage. Micro wind turbines are likely to be more expensive and more carbon intensive than solar PV if the lower efficiency of performance is applied in the LCOE and LCAGHG estimation.

However, this conclusion is drawn from limited literature in order to give a rough comparison between the two technologies. The LCAGHG and LCOE in applied situations would change along with the particular sites. For each project, it is recommended to conduct a separate estimation on LCOE and LCAGHG before making a decision.

## **2.4 The Future of Solar PV and micro urban wind turbines**

### **2.4.1 PV – cheaper, more efficient and more flexible**

The goal of Solar PV technology is to achieve higher performance with lower cost. Over the past three decades, the cost of PV shows a significant reduction along with its cumulative installed capacity and this trend is still improving (Nemet 2006). In terms of increasing performance, some research is focused on material and device design aimed to improve the solar-to-electricity conversion ratio; other research investigates low-cost manufacturing to adapt high-efficiency materials with durable performance. Two cases capturing these trends bear noting. The first is the highly efficient three-dimensional PV box, and the other is the “soft house” using high efficiency thin film.

Jeffrey Grossman at MIT has invented the super-efficient solar origami, a transparent box with folded solar cells. In his solar box, the composition of origami solar cells is derived from the tree branch structure in the nature, highly effective in capturing the sunlight. It is said to be two and a half times more efficient than traditional flat arrays (Liggett 2010). However, in terms of design integration, a solar box might need larger space, and posing difficulties for building integration.

A solar PV product trend that is friendlier to building integration is towards more flexible and thinner film panels. The efficiency of thin film continues to improve. A recent announcement from “*United Solar*” stated that they broke the record and increased the efficiency of thin film PV cells to 16.3% under lab conditions, and the module efficiency of market products is expected to exceed 12% this year (Uni-Solar 2011). On the other hand, thin film is becoming thinner. Currently, it is already possible to attach the thin film PV cells on the soft materials like fabric and curtains. In a soft house design by Sheila Kennedy shown in Figure 2.7, solar PV curtains attached with CIGS PV cells capture the sunlight that falls on movable façades. This PV curtain was believed to provide the house “about

half of the daily power needs of an average household in the United States” (Wright 2008).



Figure 2.7: Solar House designed by Sheila Kennedy  
Source: <http://inhabitat.com/solar-harvesting-textiles-energize-soft-house/>

In the future, thin film PV cells could be dramatically “upgraded” to another form – the “printable PV”, which would allow semi-conductive material to be printed onto a flexible substrate, similar to the printing of newspapers. Printable PV cells will save raw material waste, making the PV more economical and enabling faster production at a lower cost. Currently, scientists are investigating various approaches to produce cheap printed PV. The application of this technology might bring another revolution; at the time, PV will be like a layer of materials, similar to building coating, allowing even more diverse and flexible application in architecture design.

#### **2.4.2 Micro wind turbines – Lower cut-in speed, higher efficiency and less negative impacts**

The large-scale commercial wind farm has been quite well developed –the operational capacity keeps rising along with the increase of average installed individual turbine size over the past decades (Wiser and Bolinger 2006). However, micro urban wind turbines are still at an emerging stage. Even in



Europe, where most studies and practices on urban wind energy have taken place, there are still no safety, noise and installation urban design requirements related to wind turbines (Cace, Horst et al. 2007). The uncertainty of real urban wind energy output shown in several researches suggests more cautious development strategies based on the openness of wind data are needed, to ensure the credibility of this technology (Encraft, 2009, Shawn 2008). At the same time, exploring a higher performance of wind turbines and mitigating their negative impact would still be needed to justify its utilization in cities.

One approach is to develop the low cut-in speed wind turbines to deal with the slow average wind speed in urban areas. Lowering the cut-in speed will make use of the slower wind, previously not usable, and increase the energy yield. However, applying wind turbines with low cut-in speed does not associate with extra economic benefit – for the energy gain might not payback its extra cost (Ferrigno 2010).

To address the negative impact of wind turbines, some renewable enterprises like *"Quiet Revolution Company"*, also target producing quieter and more visual-pleasing wind turbines. Nevertheless, to use wind energy best, placing the wind turbine at the right location in the city to capture sufficient wind resources has great significance. In the next chapter, I will discuss the location and form factors related to wind electricity generation.

## **2.5 Conclusion**

This chapter discussed the key technical features of solar PV and micro wind turbines. The fact-based description and comparison on various aspects of both technologies are to provide a more comprehensive picture for designers in renewable decision-making. To sum up, key principles of the technologies are as follows.

- Solar PV is a material-based technology. The semi-conductive material

used in PV will not only determine the appearance of panels, but also the efficiency, average cost and life cycle carbon emission. Solar PV panels can be seen as plate-shape devices which can be placed in various ways to capture sunlight.

- A wind turbine is a complex mechanical architecture. A great variety of micro wind turbines can be found as a response to various complex aerodynamic conditions in the cities. However, urban wind turbines have some significant drawbacks such as noise, safety concern, resonance and the flicker shadow. The most serious constraint is the minimum wind speed requirement, which makes it inapplicable in many urban places. This feature calls for thorough studies on the feasibility of urban wind integration at the early urban design stage.
- Comparing two technologies in general, I found solar PV is probably more applicable and accountable in urban integration due to its higher flexibility, more stable energy sources and less negative impacts. However, depending on urban physical conditions, micro wind generation may still play an important role in specific situations, particularly if the technology advances enable more diverse, responsive and effective wind energy generating solutions to complex physical environments.
- In terms of cost and environmental impact, solar PV could be cheaper and less energy intense than urban micro wind turbines too. Wind energy usually shows very low efficiency of performance in the urban area. This shortage renders the micro wind energy more expensive and carbon intense than solar PV. However, since the cost and LCAGHG are highly correlated with the potential annual energy output, which varies greatly from location to location, the relative result between the two technologies would change accordingly as well.

## **Chapter 3: Renewable energy potential: simulation**

### **methodologies and form-related determinants**

This chapter explores form-incorporated renewable energy potential simulation methodologies for solar PV and micro wind turbines in the urban environment. Building on existing renewable energy calculation methods, it tries to link energy variables, such as the average hourly solar irradiation and wind speed, with form-related factors, through quantitative or qualitative analysis. For each technology, I firstly elaborate the formula and their variables, then examine the correlations between important variables and the urban form respectively, and the ways of incorporating their impact into renewable energy potential simulation.

The methodologies will be applied to the simulation analysis in Chapter 4, and will also be used for renewable energy potential simulation methods in the energy pro-forma of “Making the clean energy city” project.

### **3.1 Solar PV**

What differentiates urban integrated solar PV systems from PV farms is the potentials and constraints of building shapes for PV installations, as well as the impact from the shade from nearby buildings.

The annual energy output of solar PV electricity is a function of average hourly solar irradiation, effective annual solar duration, the PV installed area and the efficiency of the PV system.

#### **3.1.1 Annual Solar Energy Production Formula**

The function may be written as follows

$$E_{pv} = \sum_{i=1}^n G_{hy\_i} * A_i * H * \gamma_i * \eta \quad (A)$$

$E_{pv}$  (KWh/year) is annual electricity output from solar PV,.

$G_{hy\_i}$  (KWh/sq m) - is average hourly irradiation on surface  $i$ , which is the average hourly solar energy intensity that PV surface  $i$  receives over the solar duration time in a year.  $G_{hy\_i}$  will be affected by the geographic location, local climate and the placement of the PV. Section 3.1.1 will elaborate on the impact of the above-mentioned factors on  $G_{hy\_i}$ .

$H$  (unit/year)- is unit of local annual solar duration hours. The solar duration is the length of time in which the solar radiation falling on the plane perpendicular to the direction of the sun is greater or equal to 120 W/sq m<sup>7</sup>. This solar duration is determined by the latitude and the local climate. In our later simulation based in Jinan, the solar duration is given from the climate database of China Meteorological Administration. The annual solar duration  $H$  in Jinan is fixed as 2546.8 hours<sup>8</sup>.

$\gamma_i$ — is the annual shading adjusting factor on the surface  $i$ . It is the ratio of the actual un-shaded sunlight hours over its possible sunlight hours. Since the actual solar duration could be shortened due to the shading cast by the nearby buildings, the building arrangement would have some correlation with the shading adjusting factor. Section 3.1.3 will analyze this impact; I find that effective sunlight hours are inversely related to the building north-south distance, and quadricatically related with the orientation of the building arrays.

$A_i$  (square meter) - the area of PV surface  $i$ . It is a direct form-related factor in

<sup>7</sup> The definition is drawn from European Centre for Medium-Range weather Forecasts, <http://ecmwf.int/>

<sup>8</sup> China Meteorological Data Sharing System [http://cdc.cma.gov.cn/shuju/search1.jsp?dsid=SURF\\_CLI\\_CHN\\_MUL\\_MYER\\_19712000\\_CES&tpcat=SURF&type=table&pageid=3](http://cdc.cma.gov.cn/shuju/search1.jsp?dsid=SURF_CLI_CHN_MUL_MYER_19712000_CES&tpcat=SURF&type=table&pageid=3)

the formula. However, to link it with specific neighborhood form, Section 3.1.4 analyzes the relationship between the surface area to volume ratio (SVR) and the solar energy potentials through simulating the solar energy potential of 100 building clusters.

$\eta$  (%) - the efficiency of PV system. The system efficiency is the product of the module efficiency and the system de-rating rate. The efficiency of a PV system is about 75% of module efficiency due to the conversion loss, the unclear air quality and the less ideal solar irradiation conditions. The efficiency difference between the module and PV system is called the system de-rating rate (John Randolph 2008). In our simulation, I assume mono crystalline PV cells with module efficiency of 23% will be applied. After de-rating, the efficiency of PV systems will be 17%.

### 3.1.2 The average hourly irradiation and its determinants

- **Location and climate**

The geographic location primarily determines the direct average hourly solar irradiation. And when the extraterrestrial sunlight passes through the atmosphere, the sunlight will be decreased by the aerosols, water, vapors in the atmosphere to different degrees at different places. So the local climate condition will affect the attainable solar resources as well; for example, places with humid climate might block more sunlight.  $G_{hy\_i}$  is location-specific.

- **The orientation of PV panels**

Under given local solar conditions, to get the most from solar panels, designers need to point them in the direction that captures the most sun. There are two PV systems in terms of orientation design: the fixed PV system and the tracking PV system.

- Fixed PV systems

The slope and the orientation of PV will greatly affect its annual energy output. In the northern hemisphere, PV panels facing the due south would achieve higher energy yield than other orientations. Research shows that a surface facing due south with tilt angle equivalent to local latitude could receive the maximum insolation over a year (Mondol, Yohanis et al. 2006). Lu and Yang (2010) estimated the annual PV energy yield on different surfaces for buildings in Hong Kong. They found that the annual energy output from vertical PV panels facing east/west was only two thirds of those facing the due south, and one third of those at the optimum tilt. However, sometimes fixed panels apply the optimum winter tilt, to get the most energy in the worst season (Landau. 2011).

In design and development, the impact of orientation could be incorporated. For instance, designers could lay out the buildings more carefully, enabling the longer façades to get a more sunward orientation. In roof-integrated design, they could also apply the optimum tilt of the PVs as the slope of the roof.

- Tracking PV systems

Tracking PV systems might be an easy way to solve the problem of the changing angle of the sun caused by the earth's self-rotation and revolution movement. Since this kind of system can constantly adjust the orientation of PV panels based on the position of the sun, much higher energy yield will result. However, the tracking system is more space-demanding and usually appears to be too technical and not that aesthetically appealing. It is also much more expensive than the fixed panel systems – the cost and benefit analysis between two systems might be necessary in making the decision.

In my simulation approach, the average hourly irradiation will be estimated under the climate condition in Jinan, with the consideration of orientation of the PV panels. To get the most energy potential, I assume all flat roofs will be installed with tracking PV panels. PV will be placed on the surface of sloped roofs and

also vertical facades – the orientation of the PV is determined by the building shape. The detailed calculation methodologies are available in Appendix II.

### **3.1.3 The shading adjusting factor and the building arrangement**

In Formula A, the shading adjusting factor  $\gamma$  is supposed to carry the impact of shading on the annual solar duration. This section examines the relationship between the effective sunlight hours and building arrangement. The form factors relating to the building arrangement include building height, spacing and the orientation of building arrays.

- **Height and roof shading**

Tall buildings cast shadows on the roofs of nearby low buildings, “impairing” their access to solar energy. Since clusters comprised of buildings of the same height eliminate this problem, these clusters would be preferred in solar neighborhoods. For clusters consisting of buildings at various heights, it is recommended to arrange the buildings carefully to mitigate this problem. One effective strategy could be planning the low rise building on the sunny side and the tall buildings at the shady side, to allow more access to sunlight for low-rise buildings.

- **Spacing**

The spacing indicator is the ratio of the north-south distance between the nearest buildings over the height of the sunward building (Figure 3.1). The closer the buildings are, the more greatly they are affected by the shade from nearby buildings.

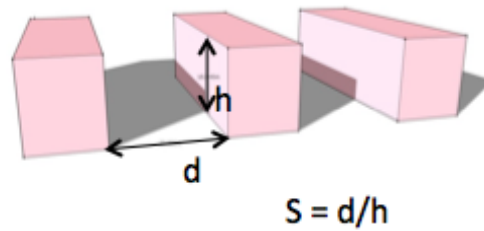


Figure 3.1 The spacing indicator

To evaluate the relationship between the spacing indicator and the annual sunlight hour on the building facade, I simulate 100 building clusters embedded with different spacing indicators. A building cluster, as defined in “making the clean energy city project”, is a basic unit of urban form that captures “a fundamental set of relationships between buildings, spaces, movement systems, and activities that underlie patterns of energy use in the urban environment”(Frenchman, Zengras et al. 2010). It reflects the “urban scale” that this thesis is focused on.

To simplify the analysis, I only examine the impact on the effective sunlight hours on the southern facade, under the controlled location of Jinan, China<sup>9</sup>. The effective sunlight hours are estimated through Autodesk Ecotect. “*Autodesk ecotect analysis sustainable design analysis*” software is a comprehensive concept-to-detail building design tool with a wide range of simulation and building energy analysis, including solar simulation based on the city climate profile. With 100 spacing indicators and the simulated effective sunlight hours from Ecotect, it is possible to analyze the correlation between the two.

---

<sup>9</sup> Here, the climate profile of Jinan City is drawn from the “Meteorological data set for China building thermal environment analysis” 2005



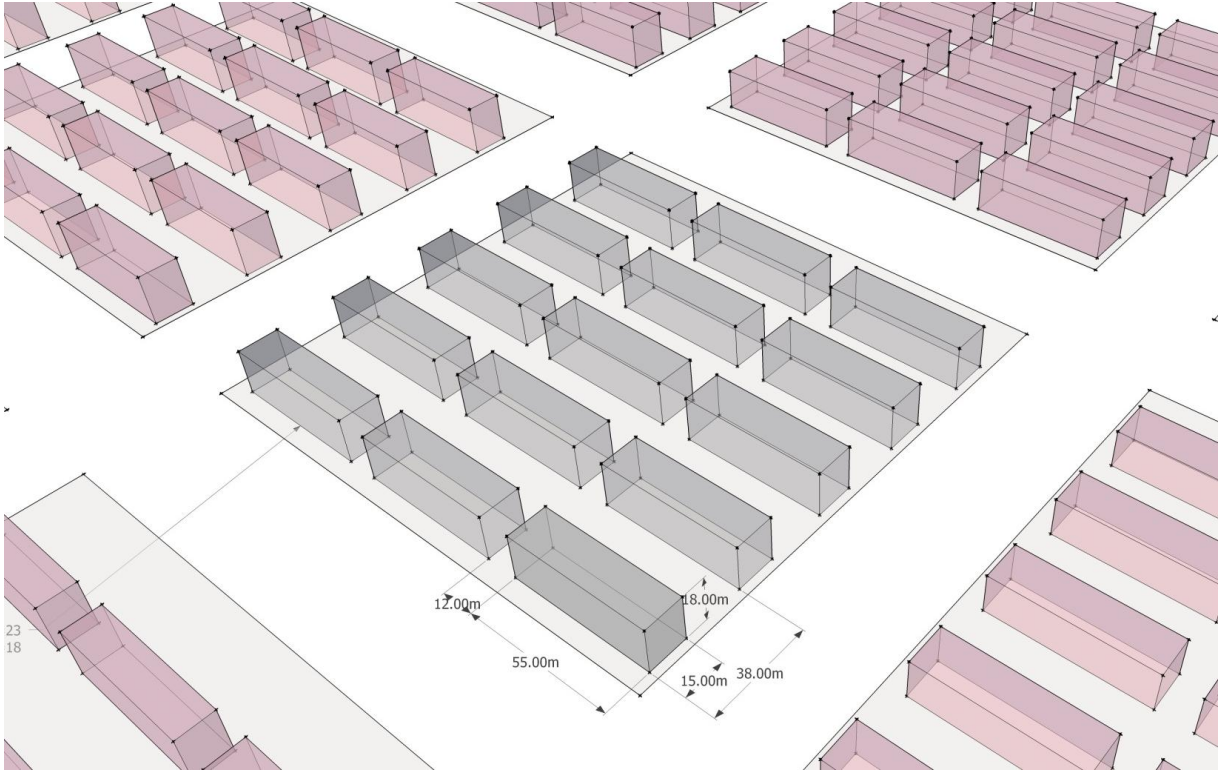


Figure 3.2: the benchmark neighborhood

In my simulation of 100 building clusters, each cluster is comprised of fifteen identical buildings. The size of each building cluster is 200 meters by 200 meters. The layout of the benchmark cluster was derived from a typical urban neighborhood in Jinan named Dongchang. I call it “slab” neighborhood in this thesis (more detailed description will be presented in Chapter 4). As shown in Figure 3.2, the north-south distance and east-west distance between two closest buildings are 23 and 12 meters, and the building height is 18 meters. Another 99 building clusters are created by modifying building height, depth, and the north-south distance relative to the benchmark case. In this way, a set of spacing indicators are embedded in the 100 cluster models. Figure 3.3 shows the 100 building cluster models, and the red one is the benchmark cluster.

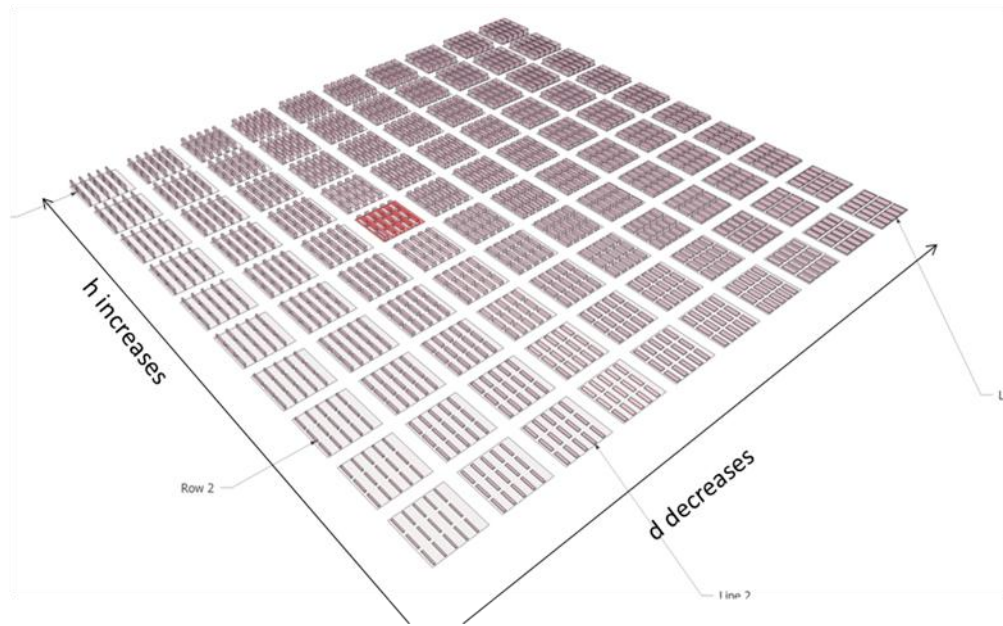


Figure 3.3: The 100 building cluster models  
*Note,  $d$  is the south-north distance between the nearest buildings, and  $h$  is the height of the buildings*

To further simplify the analysis, I assume the sunlight hours on the southern façade of the central building can be representative for all other buildings on site (Figure 3.4). Appendix I records the spacing indicators and the corresponding annual sunlight hours of the central building in the 100-model simulation.

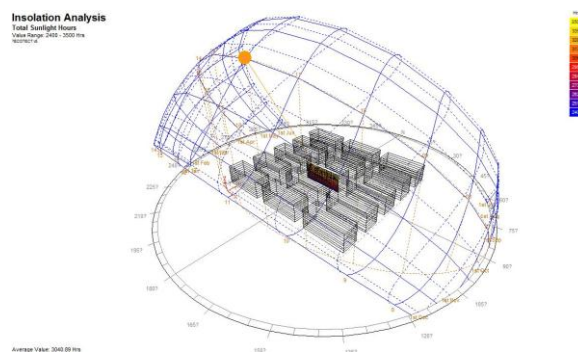


Figure 3.4: The sunlight hour simulation in Autodesk Ecotect

Figure 3.5 plots the relationship between annual sunlight hours and the spacing indicator. As shown here, under the same location, the annual sunlight hours show an inverse relationship with the spacing indicator. Annual sunlight hours

increase steeply along with the change of the spacing factor at small spacing values; however, as the spacing indicator exceeds a certain value, the sunlight hours on the buildings' southern façade levels off.

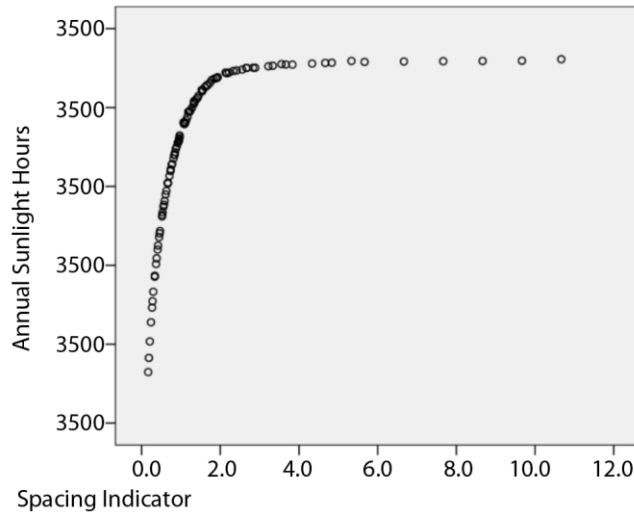


Figure 3.5 The relationship between the spacing indicators and the sunlight hours on the vertical southern facades

The function can be written as

$$H_{si} = m + n * (1 / S)$$

$H_{si}$  is the annual un-shaded sunlight hours on the southern façade, and  $S$  is the spacing indicator.  $m$  and  $n$  are two parameters that can be estimated via regression. Here,  $m$  is a positive value, and  $n$  is a negative value. These parameters in the function above are determined by location.

- **The orientation of buildings arrays**

Even with the same spacing between one another, if the building arrays are placed at different orientations, the shading pattern and, as a result, the annual un-shaded hours on the vertical façades will differ. As shown in Figure 3.6, at the same moment, the building clusters oriented in different directions present different types of shades on their vertical facades.

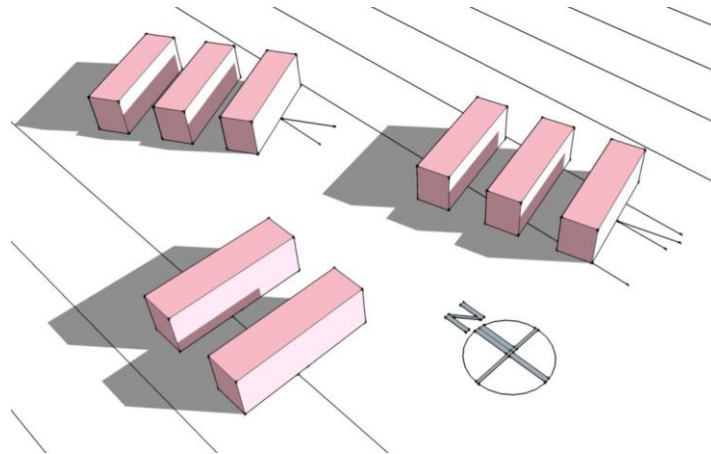


Figure 3.6 the orientation of building arrays and the shade.

To keep other factors constant, I use the benchmark model and estimate the effective sunlight hours on the southern facades when orienting it at different directions ranging from -90 (west/counterclockwise) to 90 (east/clockwise) degrees. I use “ $\sigma$ ”, which is the angle between the projection of the normal of the vertical façade and the due south (the azimuth) as the building orientation indicator, and then test the relationship between  $\sigma$  and simulated un-shaded sunlight hours.

Based on our results, there is a quadric relationship between orientation and the annual sunlight hours, shown in Figure 3.7 below. The highest value of sunlight hours occurs when the angle is zero – meaning when the clusters face true south. The function can be written as

**Error! Objects cannot be created from editing field codes.**  
**Error! Objects cannot be created from editing field codes.** (C)

$H_{oi}$  is the effective sunlight hours adjusted for the orientation.  $k$ ,  $j$  and  $l$  could be estimated via regression. In this function,  $k$  is always negative, and  $l$  is positive.  $k$ ,  $j$  and  $l$  are conditioned to the local climates and the spacing of building cluster.

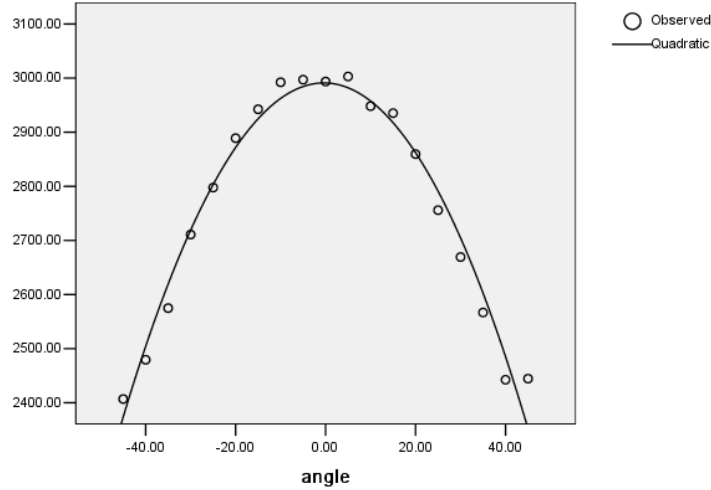


Figure 3.7 The relationship between the sunlight hours of the southern facades and the building orientation

As mentioned earlier, facing due south will also contribute to larger average hourly irradiance. Therefore, in solar neighborhood design, the east-west slab building with longer facades and facing the true south might have better performance in solar integration.

In the solar energy potential simulation,  $Y_i$  will carry the impact of the spacing and orientation. The southern vertical façade's  $Y_i$  can be calculated as

$$Y_i = (H_{si}/H_{tot}) * (H_{oi}/H_{si}^*)$$

$H_{si}$  is the effective sunlight hours adjusted by shading caused by spacing, and  $H_{oi}$  is the effective sunlight hours adjusted by the orientation based on the neighborhoods with the same spacing, and  $H_{tot}$  is the total sunlight hours in Jinan over a year.

#### 3.1.4 Surface area and surface area to volume ratio (SVR)

PV panels are mostly integrated with the roof or the sunward vertical façades of buildings. Different surface areas might have different renewable energy potential. For example, the roof is often favored over the vertical facade, for it is least

impacted by the shades and also possible to adopt PVs at the optimum tilt or accommodate tracking systems.

In order to link solar energy potential with form more clearly based on the surface area, I choose “surface area to volume ratio” (SVR) as the surface indicator to study. Building SVR is an urban form indicator, which is the total surface area over the volume of building.

To examine the relationship between the SVR and the energy potential of the neighborhood, I simulated the yearly PV electricity production of the 100 models by using formula A. In the simulation, I firstly calculate the average solar irradiance and shading adjusting factor based on the methodology discussed earlier. The installation area of the PV is assumed to be equal to the respective surface area. I neglected the shades caused by other panels. A more detailed description of my simulation methodology can be found in Appendix II. The result is the energy potential of each cluster, which is the annual solar energy output by built area<sup>10</sup>. The detailed information of 100 cluster models and the relevant solar energy potential results are listed in Appendix I.

I plot the SVR versus the energy potential of 100 building cluster models in Figure 3.8. As shown, firstly, there is a positive linear correlation between PV energy potential and the SVR. The larger the surface area to volume ratio, the more electricity output per built area it can possibly provide.

---

<sup>10</sup> I assume the height of the building floor is equal to three meters, so the total construction area can be calculated at given building dimensions of length, depth and height in each model.

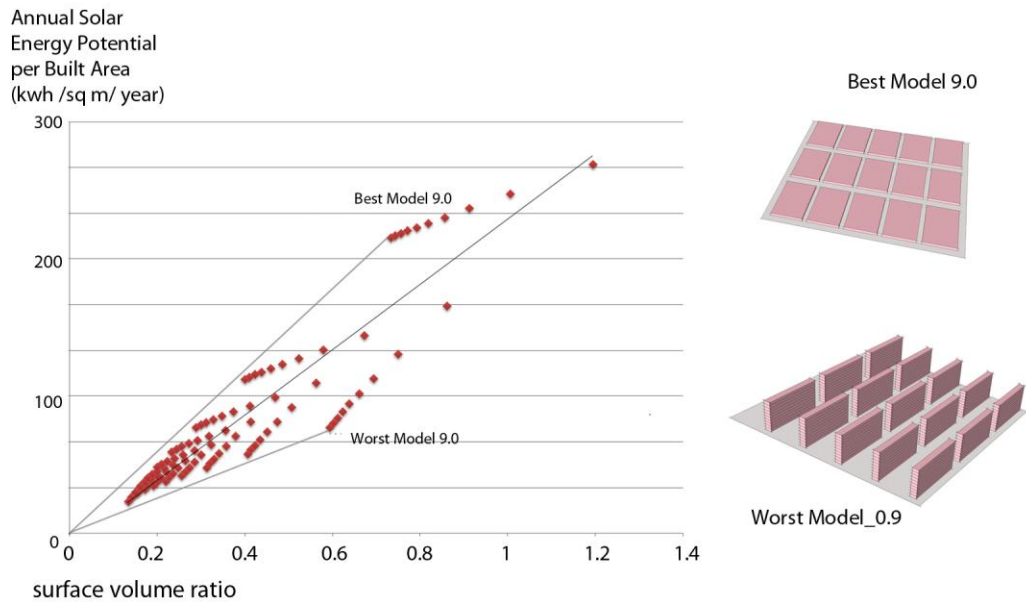


Figure 3.8 The relationship between energy yield and the surface area to volume ratio

However, for clusters with the same SVR, there are some discrepancies in energy potential. As shown in Figure 3.8, at the SVR of 0.4, there are building clusters with solar energy potential ranging from 60 to 115 kWh/sq m/year. In Figure 3.8, as the lines connect the cluster points with the origin, the slopes of these lines indicate the values of energy potential over the SVR - the steeper slope implying higher energy potential per SVR unit. A further examination on the best performing model (Model 9.0<sup>11</sup> - the one with the steepest slope) and the worst performing model (Model 0.9 - the one with the flattest slope) shows buildings with larger portion of roof area could have higher energy potential – the composition of the surfaces plays a role too. In the design and development, increasing the surface area, especially the area of the roof might be an effective strategy to promote renewable PV integration. A more detailed discussion will be carried out in later chapters.

### 3.2 Urban Wind Turbines

Wind speed is the most important factor in wind electricity production. Under the

<sup>11</sup> The way of naming the models could be found in Appendix I.

same wind regime, urban form could change the wind flow, slowing it down via its rough terrain and concentrating it through building configuration. The size of building-mounted wind turbines would also be related to the size of the buildings they are mounted on.

### 3.2.1 The formula of the wind energy output

Wind power is a function of wind speed, air density, swept area of blades, and the coefficient of performance:

$$P_w = C_p \frac{1}{2} \rho A v^3 \quad (B)$$

$P_w$  - is the power of the urban wind turbine.

$C_p$  - is the efficiency of performance, also called the capacity factor; It changes with the specific turbines and the wind speed. The maximum theoretical value is called the Betz limit, which is 59%. The capacity factor of a typical commercial wind turbine is around 30%, and as I mentioned earlier, the  $C_p$  for micro wind turbines is only between 2% and 6.4%.

$\rho$  (kg/m<sup>3</sup>) - is the air density. According to International Standard Atmosphere, at sea level and at 15°C, the air density is approximately 1.225 kg/m<sup>3</sup>. This value will be used in simulation.

$V$  (m/s) – is the wind speed. It is the most important factor for wind power generation. The wind speed depends on wind resources in the region and is also subject to the physical form of the neighborhoods. Section 3.2.2 and 3.2.3 will elaborate on these impacts respectively. The form-related factors that Section 3.2.3 tackles include height, the roughness length of the terrain and the building concentration. The estimation of  $v$  is the most complicated part in wind energy output potential simulation.



**A** (square meter) - is the swept area of the wind turbine - it can be calculated as  **$A = \pi \times R^2$** . **R** is the radius of the wind turbine. Section 3.2.4 will explain how the size of the wind turbines is constrained by the size of the building.

### 3.2.2 “V” the wind speed and local wind profile

Wind changes with seasons, temperature difference in geography, altitude, self-movement of the earth and also surrounding landscape elements like mountains or oceans. The self-spinning movement of the earth alters the wind direction; for example, it causes the wind flow from the equator to the poles to be deflected towards the east. Temperature also impacts the wind pattern. When the temperature gets cooler, the air begins to sink into the lower layer of atmosphere and causes wind flow. Recent research in Houston (TX, USA) shows that the widespread urban development caused the land area to be warmer at night, reducing the contract between the sea and the land, and altered the night wind patterns<sup>12</sup>.

Wind distribution is also critical in examining the wind energy yield. A wind distribution profile is a histogram that represents the probability of a given wind speed in 1 or 0.5 m/s “bins”. The wind profile of Jinan is shown in Figure 3.9; as can be seen, the mean wind speed is 3 m/s, and this wind profile fits well to a Weibull probability function curve. So the following function can be applied when calculating the annual wind energy output:

$$E_w = 1.91 * P_w * T * N = 1.91 * 8760 * T * N \quad (C)$$

**$E_w$**  is the annual energy output from the total wind turbines; **T** is the time length of the year – which is 8760 (365 times 24 hours); and, **1.91** is the adjustment factor

---

<sup>12</sup> More detailed info can be found via “Air Quality Worsened by Paved Surfaces: Widespread Urban Development Alters Weather Patterns”.  
<http://www.sciencedaily.com/releases/2011/06/110607121137.htm>

when adopting mean wind speed in energy output estimation under the condition that the Rayleigh distribution<sup>13</sup> is valid (Stankovic, Campbell et al. 2009),  $N$  is the total number of installable wind turbines, which is constrained by the the spacing requirement that would be discussed in section 3.26.

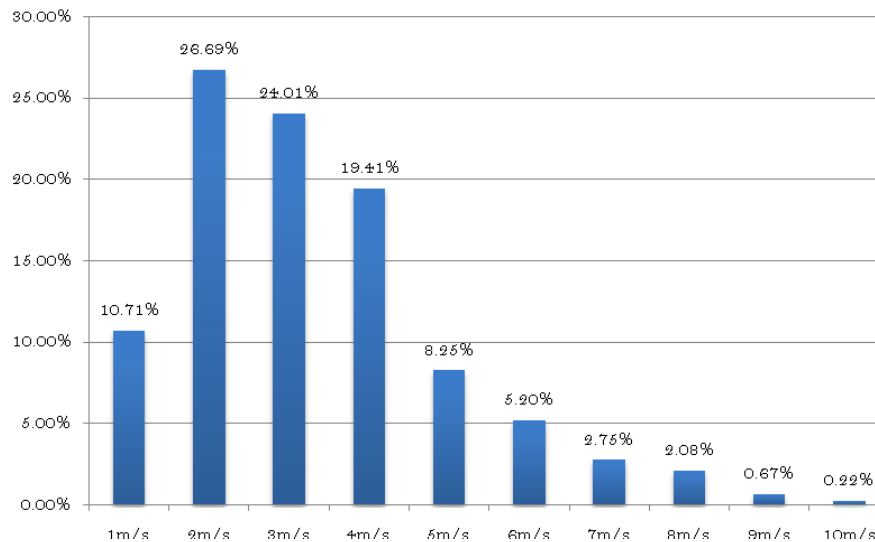


Figure 3.9 The wind profile in Jinan  
Data source: Song, Zhu et al. 2005

### 3.2.3 The wind speed and form-related factors

Buildings in cities can slow down wind speed and re-channel its direction. When wind passes through cities, the general wind speed will reduced due to the rough elements on the ground; and then its direction and speed will be greatly affected by the buildings it passes. This section discusses the impact from form- related factors including height, roughness length of the terrain and building concentration design.

- **The height of the turbines**

Generally, anywhere in the world, the higher the wind turbines are located, the richer the wind resources that can be captured. The increase of the wind speed

<sup>13</sup> Weibull is a type of the Rayleigh distribution

is faster near the ground, and less rapid at increasing heights. Above ground obstacles, the wind profile is usually approximated by a logarithmic profile with the increment of height.

- **Roughness length and turbulence**

When wind enters the urban terrain, it will be disturbed and slowed down by local features like trees and buildings. Figure 3.10 illustrates the simplest disturbing effect. When the wind passes the terrain, the building will block the wind flow, causing swirling turbulence at its downwind side. A building's disturbed zone might extend to a distance 20 times the building-height. Therefore, in urban design, one should place the wind turbines far away from the built area to avoid the turbulence zone. If the turbine has to sit in the disturbed zone, the height should be at least twice the tallest building on the upwind side (Stankovic, Campbell et al. 2009).

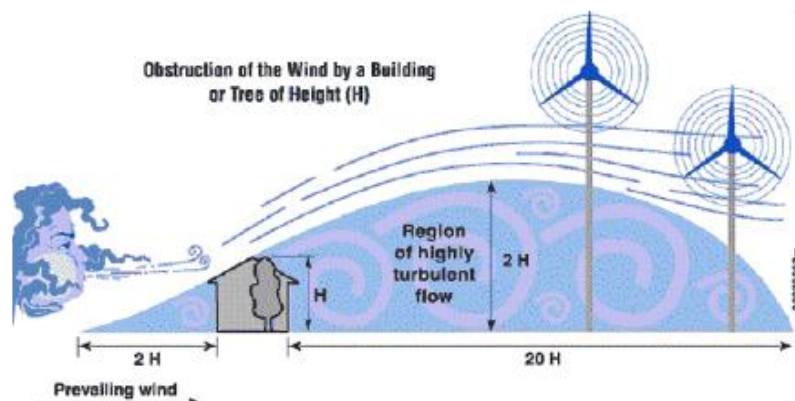


Figure 3.10 Schematic of the effect of the obstacles on the wind flow  
Source: A G Dutton 2005

“Roughness length” is a parameter that reflects the unevenness of the terrains – a combined urban form indicator related to building coverage, average building height and the variance of the building height (Wieringa 1993; MacDonald, Griffiths et al. 1998; Mertens 2006). The detailed estimation methodologies are in Appendix II. The higher the roughness length is, the rougher the terrain, and the more severely wind energy will be reduced. The roughness is higher than 0.7 in a

city center, and 0.25-0.3 in a suburban terrain, and 0.01-0.03 in an open field rural terrain (Stankovic, Campbell et al. 2009). As shown in Figure 3.11, at the same height above the ground, the wind speed at cities is much slower than that in the suburban or rural area.

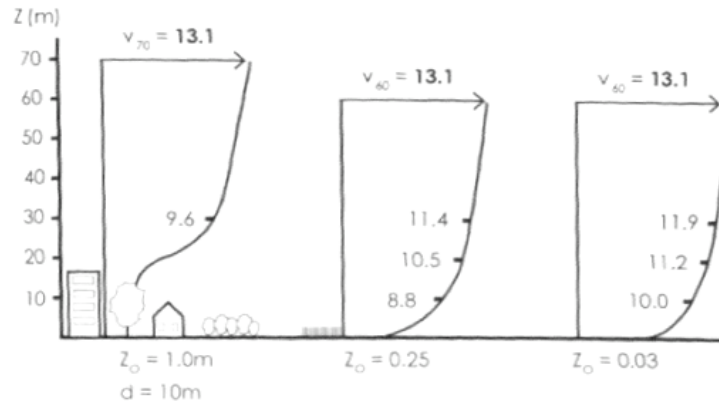


Figure 3.11 The wind speed profile associated with different terrains  
Source: Stankovic, Campbell et al. 2009

*Note,  $Z_0$  is the roughness length of the terrain. The terrains from left to right are urban terrain, suburban terrain and rural terrain.  $d$  is the displacement height, which indicates the unaffected height of the wind turbines.*

In the wind energy potential simulation, I apply the following formula taking both factors into account.

$$\frac{V(z)}{V(10)} = \frac{\ln(z / z_0)}{\ln(10 / z_0)}$$

$V(z)$  is the wind speed at operating height  $z$  (m/sec).  $z_0$  is the roughness length,  $V(10)$  is the wind speed (m/sec) at the reference height of 10m from the ground, which is the mean wind speed of Jinan City.

- **Building Concentration**

At the same time, urban wind energy integration could take advantage of building form, concentrating the wind. Two approaches could be taken here. The first one is to place the wind turbines close to building to get speed-up high wind, and the second is change the design of the entire building or structure form to concentrate the wind.

- **Close-to-building configuration**

“Close-to-building configuration” is to place the wind turbines on or near the buildings to utilize the speed-up effect of the buildings on the wind.

Among different close-to-building integration scenarios, roof-mounted strategy is the most common and sometimes also most effective as well. As shown in Figure 3.14, when wind passes a sharp-edged building, it will be separated into high-wind-speed region and low-wind-speed turbulence region. The wind speed increases by 8% - 30% in the high-wind region (A G Dutton 2005). As shown in Mertern’s wind-form research, the speed-up effect of the sharp-edged roof could help wind turbines to achieve 100% more energy yield than turbines at the same height in cities (Mertens, 2005).

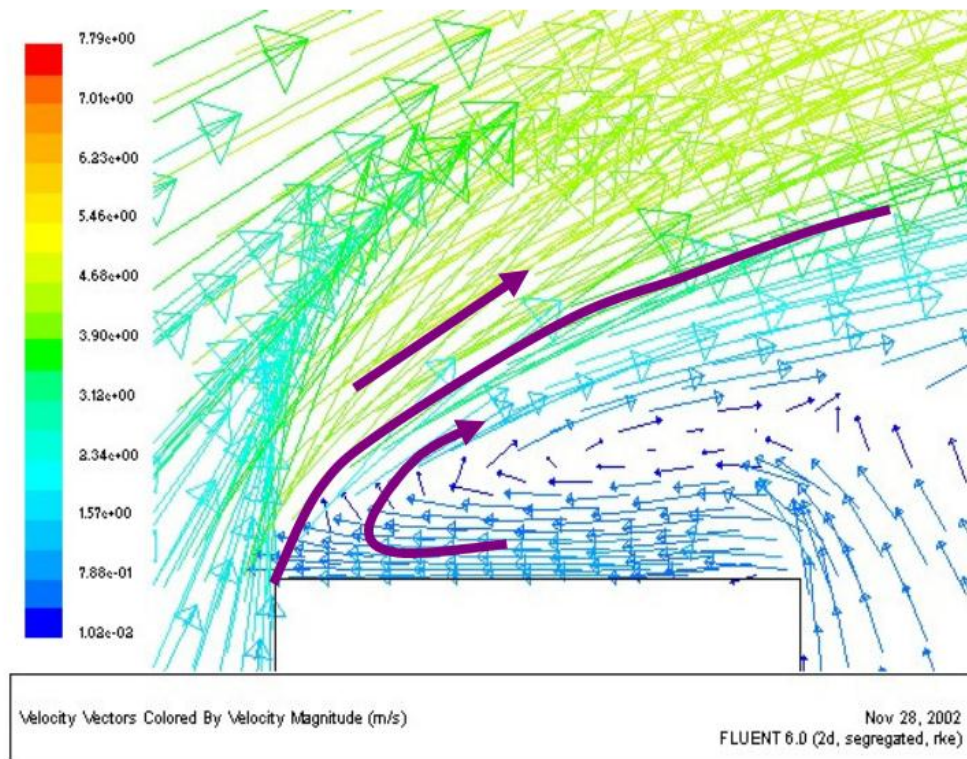


Figure 3.12 The wind flow around the building  
Source: Cace, Horst et al. 2007

Note, round-edged building could accelerate the wind speed even more. Sphere roof mounted turbines can achieve an increase of up to 300% (Mertens, 2005).

And similar speed-up effects can be found in wind turbines located besides a cylinder building.

One thing that should be noticed in design is the position of the wind turbines relative to the prevailing wind. The wind direction might also dramatically alter the speed-up effect. However, I do not include this effect in the discussion and later simulation.

- **Building Configuration**

Streamline building form is better in accommodating wind energy integration, for its shape can channel and accelerate wind flows. Stankovic did the CFD<sup>14</sup> wind speed simulations under different building configuration scenarios. The energy output results are shown in Table 3.2. These scenarios shown in Figure 3.13 include A) sharp-edge roof-mounted, B) round-edge roof-mounted, C) roof-mounted between two airfoil structures; D) square concentrator; E) circular concentrator (see Figure 3.13). According to his simulation results, the circular or square concentrator ducts with round edge in the building façades (type D and E) achieve the most additional power generation.

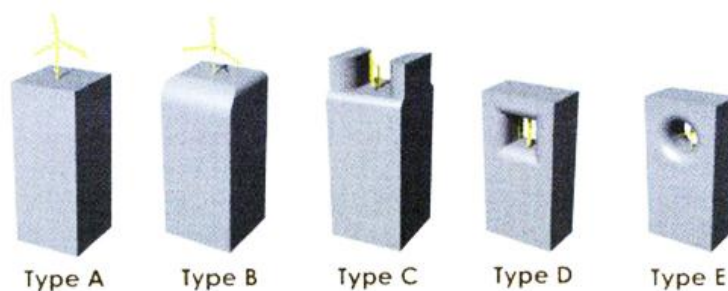


Figure 3.13 Different scenarios of the building configurations  
Source: Stankovic, Campbell et al. 2009

---

<sup>14</sup> Computational fluid dynamics

Table 3.2 the overall power production change of different building configuration scenarios

Geometry type	Overall power production change for various wind type (the power production over the regular power production )			
	Uniform	Weakly unidirectional <sup>15</sup>	strongly unidirectional <sup>16</sup>	bio-directional <sup>17</sup>
A	1.12	1.12	1.12	1.12
B	1.15	1.15	1.15	1.16
C	1.03	1.07	1.1	1.16
D	1.24	1.27	1.31	1.38
E	1.35	1.39	1.43	1.51

Source: Stankovic, Campbell et al. 2009

A wind energy concentrator research project - UWECS took the same strategy as type E and tested it in practice. In this project as shown in Figure 3.14, two kidney plan shape buildings formulate a wind duct to concentrate the wind, with a large size wind turbine placed in the gap. In the prototype test, the wind turbines are to be able to deal with a wide range of incident wind angle from -75 to +75, and it could produce 25% more energy than a same-capacity stand-alone wind turbine at the same height (Campbell, Stankovic et al. 2001)

However, in my wind energy simulation, I did not include the building configuration scenario, due to its limited application. Currently, only one building in the world – the Bahrain World Trade Center, has adopted this approach.

---

<sup>15</sup> >60 percent of the annual mean power density in the wind comes from any given 150 degree wind direction sector

<sup>16</sup> >75 percent of the annual mean power density in the wind comes from any given 150 degree wind direction sector.

<sup>17</sup> >95 percent of the annual mean power density in the wind comes from two opposite 150 degree wind direction sector.



Figure 3.14 The UWECS project  
Source: Campbell, Stankovic et al. 2001

### **3.2.5 The relationship between turbine size and building size**

Wind energy production has a linear relationship with the swept area of the blades. However, in order to avoid resonance, the size of the wind turbines should be relative to the size of the buildings they are installed with. Usually, the ratio of the characteristic building dimension over the turbine diameter should be below 0.5 to yield a stable installation (Menters, 2006). In most cases, when the diameter of the wind turbines is less than 0.1 of the building dimension, the wind turbine can achieve the highest efficiency (Jha 2011). In the later wind energy potential simulation, I use the assumption of a 0.1 ratio to estimate the size of appropriate wind turbines based on the size of buildings.

The positive relationship between wind energy output, turbine size and building size implies that building mass places some restrictions on turbine size – only buildings that are large enough can incorporate larger-size wind mills. This constraint could limit the installable capacity of building-integrated turbines and their wind energy potential.



### 3.2.6 The spacing requirement

To avoid the turbulence caused by nearby wind turbines, there is a distance requirement between the wind turbines. The spacing requirement determines the total number of turbines that could be possibly installed within a certain area. This distance is usually dependent on the type and size of the turbine, the roughness of terrain and the wind condition. Wider space can increase the energy output per turbine but decrease the number of turbines that could be applied. So there is some optimum spacing that maximizes total energy output.

In practice, wind turbines are usually placed in rows as perpendicular as possible to the prevailing wind direction, as shown in Figure 3.15. Under the unidirectional wind condition, the turbines can be sitting close to one another in the rows. However, a multidirectional wind environment requires larger spacing between the wind turbines, often necessitating around 5 to 7 diameters between the turbines in row and 7 to 8 diameters between the rows (Austrian Federal Ministry of Transport, 2005). In my wind energy potential simulation, I calculate the installable number of the wind turbines on a given roof area according to a spacing requirement based on Jinan wind conditions.

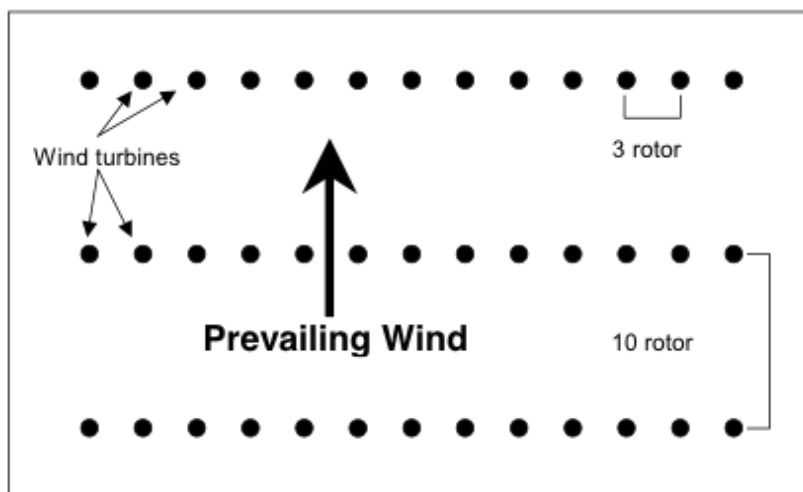


Figure 3.15 A Illustration of Turbine Spacing (3 x 10 spacing)  
Source: Austrian Federal Ministry of Transport, 2005

### 3.3 Discussions and Conclusion

#### 3.3.1 The impact of local climate conditions

Both solar and wind energy potential are firstly subject to the location and local climate conditions. The same neighborhood, located at different places will yield vastly different energy output. Taking solar energy as an example, as shown in Figure 3.16 and Table 3.3, if the installed location is changed from Jinan to Urumqi, a city with rich solar irradiance, the solar energy potential<sup>18</sup> of the earlier benchmark neighborhood will increase by 57%, whilst the potential would decrease by 72% if it changed to Chengdu which is humid and cloudy. This suggests that, even though solar energy is widely available in the world, some locations might not benefit much from PV integration due to their climate conditions. For every renewable application project, a careful examination on the local renewable resources is necessary.

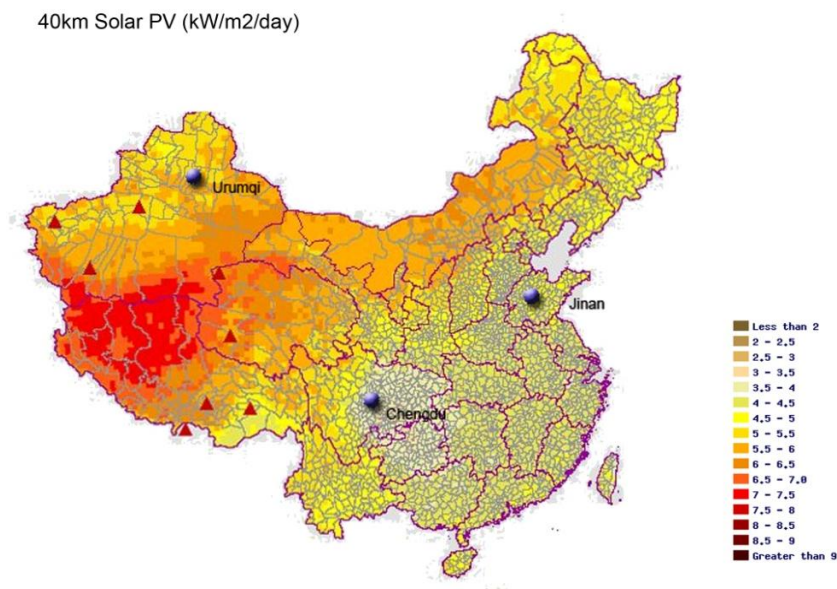


Figure 3.16 The location of the three cities in China's solar energy resource distribution map  
Source of the map: Solar and Wind Energy Resource Assessment (SIRA, UNEP/ GEF)<sup>19</sup>

<sup>18</sup> The same estimation methodology has been applied. The solar duration and the solar irradiance data of three cities are both from Song, F (2005) Meteorological data set for China building thermal environment analysis.

<sup>19</sup> <http://www.geni.org/globalenergy/library/renewable-energy-resources/world/asia/solar-asia/solar-china.shtml>

Table 3.3 The comparison of solar energy potentials of the benchmark neighborhood model in three different cities in China

City	The electricity energy potential per square meter (KWh/m <sup>2</sup> )	Change in percentage
Jinan	51.70	0.00%
Urumqi	81.05	56.77%
Chengdu	14.53	-71.89%

### 3.3.2 Form-related factors and the next step

Based on the formula and the analysis of the relevant form-related factors, we can see urban form makes a difference in renewable energy potential. For solar PV, the determinants include the PV slope, orientation, the spacing and also the surface area. For micro wind energy, the factors are building height and size, the roughness of the terrain and building configurations.

However, the analysis of the determinants in the formula only shows the correlation between a separate determinant and a variable in the estimation formula. The degree of importance of each determinant is unclear, the potential from the sun and the wind in the same neighborhood is uncertain and the combined form implications are also still unknown. Therefore, in the next chapter, I apply these formulas to simulate the renewable energy potential of four different neighborhood prototypes in Jinan, trying to distill the key form-related determinants and explore the design implications.

## **Chapter 4: The renewable energy potential of the four neighborhoods in Jinan**

This chapter applies renewable energy potential simulation methodologies to the four different neighborhoods in Jinan. It attempts to draw out key urban-form determinants through examining the correlations between renewable energy potential and urban form in the real world.

The simulated results suggest that solar energy is the dominant source of renewable energy potential across all four neighborhoods in Jinan. Surface area, especially the roof area has the greatest impact on the neighborhoods' solar energy potential, with other relevant factors being the style of roof, the FAR, and the building surface area to volume ratio.

### **4.1 The four neighborhoods in Jinan**

According to the empirical studies on neighborhood-form in “Making the Clean Energy City in China” project, there are four types of neighborhoods in Jinan: the “traditional”, the “grid”, the “enclave” and the “high-rise superblock”. These four neighborhood prototypes are very distinctive from one another. In my simulation, one representative neighborhood of each type is selected for the renewable wind and solar potential simulation.

#### **4.1.1 The “traditional” neighborhood**

This type of neighborhood is characterized by 1-3 story courtyards and narrow alleys. The courtyard layouts face south-north, enclosed by walls and/or low-rise traditional buildings with sloped roofs. Alleys in these neighborhoods run east-west with widths between 3 and 8 meters. The building coverage is very high in traditional neighborhood. “Zhangjia Village,” an urban village in Jinan, is the

representative traditional neighborhood in this study (Figure 4.1 and Figure 4.5).

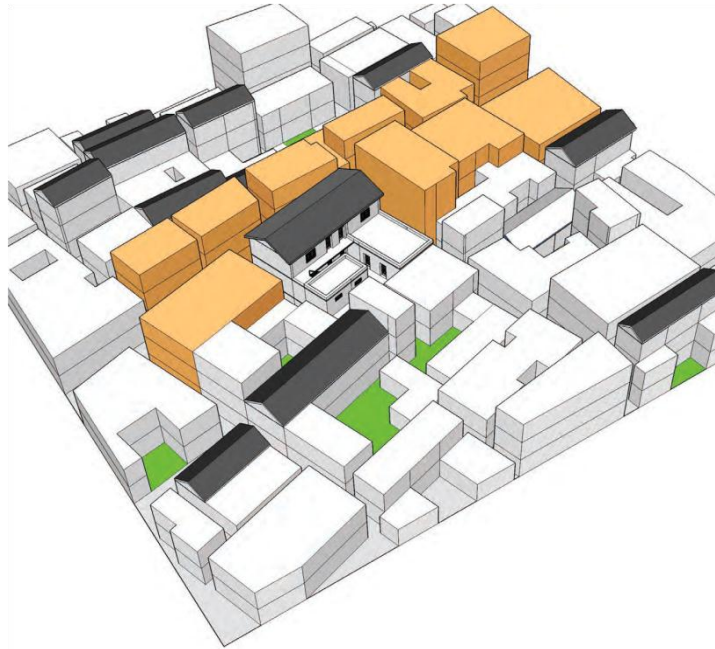


Figure 4.1 The typical traditional neighborhood in Jinan (The model is Zhangjia Village)  
Source: “Making the Clean Energy City” in China research project, MIT, 2010  
Note, the green space is the courtyard, and the orange buildings are commercial facilities.

#### 4.1.2 The “grid”

The grid is a typical street layout in modern city planning. The grid neighborhood typology was introduced into Jinan in the early 1920s during the semi-colonial period in China. The dimension of a typical grid block in Jinan is about 160 meters by 160 meters. The blocks were originally composed of traditional courtyards, but they have evolved into diverse and hybrid building forms including high rise towers and slab housing. The grid neighborhood is very open: public streets running between small blocks make the district very accessible. The “Old Commercial Street” is the typical grid neighborhood in Jinan (Figure 4.3).

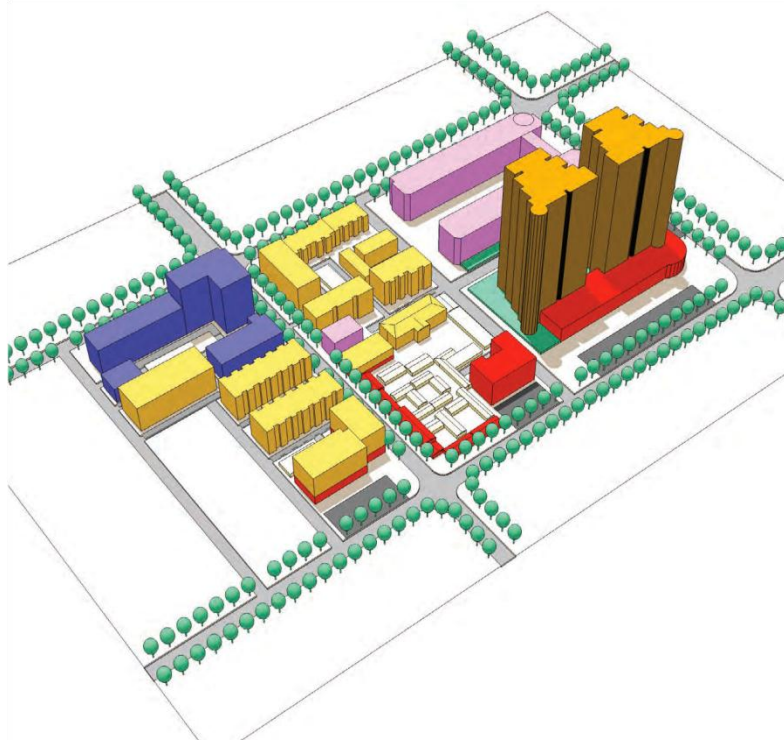


Figure 4.2 The typical grid neighborhood (The model is the “Old Commercial Street”)  
Source: “Making the Clean Energy City in China” research project, MIT, 2010

#### 4.1.3 The “enclave” / slab

The enclave neighborhood is a typical residential development from the mid-1980s. They were the original public housing developed by state-owned enterprises or governmental institutions. Each enclave neighborhood is enclosed and can be identified individually according to its occupants’ vocation. Its typical layout is characterized as regular arrays of east-west six-story slabs with regulatory north-south spacing in between. Internal roads between the buildings are often used as the outdoor space of the neighborhood as well (Frenchman, Zegras et al. 2010). Since my analysis is more focused on the physical form, according to its layout, I also termed the “enclave” type neighborhood in Jinan as “slab” type. The Dongchang neighborhood serves as a typical enclave neighborhood in our analysis is, and is the basis for the benchmark model.

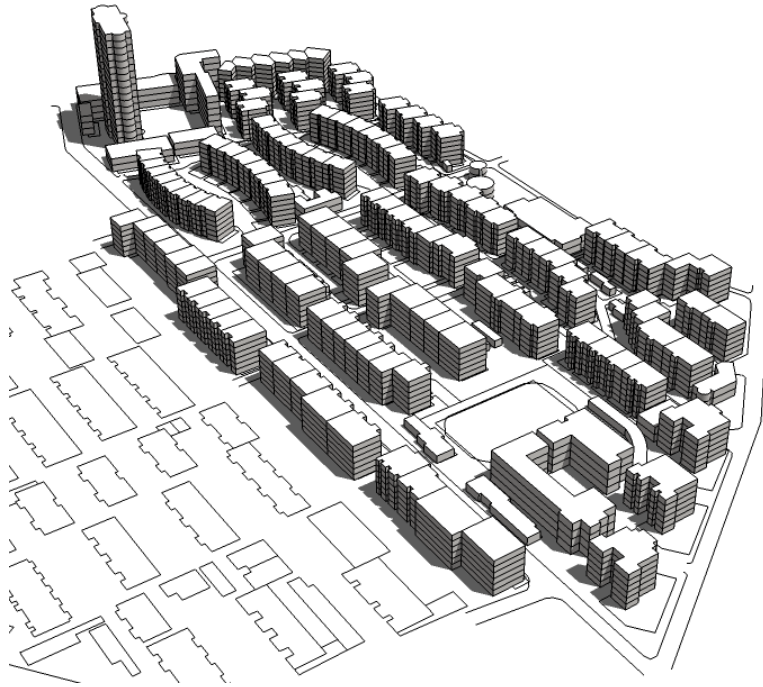


Figure 4.3 The typical enclave neighborhood (The model is Dongchang)  
Source: “Making the Clean Energy City” in China research project, MIT, 2010

#### 4.1.4 The “High-rise Superblock”

The high-rise superblock is a common residential development pattern in 21st century China. A high-rise building is defined as a building over 15 stories. The superblock neighborhoods are characterized by pure residential high-rise towers or slabs erected in the large open space. They are usually gated communities with limited access points, significantly isolating them from the surrounding urban environment (Frenchman, Zegras et al. 2010). Sunshine 100 represents the typical high-rise superblock neighborhood in Jinan.





Figure 4.4 The typical superblock neighborhood (The model is Sunshine 100)  
Source: “Making the Clean Energy City” in China research project, MIT, 2010

Clearly, the four types of neighborhoods are very distinctive from one another. For each type of urban form, one representative neighborhood is selected for the renewable wind and solar potential estimation.

The related form indicators are drawn from the GIS database of “Making the Clean Energy City in China.” This database is derived from high-resolution aerial photos and visual surveys of related neighborhoods<sup>20</sup>. Table 4.1 summarizes the key form indicators of the four neighborhoods. The GIS maps of the four neighborhoods are shown in Figure 4.5

---

<sup>20</sup> The survey was done by Tsinghua University and the GIS data provided by Beijing Normal University, as part of the “Making the Clean Energy City” project



Table 4.1 The key form indicators of the four neighborhoods

	Zhangjia Village (Traditional)	Dongchang (Enclave)	The Old commercial District (Grid)	Sunshine 100 (High-rise superblock)
Size (1000 sq m)	513.7	145.7	487.6	552.2
FAR	1.2	1.9	1.7	2.1
Building coverage	54.0%	36.4%	31.0%	14.4%
Building surface volume ratio	0.32	0.21	0.14	0.15
Average building story	2.2	5.3	5.5	10.1

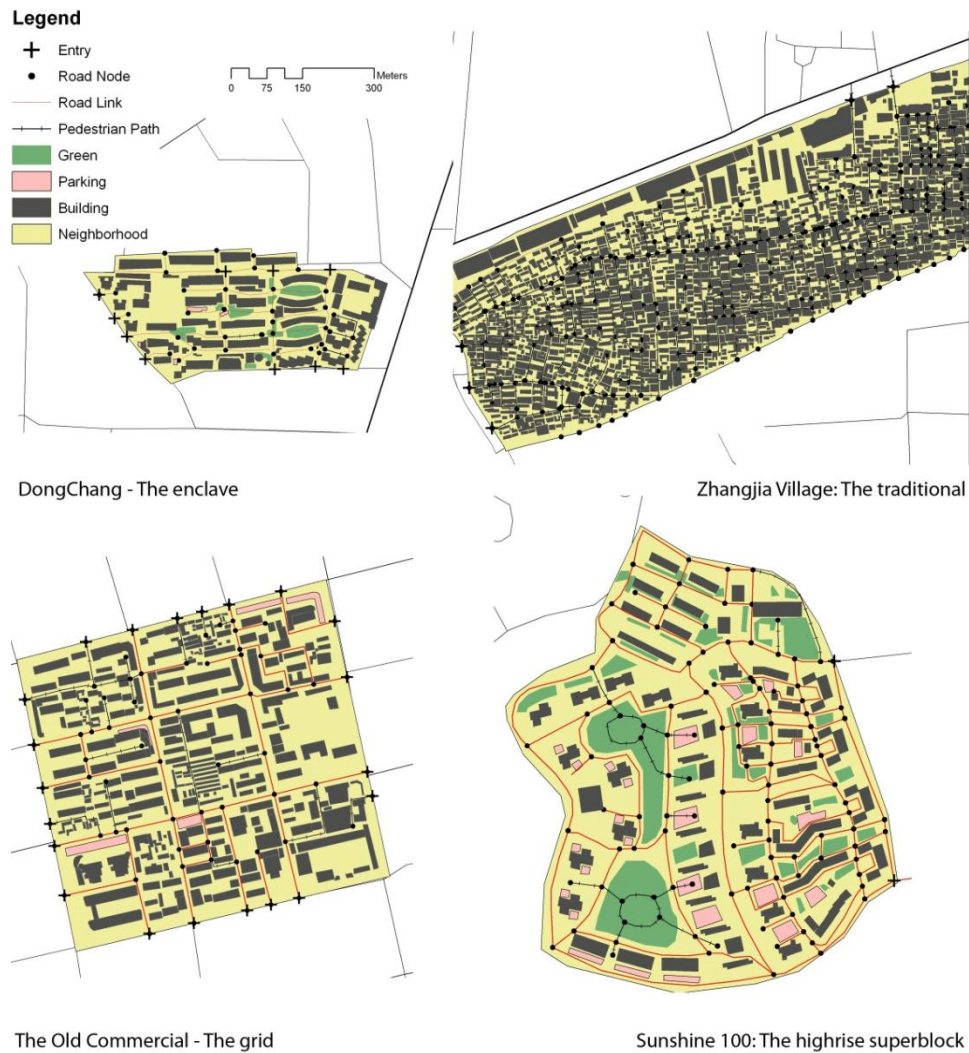


Figure 4.5 The GIS maps of the four Jinan neighborhoods  
Source: "Making the Clean Energy City" in China research project, MIT, 2010

## **4.2 Simulating the renewable energy potential of the four Jinan neighborhoods**

In neighborhood renewable energy simulation, I assume that the installation of wind turbine excludes the possibility of installing PVs on the same surface, and wind turbines will only be placed on buildings higher than 15-stories. I take both solar and wind potential into account, and the renewable energy potential is the combined result of both.

### **4.2.1 Methodologies and assumptions**

For solar energy estimation, only the potential from the roof-mounted and southern-facade-integrated PV are considered<sup>21</sup>. According to formula A in Chapter 3, the inputs include the average hourly irradiation, roof area, the southern surface area, and the effective solar duration.

- Consistent with previous simulations, the efficiency of PV is assumed to be 17%.
- The solar duration in Jinan is 2546 hours.
- The average hourly irradiation and the shade adjusting factor are estimated based on the methodologies described earlier.
- For shading adjusting factor calculation, we assume all the building arrays are facing due-south, and the spacing factor is estimated based on the average height of the buildings and the average distance between the buildings measured from the GIS dataset.
- In terms of the surface area, we assume the installed PV surface area is equal to the roof area on the top, and the roof area is equal to the site area multiplied by the building coverage; 30% of the southern façade would be

---

<sup>21</sup> The renewable energy potential simulation method can be found in Appendix II – a flat roof will be installed with the tracking PV system and a vertical façade will have PV panels installed parallel to the surface. For sloped roofs we assume that the PV panels are placed in parallel to the slope.

covered by PV panels.

For wind, only roof-mounted turbines for buildings higher than 15 stories are taken into account. The wind energy potential is calculated based on formulas B and C in Chapter 3.

- The wind speed is estimated based on average wind speed at the height of 10 meters in Jinan, which is 3m/s. It is then adjusted for height, the roughness length of the neighborhood and also the roof-mounting concentration.
- The size and the total number of roof-mounted wind turbines is generalized according to the building dimensions.
- The capacity factor is assumed to be 4%. More detailed methodologies are provided in Appendix II.

#### 4.2.2 Zhangjia Village – the traditional neighborhood



Figure 4.6 Photos of Zhangjia Village

Source: "Making the Clean Energy City" in China research project, MIT, 2010

Zhangjia Village is the traditional low-rise high-density neighborhood. The building surface volume ratio is 0.32. Its building coverage is 54%, the highest among the four neighborhoods.

However, there are many traditional double sloped-roof buildings in Zhangjia Village, which are not ideal for solar PV integration. For these roofs, we can only assume that the sunward slopes, which are southern, eastern and western-facing will be integrated with fixed PV panels<sup>22</sup>. Since courtyard buildings are interconnected or perpendicular to one other, the solar exposure area of southern facades is smaller<sup>23</sup>.

Because the buildings in Zhangjia Village are too low, the wind speed on the roof doesn't reach the minimum speed for wind turbine installation. The contribution from wind energy is zero.

According to the simulation, Zhangjia village's renewable energy potential is 32.5 KWh /sq m/year. All the renewable energy is generated from solar PV, where the roof-mounted PV contributes around 90% of the total. The total renewable energy production is about one sixth of the annual total in-home residential energy consumption per square meter. This data is drawn from empirical surveys in "Making the clean energy city" project. The roof shape lowers the renewable energy potential dramatically. If the roof were flat and installed with tracking PV panel fully, the renewable energy potential would be doubled to be as high as 68

---

<sup>22</sup> For Zhangjia Village, the roof areas are calculated differently. In the simulation, we roughly assume that all the roofs in Zhangjia Village are double-sloped. Based on visual observation, the neighborhood is roughly comprised of identical buildings oriented differently, with one third of the buildings laid out north-west and two thirds east-west. According to GIS measurements, a typical building layout plan is on average 19 meters on the south-north side by 9 meters on the east-west side. The ratio of the short edge to the long edge is usually 1:3. The average building height is 6.3 meters, and roof slope 20 degrees. All the southward, westward and eastward sides of the roofs are installed with solar PV panels. In this way, I calculate the roof area at different orientations.

<sup>23</sup> I assume that only the southern façade of the east-west buildings would be integrated with the solar PV. I also assume one-third of the southern façades are blocked by surrounding buildings. With these assumptions, I roughly estimate the exposed southern façade.

KWh/sq m/year.

#### 4.2.3 Dongchang – the slab neighborhood



Figure 4.7 Photos of the Dongchang neighborhood  
Source: 'Making the Clean Energy City in China', MIT research project, 2010

The Dongchang neighborhood is comprised of east-west slab construction buildings, with an average height of 16.4 meters. It is the basis of the benchmark models used in our simulation in Chapter 3.

In Dongchang neighborhood, there is one 72-meter-high building. We assume that this building is installed with urban wind turbines – thus, all the wind potential is from this building.

According to the estimation, the renewable energy potential for Dongchang neighborhood in Jinan is estimated to be 36.4KWh/sq.m. Almost all the energy is produced from solar PV. Roof-mounted tracking PV systems produce over 80%



of the solar energy potential. Due to the spacing requirement of the wind turbines, low wind speed and the small size of the turbines, wind energy potential is not that much, less than 1% of the total. Even on the highest building in Dongchang, roof space generates much more energy yield if installed with solar PV versus wind turbines.

#### 4.2.4 Old Commercial District– The grid neighborhood



Figure 4.8 Photos of the Old Commercial District  
Source: 'Making the Clean Energy City in China', MIT research project, 2010

As shown in Figure 4.8, there are a variety of building types in the grid neighborhood. There are high-rise towers of over twenty stories, mid-rise slabs and low-rise traditional courtyards. Although the average building height of the Old Commercial District is almost the same as enclave neighborhoods, the variety of heights is much greater than in the other neighborhoods.

In the Old Commercial District, there are six buildings that are over fifteen stories.

We assume that these six buildings will be installed with the wind turbines<sup>24</sup>. For solar integration, we took the average building footprint and height derived from the GIS dataset and applied them to estimate the building surface<sup>25</sup>.

In this analysis, the energy potential in grid neighborhoods is almost as same as in enclave neighborhoods. This analysis undoubtedly contains some error, for the simulation neglected the shading effect on the roof of the buildings. Based on work done by another research on the “Making the Clean Energy City” project, roof shading would be around 5% on average across the year<sup>26</sup>. The real energy yield from solar energy might be somewhat smaller.

#### 4.2.5 Sunshine 100 – the high-rise super block



Figure 4.9 Photos of high-rise neighborhoods  
Source: ‘Making the Clean Energy City in China’, MIT research project, 2010

<sup>24</sup> In my simulation, I use the average height of 75 meters and the average roof area of the six highest buildings to estimate the wind potential.

<sup>25</sup> I use the average perimeter, height and the area of the buildings derived from GIS dataset. I assume that all the buildings lower than 15 stories are identical. The ratio of the long edge to the short edge in each building is 3:1. The average area of the southern façade is calculated accordingly.

Sunshine 100 is comprised of towers that are over 20 stories and some mid-rise slabs. The building coverage is the lowest among the four neighborhoods, at only 14.4%, but the average height is the highest at 30 meters.

In the simulation, I assume that the roofs of the seven highest towers will be installed with wind turbines, and the rest of the buildings will be installed with PV panels.

The simulated potential renewable energy supply is 9.5 KWh/sq m/year, with most of the renewable energy generated from the solar PV. Even though 10% of the roof area is installed with wind turbines, their annual energy yield is only 0.11 KWh/sq m, less than 2% of the total renewable energy potential. If these roofs were installed with PV, the additional annual solar energy potential these roofs could provide is 0.58 KWh/sq m. In terms of the utilization of the roof area, solar PV is more efficient than wind turbines.

### 4.3 The renewable energy potential and the form determinants

Table 4.2 The simulated renewable energy potential of four Jinan neighborhoods

Neighborhood	Zhangjia Village	Dongchang	Old Commercial District	Sunshine 100	Average
Total renewable energy potential per built area (KWh/sq.m/year)	32.50	36.40	31.1	9.50	27.38
Solar (KWh/sq.m/year)	32.50	36.37	31.02	9.39	27.32
Wind (KWh/sq.m/year)	0.0	0.03	0.08	0.11	0.06
The average annual in-home residential energy consumption per built area* (KWh/sq.m/year)	176.1	198.6	200.0	195.0	192.43
Renewable energy as a percentage of in-home energy consumption (%)	18.46%	18.33%	15.55%	4.87%	14.23%

*Note, the data of the average annual in-home residential energy consumption per built area of four neighborhoods are from "Making the Clean Energy City" in China project, MIT, 2010*



Table 4.2 presents the results for estimated renewable potential as well as current residential energy consumption of the four neighborhoods. Comparing the renewable energy potential to the existing in-home residential energy consumption, I found out that the renewable energy potential on average could meet 14% of the total energy demand across the four neighborhoods in Jinan. Its contribution, even within the existing urban form that was not particularly designed to accommodate its integration, is still quite significant.

Solar energy is the dominant source of the renewable energy potential across all the neighborhood types. This fact suggests that PV integration would receive the most attention in achieving the renewable potential of neighborhoods in Jinan. Moreover, building surface area and orientation are the key factors affecting solar energy potential.

#### **4.3.1 Solar energy – the major contributor to renewable energy potential in Jinan**

According to the simulation results, solar energy comprised more than 98% of the renewable energy potential in all four neighborhoods. It is both more efficient than wind energy and more applicable to different urban forms.

Due to minimum wind speed constraints, wind turbines could only be installed on buildings that are high enough. The slow wind speeds resulting from the rough urban environment would lead to poor wind energy output, and the spacing requirement limits the number of turbines installable within the limited roof space available. As shown in the Sunshine 100 case, even on high buildings, roof-mounted wind turbines cannot generate as much renewable electricity as solar PV in Jinan.

For solar energy potential, the surface area – especially roof area – FAR, and building orientation are the determining form-related factors in our analysis.

### 4.3.2 The building surface area to volume ratio (SVR)

The relationship between the building surface area to volume ratio (SVR) and its energy potential is shown in Figure 4.10. Zhangjia Village has the highest SVR, but not as much energy potential as Dongchang. This is mainly because the double-sloped roofs<sup>27</sup> in Zhangjia Village reduce its solar energy potential. The Old Commercial District shows higher renewable energy potential than Sunshine 100 though it has a similar SVR, mainly due to its higher roof coverage. This reason is in line with the finding in the last chapter regarding the impact of SVR and roof area ratio on the energy potential of 100 neighborhood models.

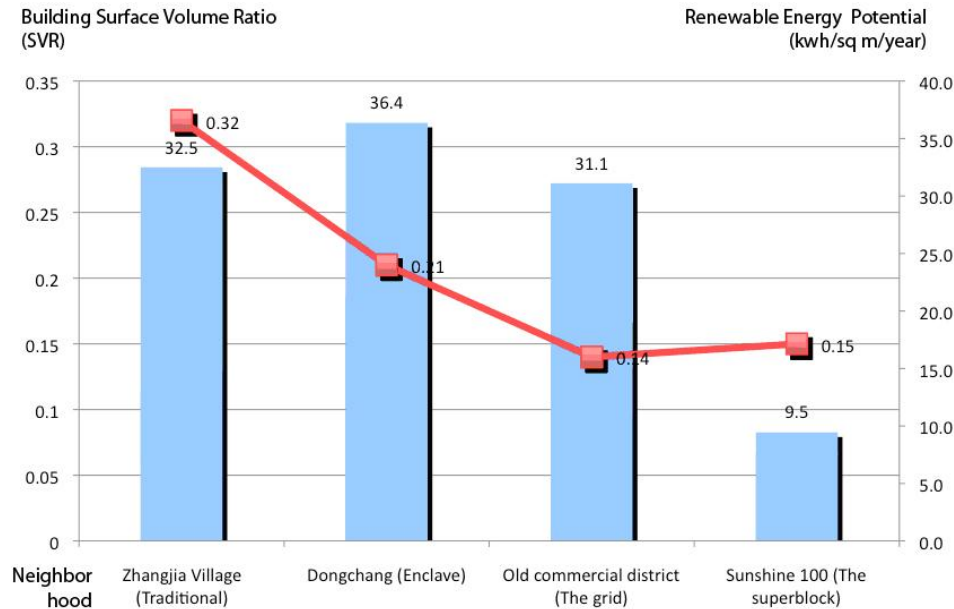


Figure 4.10 The relationship between building surface volume ratio and renewable energy potential

### 4.3.3 Floor area ratio

Floor area ratio (FAR) is an important urban form indicator in design and

<sup>27</sup> The double-sloped roof can efficiently capture solar energy only on its sunward side. The flat roof provides the possibility of installing highly efficient tracking PV systems (in our simulation, we assume tracking PV panels are installed on all flat roofs) with much higher energy yield by area.

development. It is the ratio of the built/constructed area over the site area. As shown in the Figure 4.11, there is not a positive correlation between FAR and the renewable energy potential (REP). Sunshine 100 has the highest FAR, but lowest REP. In addition, as we mentioned, Zhangjia Village – the neighborhood with the lowest FAR – would have the highest REP at over 60 KWh/sq m/year if its roofs were flat. This implies that there could be a negative correlation between FAR and REP.

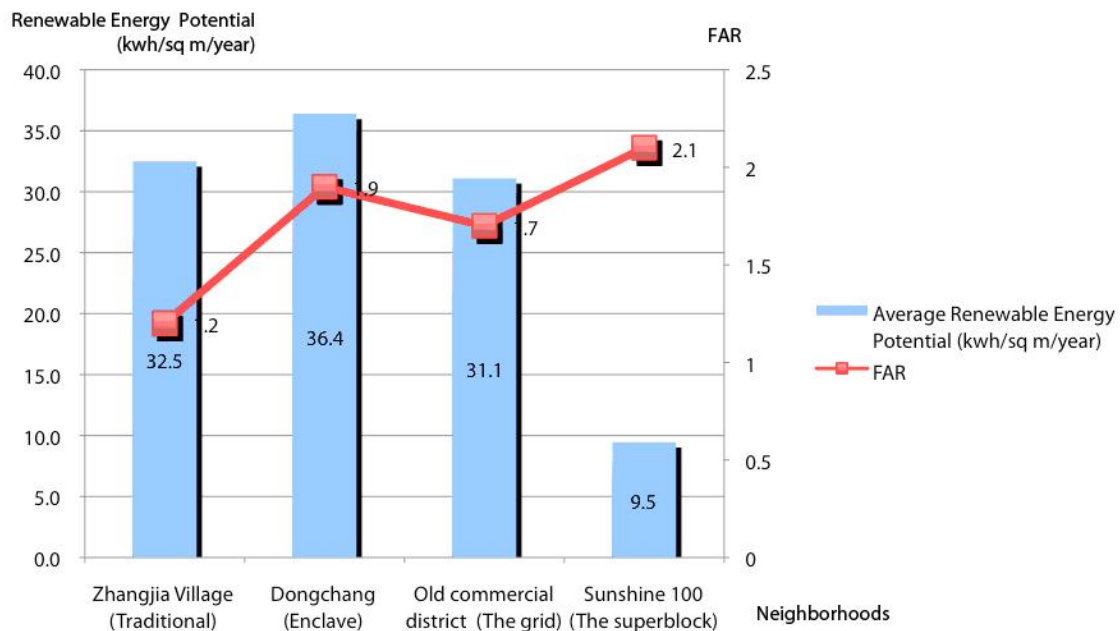


Figure 4.11 The relationship between FAR and renewable energy potential

### 4.3.4 Roof area

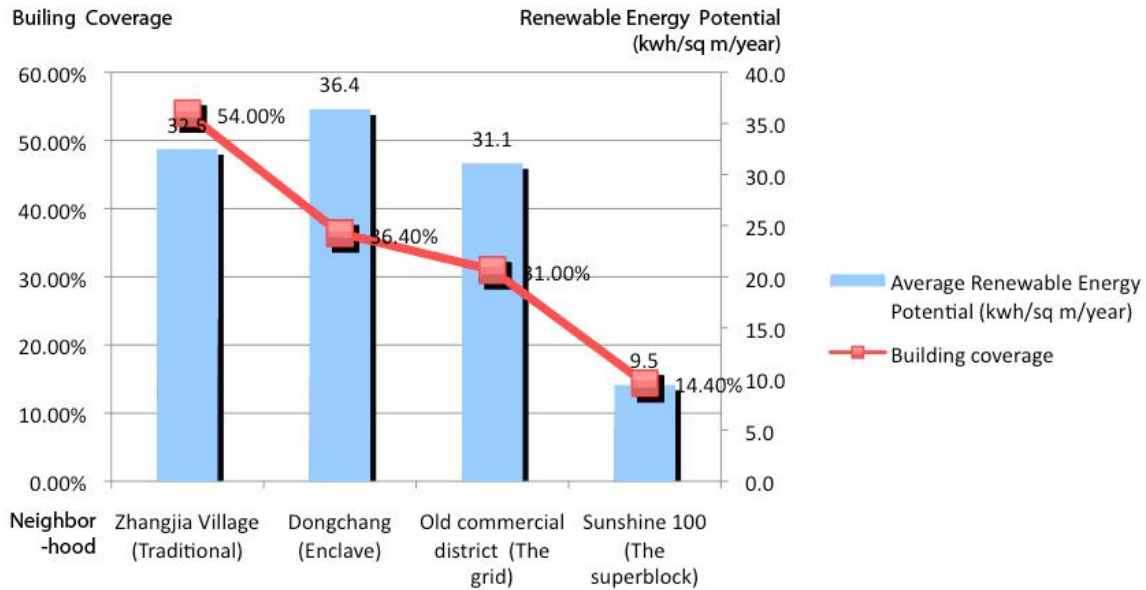


Figure 4.12 The relationship between building coverage and renewable energy potential

As shown in Figure 4.12 there is a very significant positive correlation between building coverage and renewable energy potential in the Dongchang, Old Commercial District and Sunshine 100 neighborhoods. The only outlier here is Zhangjia Village due to the roof shapes there. Since building coverage is the ratio of built area to site area, which is almost equal to the roof coverage, the importance of roof area can be seen.

To sum up, for cities like Jinan, solar would be the major source for renewable energy potential. Neighborhoods with lower FAR and higher roof coverage are likely to have higher renewable energy potential. The form of the roof would have a substantial impact as well. In real developments, the challenge is in how to incorporate these considerations into the design without undermining other neighborhood amenities. Further discussions on design principles and appropriate neighborhood prototypes will be presented in the next chapter.

Note that our conclusions only apply to cities with climate conditions similar to Jinan's, which is less windy but receives strong solar irradiation. The relative composition of solar and wind energy in the overall renewable energy potential would change by location. But the higher potential of solar PV within these types of urban form would remain.

## **Chapter 5: The urban design implications for renewable energy integration**

This chapter interprets the determinants I found in chapter 3 and 4 into design principles for renewable energy integration. The discussion concentrates on the form implications of solar energy – particularly surface area and roof design – due to its primary significance in determining urban renewable energy potential. Discussion of the form implications for wind energy follows. Combined design for both solar and wind energy will also be discussed at the end of the chapter.

### **5.1 Surface area and its physical form implication**

As demonstrated in the last chapter, surface area, especially roof area, is a very important factor in shaping the renewable solar potential of a neighborhood. To draw more intuitive and instructive implications for urban design from the abstract correlation, I further analyze the surface-form relationship at a given FAR.

In many cases, designers must work with an FAR that is pre-determined by other programmatic or policy considerations in a project. Because FAR may impact the solar energy potential per built area as well, keeping it constant will enable the study of more specific surface-form relationships. The key question I want to answer in the discussion of surface is how to create more solar potential through the surface-form design at a given building density, while ensuring the livability and quality of the urban spaces.

#### **5.1.1 Low FAR neighborhoods offer a greater potential for change**

To get an idea of the impact of FAR, I examined its relationship with renewable

energy potential based on the simulation results for 100 building cluster model presented in Chapter 3<sup>28</sup>.

As shown in Figure 5.1, the larger the FAR, the smaller the potential energy supply per built area that PV integration could provide. It is easy to explain this correlation, as there is always a maximum amount of solar energy available at a given plot. Due to the limited area of the given site for placing solar PV relative to the larger size of the development, for projects with high renewable energy production requirements, a high-FAR development strategy might not work.

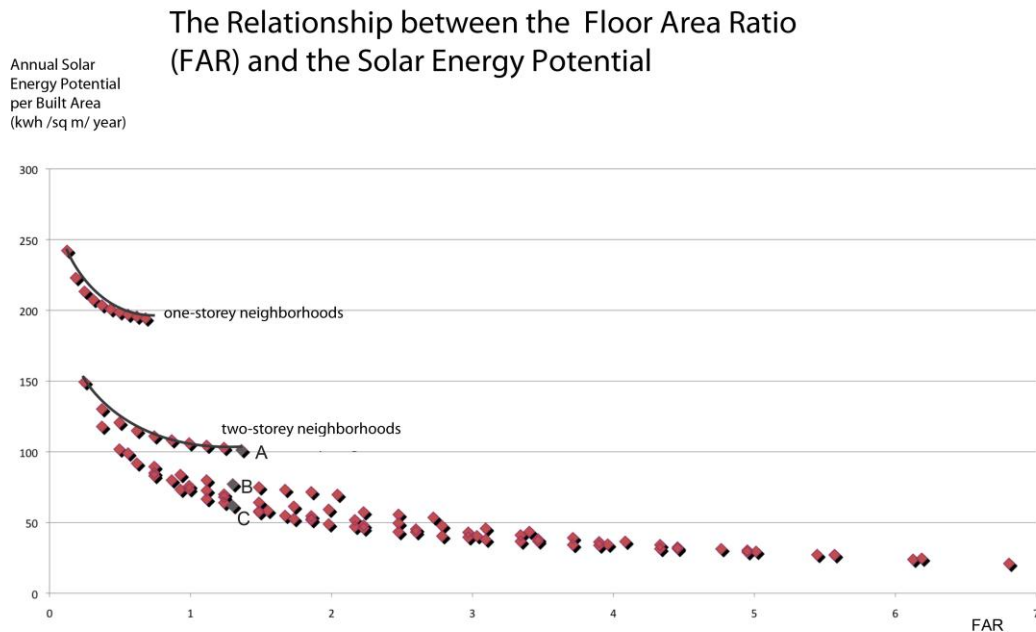


Figure 5.1 The relationship between FAR and solar energy potential for the 100 models  
Note: A, B, and C indicate the three building clusters discussed in Table 5.1

However, among developments with the same FAR, there is some variation in the renewable energy potential. And, the range of variation decreases as the FAR increases. As we can see from Figure 5.1, building clusters with the same FARs of 1.3<sup>29</sup> could have energy potentials ranging from 55 to 100 KWh/sq meter/year,

<sup>28</sup> Note that at the same size, the building volume is correlated to the building volume per site area; in the 100 models simulated, it is proportional to the floor area ratio (FAR).

<sup>29</sup> In Figure 5.1, A, B and C are of the same FAR of 1.3, however, the annual solar energy potential can range from over 100 kwh/sq m/year in A Cluster to 55 kwh/sq m/year in C Cluster.

whereas the energy potentials of neighborhoods with the FAR of 3 span a much smaller range, between only 40 and 50 KWh/sq meter/year.

For urban residential development, the FAR usually falls between 1 and 2. As we can see from Figure 5.1, within that range of FAR, urban form, and more specifically building shape and prototypes can have a significant impact in increasing the renewable energy potential.

#### **5.1.2 Low-rise and large roof area**

Further study on the form of specific building clusters shows that, at a given FAR, low-rise neighborhoods with high roof coverage yield higher solar energy potential.

- **Low rise**

There are two curves in a higher position on Figure 5.1, indicating better renewable energy performance among the 100 models. The highest and second highest curves are the one-story and two-story neighborhoods, respectively. This implies that, at the same FAR, low-rise clusters would have higher solar energy potential. The reason for this lies in their surface area composition; as neighborhoods with the same FAR would also have the same overall building volume, low-rise flatter neighborhoods would usually have a larger roof surface area, enabling greater solar energy generation than the vertical surfaces of high-rise neighborhoods.

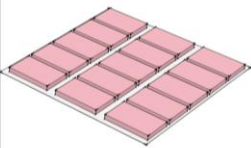
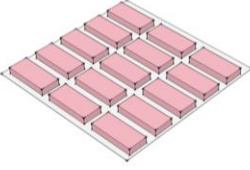
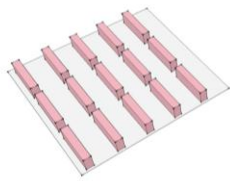
- **Larger roof area**

Figure 5.1 also highlights the energy potential of three building clusters - A, B and C - that share the same FAR; their form characteristics are shown in Table 5.1. Model A is the most PV-friendly form, achieving the highest solar energy potential. This neighborhood does not have the highest surface area to volume ratio, but its average height is the lowest and the ratio of roof area to total surface area is the



highest; whereas model C has the largest surface area to volume ratio, but its roof area is a smaller proportion of total surface area, resulting in the lowest solar energy potential.

Table 5.1 The renewable energy potential comparison among Model A, B and C

Building Cluster Type	A	B	C
Building Form			
The Solar Energy Potential (kwh/sq m/year)	101.2	74.9	64.1
The Building Surface Volume Ratio	0.399	0.347	0.434
Roof Area over the surface area ratio	71.6%	47.1%	12.3%
Average Building height (meter)	6	9	21

Note that the total surface area of a neighborhood could still influence its renewable solar potential, but the important point is that the composition of the surface area, and especially the roof area to total surface area ratio, is significant.

### 5.1.3 Urban form implications: the low-rise perimeter prototypes

In cities, neighborhood forms like Model A are rarely found, except for in some industrial developments. Such big, flat boxes would often lead to poor ventilation and the uneven access to sunlight in buildings. Still, the implications of the findings about height and surface area composition could be instructive. Since these form characteristics including height, FAR and roof coverage are embedded in development prototypes, the implications are meaningful for selecting renewable energy-friendly prototypes based on their general form characteristics.

The “Making the Clean Energy City” in China research team also scanned sustainable urban development projects around the world and identified six sustainable neighborhood form prototypes (Frenchman, D., J. Wampler, et al. 2011). These six sustainable urban form prototypes are categorized based on the building forms, arrangements of buildings and open space, and circulation systems. Among those prototypes, the slab and the small perimeter block are the two most popular low/mid-rise prototypes. A slab neighborhood was described in the last chapter. The perimeter block is defined as a rectangular block with linear buildings sitting along its edges and enclosing a yard in the center (Figure 5.2). Drawing from the earlier findings, at the same FAR the perimeter block should have a higher renewable potential than the slab neighborhood since it has a higher roof area to total surface area ratio.

To better compare these two different prototypes, I simulate the solar energy potentials of a benchmark slab neighborhood model (the benchmark model based on Dongchang neighborhood in Jinan) and a perimeter block neighborhood model (Figure 5.2) with similar FARs, both facing due south. The perimeter block is derived from a typical Barcelona block; the block size is 113 meters by 113 meters, with a building depth of 25 meters and a height of 11 meters. The width of the street, which is also the distance between the two closest buildings, is 20 meters. Table 5.2 lists the results, with the perimeter block showing higher solar energy yield. It suggests that it may therefore be a direction for creating more energy productive and livable housing forms.

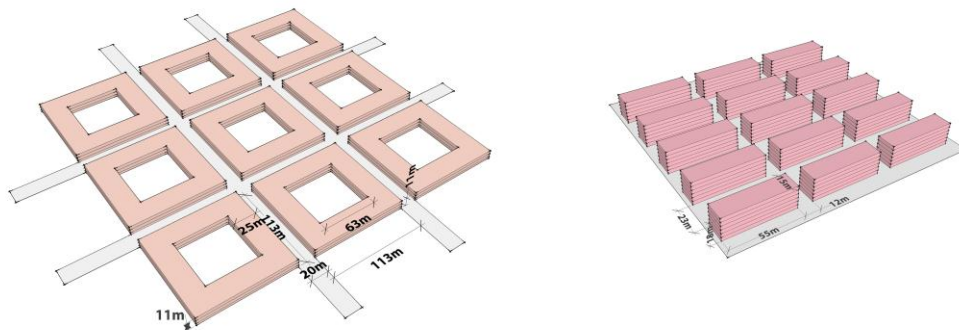


Figure 5.2 The perimeter block model and slab models

Table 5.2 A form-energy comparison between the perimeter block and slab prototypes

Neighborhood Prototype	Form-related Factors				Energy
	Average Height ( meter)	Surface Volume Ratio	FAR	Roof Area ratio over the total surface area	Solar energy potential (KWh/square meter/year)
Slab	11	0.2253	1.86	24.7%	53.01
Perimeter Block	18	0.1433	1.79	63.4%	59.22

#### 5.1.4 Summary

FAR places constraints on the renewable energy potential of neighborhoods. For urban residential developments with FARs ranging from 1 to 2, the design of the urban form in terms of surface area could significantly change the renewable energy potential. Relatively low-rise, high roof area, or high building coverage forms would be more solar friendly. Those building forms are usually very flat and close to the earth to harvest the maximum solar energy via rooftop solar PV systems.

The trend in urban development in developing countries like China suggests that FARs could be even higher. In high-density developments the same principles of maximizing roof coverage can be applied to ensure relatively high solar energy potential. As shown earlier, designers could adopt the perimeter blocks like Barcelona at the height of 6-7 stories – more dense than current Chinese towers in such projects - but possibly resulting in greater renewable energy potential with its larger roof area.

Designers could also intersperse uniform, relatively low-rise development with small-footprint high rises at intervals to achieve both high density and maximal solar potential, or even combine towers and courtyards into the same building. I will further discuss this “low-high rise” in a later section.

## **5.2 Roof Design**

Roof design at a building or sometimes building cluster influences the solar energy potential greatly. Designing roof tilts carefully and innovatively, and creating roof-like surfaces are two useful renewable energy design strategies.

### **5.2.1 Designing roof tilts**

The simulation of Zhangjia Village's renewable energy potential in Chapter 4 reveals the potentially significant impact of roof shape. In real world developments, fixed PV panels on sloped roofs are more often adopted due to economic and aesthetic concerns.

With sloped roofs, the slope and orientation of the roof is probably the most essential consideration. Traditional double-sloped roofs usually have one shady side with poor access to solar energy, as in Zhangjia Village. In new developments, in order to gain the benefits of sloped roofs and also maximize the attainable solar energy, designers could apply either one-sloped roofs or asymmetrical double-sloped roofs.

On a one-sloped roof, the entire roof area tilts at the optimum angle towards the sun, utilizing the entire roof area to collect solar radiation. Asymmetrical double sloping roofs with the sunward-facing slope having a larger area would also collect more sunlight than symmetrical double-slope roofs. As shown in Figure 5.3, the sustainable neighborhood “Vauban” in Freiburg, famous for its PV integration, adopted both strategies to increase the PV potential.



Figure 5.3 Photos of PV roofs in Vauban

Source: <http://www.frsw.de/fotos09sep/vauban-solar1-090923.jpg> (top)

<http://www.greenchannel.tv/addons/albums/images/5443684.jpg> (bottom left)

[http://www.naturconcept-eco.de/angebote/guided\\_tour\\_vauban.php](http://www.naturconcept-eco.de/angebote/guided_tour_vauban.php) (bottom right)

Similar principles can be applied to the design of shading on building facades.

Figure 5.4 shows the energy-efficient office building ENERGY-base, in which the inclination of the window shading structure is set according to the local latitude to optimize solar energy generation (Waldhör, 2010/03).



Figure 5.4 The PV shading façade in the ENERGYbase building  
Source: Waldhör, 2010/03

### 5.2.2 Create and utilize more roof-like area

In roof design, it is also possible to increase the roof-like area, and thus renewable energy potential, through projection design strategies. One effective approach is incorporating outdoor or extended shading structures that can create roof-like area for PV panels.

Canopies and outstretched eaves can be used to create pleasant semi-closed spaces, while also advancing solar PV integration. Figure 5.5 shows how to extend eaves as shading structures mounted with PV to increase renewable energy potential. Figure 5.6 is a PV panel canopy covering several buildings in Masdar. There, the PV panels will be mounted on a canopy structure, providing shade for the building's roof terrace and their open space while at the same time generating solar power for the facility (Whitmore 2010). For the small perimeter blocks discussed earlier, it would also be possible to add transparent PV ceiling/shading structures in the courtyard spaces to further increase solar energy potential.





Figure 5.5 Extended PV eaves on Tsinghua University's environment and energy-efficiency building. Source: [http://catalog.iguzzini.com/projectdetails.aspx?project=PRJIG\\_338](http://catalog.iguzzini.com/projectdetails.aspx?project=PRJIG_338)



Figure 5.6 The PV canopy in Masdar  
Source: <http://cdn.lbecoist.com/wp-content/uploads/2010/04/masdar-sustainable-city.jpg>

### 5.3 Shading concerns

The orientation, spacing and height of buildings all impact the shading of solar PV on roofs or vertical facades. While shading of a roof significantly decreases its solar energy potential, sunlight access on vertical facades might be more significant due to livability concerns than for solar energy potential.

### 5.3.1 Orientation

As discussed in Chapter 3, neighborhood orientation can have a substantial impact on renewable energy potential by changing the effective solar duration.

To evaluate the significance of orientation in “perimeter block” and “slab” neighborhoods, I estimated the solar energy potential of these two neighborhoods over a year (KWh/square meter/year) at two different orientations, with the prototypes’ long-edge facades facing due south and southeast, respectively<sup>30</sup>. The results are shown in Table 5.3 below. The square perimeter block oriented due south shows a similar energy potential to its counterpart facing southwest, whereas there is a substantial drop in solar energy potential when the slab neighborhood prototype is oriented southwest.

That result could be due to the fact that over 90% of the solar energy potential of the perimeter block is from the roof, so the orientation is not as crucial. It might also be due to its square perimeter forms – there is no long edge in an individual building or building cluster so its orientation will not greatly affect the energy potential from the surface. However, for slab neighborhoods the orientation plays quite an important role in the energy potential from the vertical facades. As shown in Table 5.3, the energy potential from the façade decreases when the neighborhood faces southwest. A more detailed result of this study is attached in Appendix III.

---

<sup>30</sup> When orientated to the south, the energy potential calculation only takes the roofs and vertical southern facades into account. When the orientation is to the southwest, the energy potential from the roof as well as both the southwestern and southeastern facades would be taken into account.



Table 5.3 The solar energy potential of four geometric prototypes of the neighborhoods

Geometric type	The percentage of energy potential from façade-integrated PV	The percentage of energy potential from the roof-mounted PV	Solar energy potential per construction area (KWh/square meter/year)
Slabs – orienting due south	37.05%	62.95%	53.01
Slab – orientating southwest	33.62%	66.38%	50.28
The Perimeter Block – orientating due south	6.07%	93.93%	59.22
The Perimeter Block Orientating southwest	8.34%	91.66%	60.68

The finding regarding neighborhood orientation could also be instructive in renewable energy integration. For the slab neighborhood, to get more solar radiation, buildings should be carefully laid out to orient their long edges due south. On the other hand, the flexibility in its orientation allows the perimeter block to rotate or transform its layout more freely, and incorporate other design considerations such as the prevailing wind direction. The diverse layout of the block units could encourage the creation of more interesting urban public spaces and contribute to the people's quality of life. The pleasantness of semi-private space within blocks would add great value to a development.

### 5.3.2 Building height planning and shading

Building height planning could mitigate the negative impacts of shading. While laying out the buildings, arranging buildings with the same height together in clusters could ensure good access to sunlight on all the roofs. Otherwise, placing tall buildings on the shady part of a site could also be a useful design principle.

### 5.3.3 Spacing

Spacing between close buildings could affect shading as well, as shown in Chapter 3, in terms of the effective solar duration on vertical façades. However, its impact on the total solar energy potential is not that significant for several

reasons. One reason is that the larger the spacing between buildings, the less area will be built, and thus, the less roof area will be available for PV. In addition, the energy potential from vertical facades is usually less than that from roofs', mainly due to the lower intensity of solar radiation.

Nevertheless, spacing has a great impact on urban quality of life. It affects vertical windows' access to sunlight greatly, and solar access within units is important to the health of residents. Spacing is also related to the availability of outdoor space, the space within the urban fabric used by the public either for greening – connecting people with nature – or as a place for activities connecting people to other people. So spacing is of great importance to quality of people's life.

#### **5.4 Wind energy in the city – integrating with open space**

Wind energy shows limited potential in urban areas according to our simulation in Jinan. For cities with similar climate conditions to use the wind energy, it would be better to place the wind turbines in open spaces, rather than in the city center. Note the important caveat that wind potential is city-design and location specific. For examples, cities with many rather large open spaces, akin to Swiss cheese, might have higher wind energy potential than uniform, densely-packed urban fabrics.

The minimum wind speed requirement makes it difficult to incorporate wind energy into many places in cities. Due to safety concerns and the need for higher wind speeds, urban wind turbines are usually located on top of buildings. Rough urban terrain reduces wind speeds, so wind turbines mounted in lower positions would not see high enough wind speeds. This is the reason why roof-mounted wind turbines could not work in Zhangjia Village in our simulation. Note, there are cases where micro turbines have been installed on low-rise buildings, but their energy output is quite small.

But even in high-rise neighborhoods with turbines installed to catch higher-speed winds, the potential energy contribution from those roof-mounted wind turbines is still restricted. Turbulence would lower the efficiency of turbines' performance, lowering wind energy output. Spacing requirements between turbines would also prevent the full use of available roof space. As simulated in Jinan, installing solar PV on a roof would yield more energy than installing wind turbines.

An effective way to increase wind energy gain would be to place wind turbines on the windward edge of the city and adjacent to open space. This would produce energy more efficiently and with a greater capacity by catching higher-speed winds at the periphery before they slow down over the rough urban surface. The windmills could stand alone and be of a size and capacity not possible for wind turbines mounted on buildings. These windmills could be arranged in a line perpendicular to the prevailing wind direction at the city edge. Other locations could be on ridges, or along riverfronts or other shorelines where there is access to prevailing winds. For example, in Lackawanna, New York, eight new windmills have been built on the shoreline. There, they not only supply clean wind energy, but also change the image of the community.



Figure 5.7 Urban windmills in Lackawanna, New York

Note that, there are controversies on locating urban wind turbines in open spaces in local communities centered on the concern of visual pleasure. The scale of the turbines in relation to the scale of other city features – this may also determine

whether they are considered beautiful/acceptable or not. The selection of these “public” turbines should take this into consideration.

## **5.5 Combining solar and wind energy in urban development**

Combining wind and solar energy within developments would diversify energy sources. Even though wind does not show much potential at the moment, future technology development could enable more productive micro wind turbine generation. A combined strategy is an essential part of the design palette in utilizing and diversifying renewable energy sources in cities. It could be achieved through planning and also through building design strategies.

Spatial planning of renewable energy could locate different types of renewable energy production in optimal locations with the urban area, diversifying and maximizing the renewable energy potential. As discussed above, wind energy would be best sited adjacent to open space rather than in the built area of cities, while PV panels would yield higher and more reliable energy potential in an urban center, especially in low-rise courtyard neighborhoods.

In terms of urban design, a new urban form prototype – the “low-high rise” could provide the possibility of integrating both solar and wind energy. The “high-low rise block” combines the low-rise courtyard block with towers, creating a dense, hybrid urban form. The large roof area of the low-rise courtyard could accommodate PV integration, and the wind could be integrated into its high-rise tower. This block could be placed at the windy urban edge, with towers lining up at designated locations to capture the wind energy. Figure 5.8 shows an example of the low-high rise block, which is a new sustainable prototype proposed in the “Making the Clean Energy City” in China project. This proposed prototype is an integrated and comprehensive sustainable development example, rather than a simplified physical building structure suitable only for renewable energy generation. As we can see in Figure 5.8, the hybrid form allows a combination of

different uses and functions within one block, and it also incorporates an innovative connective wind ventilation system for heating and cooling. The fine-grained design of roofs, façades, building junctions and courtyards also create a variety of interesting public or semi-private spaces for users.

Further design steps could be taken, changing the generic form of this prototype to increase its renewable energy potential. For example, the edges of the tops of the towers could be rounded to speed up the wind for roof mounted wind turbines. Combining all of these individual elements could have a rather powerful influence on the urban form and design of cities.

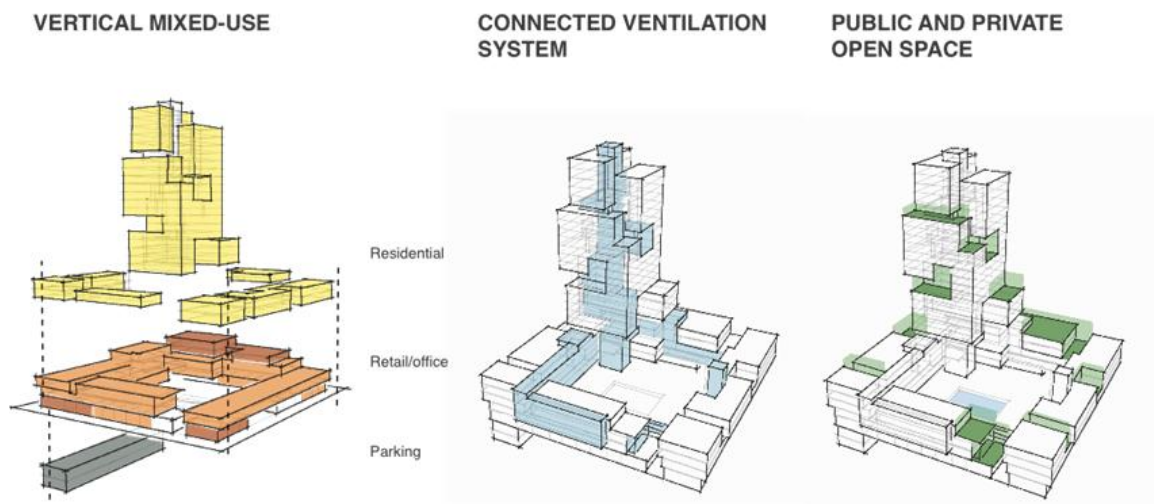


Figure 5.8 The high-low rise Prototype

Source: The final work of the “Making the Clean Energy City” in China China” MIT-Tsinghua Joint Urban Design Studio

## 5.6 Summary

To summarize, creating and positioning the right places for locating renewable energy facilities is the foremost concern for both solar and wind energy integration. A renewable-friendly form creates more area for the installation of renewable energy facilities, and thus the capture of more energy from nature. The neighborhood design principles for sun and wind energy potential include:

- ◆ Relatively low-rise and high roof-coverage neighborhood forms have a higher solar energy potential. From this perspective, the low-rise perimeter block form seems ideal.
- ◆ Roof tilt can maximize solar exposure, as can extensions of horizontal roof-like surfaces. It is best to design neighborhoods with predominantly flat roofs, or with carefully crafted roof angles and extensions (into the public realm, for example) to maximize renewable energy potential.
- ◆ Different form typologies are more and less sensitive to orientation. Perimeter block types with interior courtyards can be oriented in several directions without much loss of solar potential, whereas slab neighborhoods must be oriented south or their potential drops significantly. Spacing does not show much significance for solar energy potential, but it is important for quality of life.
- Context affects wind potential greatly. It is best to place wind turbines at the edges of open spaces, where turbulence is lower and wind speeds higher than among built structures.
- From the city planning perspective, designers should locate renewable sources at optimal locations based on their energy producing features mentioned above.
- It is possible to incorporate solar and wind energy within the same development, providing basically uniform low-rise development with high roof coverage for solar potential, punctuated by high-rise buildings at significant intervals to minimize turbulence and maximize wind potential. This “high-low rise” block accommodating both strategies could serve as an innovative urban form in the future.

## Chapter 6: Conclusion

### 6.1 The role of the renewable energy integration

Currently, renewable energy integration is only a small section of the much larger framework of sustainable development. In the sustainable neighborhood rating system LEED-ND,<sup>31</sup> for example, “on-site renewable energy sources” are only a credit option earning 3 points out of a total of 106.5 possible points. These sources are given a similarly insignificant weighting in the BREEAM<sup>32</sup> sustainable neighborhood rating system. Even within zero energy building criterion, on-site energy supply is regarded as less crucial than energy efficiency strategies (P. Torcellini 2006)

In fact, renewable energy integration could make a significant contribution to the sustainability of development. According to our simulations for four neighborhoods in Jinan, the renewable energy potential could satisfy a significant portion – 14% on average – of total energy use.

What is more, given that zero energy building and neighborhood design is the trend for new development; renewable energy integration will be an indispensable component in the future. The Energy Committee in European Union has already announced that all buildings built after 2019 in Europe should produce their own energy on-site. Therefore, an understanding of the relationship between form and renewable energy potential could help designers incorporate

---

<sup>31</sup> LEED-ND is short for Leadership in Energy & Environmental Design for neighborhood development, which is an internationally recognized green building certification system, providing third-party verification for sustainable neighborhood development.

<sup>32</sup> BREEAM stands for the Building Research Establishment Environmental Assessment Method and rating system of buildings. It is a program of the Building Research Establishment (BRE), an organization based in the UK.

both renewable energy and energy efficiency strategies appropriately into the design of cities, meeting the energy demand with the on-site renewable supplies.

Another underlying benefit of the renewable energy integration is the impetus it provides for creating forms that are more responsive to nature. In order to achieve higher renewable energy yield, designers could adjust, or even transform the form to optimize solar and wind conditions. The emphasis on the natural context of could be invaluable for planners and architects in creating a more functional and enjoyable living places.

## **6.2 The relationship between urban form and renewable energy potential**

The design of cities affects the potential for utilizing renewal energy sources. Different neighborhood forms produce different renewable energy potentials. Comprehensive design approaches could be adopted to increase the renewable energy potential of the development. The key findings of this thesis are summarized below.

### **6.2.1 Regarding renewable energy technologies**

Solar PV and urban micro wind turbines are vastly different technologies due to the characteristics of the energy sources they utilize. Climate conditions, as the foremost constraint, should be examined before the selection of technologies.

Solar PV is a material-based technology. In most situations, it is more flexible in how it is applied in the built area. Its flexibility and efficiency are likely to keep improving in the future, with its application in urban development becoming even more popular.

Micro wind turbines take a variety of complicated mechanical forms in response to different urban wind conditions. As an emerging technology, urban wind turbines still need to confront many constraints such as minimum wind speeds.



The low efficiency of their performance in cities often causes them to be more costly and carbon intense than solar PV. However, technological advancement may enable micro wind turbines to capture flowing wind energy in more innovative, responsive and efficient ways, greatly increasing its potential in the future.

### **6.2.2 The Relationship between form-related determinants and renewable energy potential**

I found out that the relationship between urban form and renewable energy potential is quite significant. The vast differences in renewable energy potential across four existing Jinan neighborhoods demonstrate the importance of urban form.

In terms of solar energy, urban development characterized by lower building heights and higher roof coverage offers higher potential. Such forms also provide opportunities to leverage this potential through the design of the development, by creating human-scaled public spaces and active streetscapes. For developments with similar FAR, roof area plays a key role in maximizing solar energy potential. Appropriate orientation of the surface area can have a great positive impact, too.

Height helps wind turbines to capture more wind energy, since wind speed often increases with height. Building shapes can accelerate wind speed, as well; for example, curving roof shapes and duct designs can funnel the wind. But due to the dampening effects on wind speed and the turbulence produced by rough urban terrain, the wind energy potential in built areas as they are currently designed is quite restricted. On the contrary, open spaces with smooth terrain are more suitable for incorporating micro wind turbines, especially when they face the prevailing wind.

### 6.2.3 Urban design implications for renewable integration

Understanding the relationship between the renewable energy potential and urban form characteristics, I summarize the design suggestions as follows:

- ◆ Incorporate renewable energy planning at the city planning level. Install appropriate renewable energy sources in appropriate locations. For instance, save open spaces for urban wind turbines and place solar PV panels within low-rise perimeter block neighborhoods, to maximize the aggregated renewable energy potential at the city level.
- ◆ Solar energy is the major component of the total renewable energy potential across all neighborhood types in cities with climate conditions similar to Jinan's. Adopting solar energy in built areas would generate more significant renewable energy than wind turbines, so it would be wise to make solar energy the focus of renewable energy design in cities.
- ◆ Apply flat-roofed, low-rise buildings with large roof areas for solar PV integration. The low-rise perimeter block, carrying all the above-mentioned features, could be a successful and increasingly popular renewable and sustainable development prototype here. Minimally constrained by the orientation buildings for the consideration of renewable energy potential, it could also facilitate the creation of more interesting and livable open space and circulation systems within the urban environment.
- ◆ Optimizing the slope and orientation of roof surfaces or shading structures plays an important role in solar potential. Balancing aesthetic concerns with PV energy potential is the key. One strategy to meet both objectives is to include single-sloped roofs or unsymmetrical roofs with longer slopes facing the sun.

- ◆ With a given building form, creating more horizontal surface area for installing PV panels, through roof-like structures such as canopies or building projections is another design strategy to augment solar energy potential.
- ◆ Arranging wind turbines at the edges of windy urban open spaces could be a useful principle for urban wind energy design. Such places include, for example, waterfronts, the edges of parks, natural wind corridors like canyons or ridgelines, and the windward urban edge facing the prevailing winds. Such open space arrangements also enable the incorporation of the stand-alone wind turbines, of larger size than roof-mounted turbines.
- ◆ High-rise towers can also be placed within a predominantly lower-height urban fabric to achieve FAR's appropriate to land-scarce developing countries like China. These high-rise point towers have a rather small footprint, and if carefully placed to take into account shadow effects, their incorporation into a predominantly low-rise fabric should have minimal effect on overall solar energy performance. Incorporating point towers also creates possibilities for incorporating wind energy.
- ◆ In terms of combined solar and wind design, the hybrid high-low rise building block might be an innovative and promising development prototype for the future. This form could accommodate solar integration via its low-rise courtyard podium, and the possibility of incorporating wind turbines on carefully located high-rise towers. Suitable for application in various climate conditions, this prototype could help in increasing the renewable energy potential and diversifying the energy supply of the development, while providing a fully viable and livable urban design form.

### **6.3 The contribution to the “Making the Clean Energy City” in China project**

Built on existing research within the “Making the Clean Energy City” in China project, this thesis offers a new perspective on examining the impact of urban form on renewable energy potential through quantitative analysis. It tests and

applies the simulation methodology for solar and wind energy potential, and it also abstracts the design implications for future development as listed above. However, its greatest contribution lies in its improvement of the energy evaluation tool – the Energy Pro-forma.

### **6.3.1 A climate, form and technology integrated metric**

In the Energy Pro-forma, a metric comprised of climate, form and technology is developed for use in solar and wind energy potential simulation. Formulas A, B and C in Chapter 3 are applied, and the relevant variables in the formulas are estimated through respective functions based on the given inputs of the pro-forma<sup>33</sup>. All of these functions and formulas are integrated into a spreadsheet that can simulate the renewable energy potential of a new urban development with inputs. The inputs can be categorized as below:

- **Climate and location**

The climate and location inputs include latitude, local mean wind speed and average annual solar duration, and other variables. In this pro-forma, which is Jinan-specific, climate and location inputs are constant across all the neighborhood types.

- **Urban form**

Most of the urban-form related inputs are consistent with the existing urban form inputs in previous energy pro-forma. However, the renewable section does bring some new form-related variables, such as roof type and inclination, and also buildings' north-south distance. These inputs specify the urban form further and can help designers to pay more attention to the form-energy relationship in design, especially the way that buildings respond to nature.

---

<sup>33</sup> the correlations of the inputs and variables are discussed in chapter 3 and their related functions are listed in appendix II.

- **Technology efficiency**

Distinct from the simulation analysis in this thesis using the optimistic estimates of technology efficiency, the pro-forma simulation provides three levels of energy efficiency for each technology due to concern about accuracy. For example, the efficiency of wind has three categories of 6%, 4.5% and 3%. Designers could choose to use the lower efficiency estimate if wind conditions on a site were not ideal enough.

This metric will guide designers from urban form and renewable energy technologies to the relevant energy variables, and then to the renewable energy potential of a new development. It will also provide a clearer understanding of how the interaction of location, urban form and technologies can influence the renewable energy potential of a development. A detailed metric explaining how these inputs relate to the variables and the final simulation results is available in Appendix IV.

### **6.3.2 Complete the framework of the Energy Pro-forma**

Incorporating this methodology for simulating solar and wind energy potential will advance the Energy Pro-forma in the “Making the Clean Energy City” in China project. Previously, the Energy Pro-forma could only show relationships between form and energy demand. The addition of the renewable energy source module gives credit to urban form’s contribution to sustainability from the energy supply perspective. Addressing both energy demand and supply potential could yield more comprehensive sustainable development proposals. Since the Energy Pro-forma directly illustrates their relationship, it is instructive for designers as they balance the two strategies.

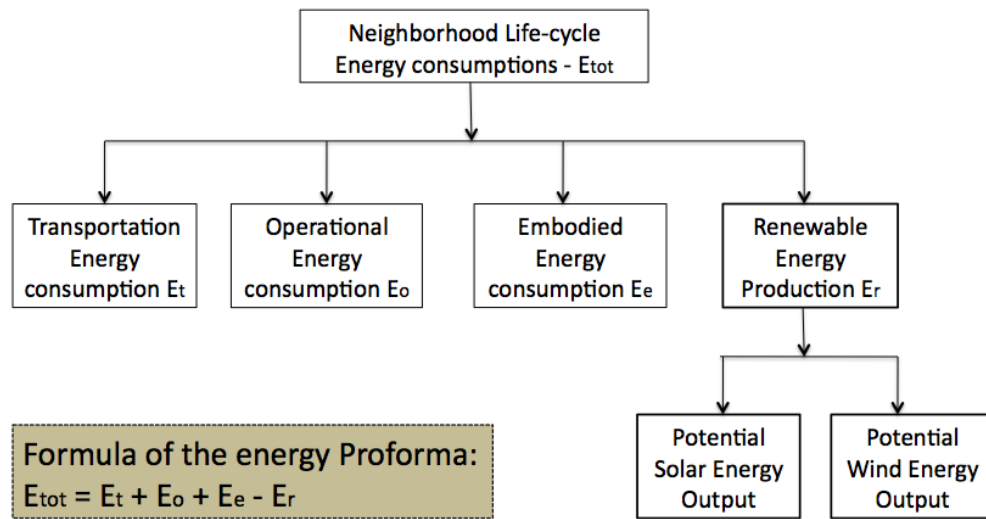


Figure 6.1 The structure of the new Energy Pro-forma

## 6.4 Directions for future work

The limitations of the thesis include its very specific scope and the very simplified assumptions used in its simulation analysis; all the finding and conclusions are based on this scope and these assumptions. Future directions for further study could extend this scope. Researchers could also focus on more on trade-offs between the renewable integration and other design considerations and a fuller discussion of livability issues.

### 6.4.1 Extend the scope

This thesis only explores renewable energy generated from solar PV and wind turbines, both producing electricity. It does not discuss the renewable sources from the earth and water, such as the geothermal energy and mini hydro power plants, both of which could also be used at the urban development scale. Even under the solar energy category, other systems, such as solar thermal, which would provide an energy supply in the form of heat, are not included either. Solar hot water systems use different working principles from PV and could yield a

different renewable potential even from the same neighborhood form. However, an elaboration of the differences between the two could be helpful to designers in technology selection.

In order to distill the key urban form factors, simulations in this thesis have been carried out assuming extremely simplified urban forms, such as the 100 models in Appendix II. Dedicated design at the building level such as shading structures for solar integration, and streamlined forms to augment wind energy could make a difference as well, but understanding their impact on overall renewable energy potential would require further study.

This analysis also relies on highly optimistic assumptions regarding solar PV. I assume that all the flat roofs will be installed with tracking PV panel systems, and that the efficiency of the PV systems is as high as 17%. The solar energy potential could be lower in reality if the assumptions are not accurate.

#### **6.4.2 Trade-offs**

There many discussions that could be done regarding trade-offs between the impacts of urban form on energy efficiency and renewable energy production, and balance between costs and benefits produced.

Promoting the integration of renewable energy could be contradictory to other design considerations. Taking the composition of the surface area for example, roof area is more important than vertical surface area for solar energy production potential. However, in terms of the access to the sunlight of the users, larger portion of vertical surface area would be more beneficial for users in the units of buildings. The balance could only be found through the trade-off analysis. Also, the optimal orientation of a building block for solar energy might not be the same as for building ventilation, and this needs further study as well.

In terms of cost-benefit trade-offs, although I mentioned that the cost of the technologies would be quite expensive, I did not include cost in later discussion of design strategies. With a limited budget, cost-effectiveness analysis could be crucial as well. Even among the products within these renewable energy categories, the cost–effectiveness trade-off between expensive but effective tracking panels versus cheaper fixed panels could be an issue to pay attention to.

#### **6.4.2 Livability**

Focusing on the form-and-energy relationship, this thesis did not consider deeply the impact of the renewable energy integration on the people’s behaviors and livability of a neighborhood. Issues to consider would include, for example, how to balance the visual unpleasantness (to some) of wind turbines and renewable energy development in the community, and whether the introduction of renewable energy projects could change people’s lifestyles and behavior. Sustainable urban development is a comprehensive topic encompassing both the form of buildings and people’s way of life. Further discussion of the coordination between these various dimensions would contribute to more enjoyable and popular renewable energy and development plans.



## Bibliography

- Austrian Federal Ministry of Transport (2005). WIND POWER PROJECT SITE: Identification and Land Requirements. Albany, NY, Global Energy Concepts and AWS Truewind, LLC.
- A G Dutton, J. A. H., M J Blanch (2005). The Feasibility of Building-Mounted/Integrated Wind Turbines (BUWTs): Achieving their potential for carbon emission reductions. , Energy Research Unit, CCLRC.
- Allen, S. R., G. P. Hammond, et al. (2008). "Energy analysis and environmental life cycle assessment of a micro-wind turbine." Proceedings of the Institution of Mechanical Engineers Part a-Journal of Power and Energy 222(A7): 669-684.
- "Air Quality Worsened by Paved Surfaces: Widespread Urban Development Alters Weather Patterns". Retrieved July 13rd, 2011, from <http://www.sciencedaily.com/releases/2011/06/110607121137.htm>
- Bahaj, A. S. a. M., L. and James, P. A. B. (2007). "Urban energy generation: Influence of micro-wind turbine output on electricity consumption in buildings." Energy and Buildings 39(2): 154--165.
- Butera, F. (2007). Towards the Renewable Built Environment. Urban energy transition : from fossil fuels to renewable power. P. Dorege, ELSEVIER.
- Cace, J., E. t. Horst, et al. (2007). Urban Wind Turbines: Guildlines for small wind turbines in the built environment. Wind Energy Integration in the Urban Environment. Wineur.
- Campbell, N., S. Stankovic, et al. (2001). Wind Energy for the built environment (Project WEB) Procs. European Wind Energy Conference & Exhibition. Copenhagen.
- Chirs Whitmore.( 2010). "SunPower to build 1MW Masdar Institute roof installation". Retrieved July 13rd, 2011, from [http://www.pv-tech.org/news/sunpolr\\_to\\_build\\_1mw\\_masdar\\_institute\\_roof\\_installation](http://www.pv-tech.org/news/sunpolr_to_build_1mw_masdar_institute_roof_installation)
- China Meteorological Data Sharing System. <http://cdc.cma.gov.cn/>
- Dominique Gauzin-Müller, N. F. (2002). Sustainable architecture and urbanism : concepts, technologies, examples. Basel ; Boston Birkhauser.

- EIA and U. S. E. I. Administration (2010). International Energy Outlook 2010
- European Centre for Medium-Range weather Forecasts. <http://ecmwf.int/>
- Frenchman, D., C. Zengras, et al. Making the 'Clean Energy City' in China (draft). (Cambridge: Massachusetts Institute of Technology with Tsinghua University). Research sponsored by the Energy Foundation, China. Page 84
- Frenchman, D., J. Wampler, et al. (2010). Clean Energy Neighborhoods. (Cambridge: Massachusetts Institute of Technology with Tsinghua University). Research sponsored by the Energy Foundation, China. Page 176
- Frenchman, D., J. Wampler, et al. (2010). Clean Energy Development Patterns. (Cambridge: Massachusetts Institute of Technology with Tsinghua University). Research sponsored by the Energy Foundation, China. Page 41
- Ferrigno, K. J. (2010). Challenges and strategies for increasing adoption of small wind turbines in urban areas, Massachusetts Institute of Technology, Engineering Systems Division: 80 p.
- German Solar Energy Society (DGS) (2008). Planning and Installing Photovoltaic System: A Guide for Installers, Architects and Engineers, Earthscan in UK and USA.
- Global Wind Energy Council <http://www.gwec.net/>
- Hankey, S. and J. D. Marshall (2010). "Impacts of urban form on future US passenger-vehicle greenhouse gas emissions." Energy Policy **38**(9): 4880-4887.
- Hoffert, M. I., K. Caldeira, et al. (1998). "Energy implications of future stabilization of atmospheric CO<sub>2</sub> content." Nature 395(6705): 881-884.
- Jacobson, M. Z. (2009). "Review of solutions to global warming, air pollution and energy security." Geochimica Et Cosmochimica Acta 73(13): A581-A581.
- Jha, A. R. (2011). Wind turbine technology. Boca Raton, FL, CRC Press.
- Jiahua, Pan, et al. Understanding China's Energy Policy. A background paper prepared for stern review on the economics of climate change, the Chinese Academy of Social Sciences(CASS), 2006.
- Jiang, Y. (2010). Does energy follow urban form? : an examination of

- neighborhoods and transport energy use in Jinan, China, Massachusetts Institute of Technology: 163 p.
- Landau., C. R. (2011). "Optimum Orientation of Solar Panels." Retrieved 0401, 2011, from <http://www.macslab.com/optsolar.html>.
- Lazarus, N. (2009). BedZED: Toolkit Part II - A practical guide to producing affordable carbon neutral developments, BioRegional Development Group.
- Luque, A. and S. Hegedus (2003). Handbook of photovoltaic science and engineering. Hoboken, NJ, Wiley.
- Liggett, B. (2010). "Solar Origami: MIT Working on Super Efficient Folded Solar Panels." from <http://inhabitat.com/solar-origami-mit-working-on-super-efficient-folded-solar-panels/>.
- MacDonald, R. W., R. F. Griffiths, et al. (1998). "An improved method for the estimation of surface roughness of obstacle arrays." Atmospheric Environment 32(11): 1857-1864.
- MacKay, D. (2009). Sustainable Energy – without the hot air. Cambridge, England, UIT.
- Manfred Lenzen, R. W., Barney Foran (2007). Direct versus embodied Energy - The need for urban lifestyle transitions. Urban Energy transition: from fossil fuel to renewable power. P. Droege, Elsevier Science.
- McKinsey & Company. (2009). "China's green revolution: Prioritizing technologies to achieve energy and environmental sustainability." Retrieved 1101, 2010, from [http://www.mckinsey.com/locations/greaterchina/mckonchina/reports/china\\_green\\_revolution.aspx](http://www.mckinsey.com/locations/greaterchina/mckonchina/reports/china_green_revolution.aspx)
- Mertens, S. (2006). Wind Energy in the built environment : concentrator effects of buildings. Essex, Multiscience Publishing.
- Mithraratne, N. (2009). "Roof-top wind turbines for microgeneration in urban houses in New Zealand." Energy and Buildings 41(10): 1013-1018.
- Module Pricing in Solar buzz . <http://www.solarbuzz.com/facts-and-figures/retail-price-environment/module-prices>.
- Mondol, J. D., Y. G. Yohanis, et al. (2006). "Optimal sizing of array and inverter for grid-connected photovoltaic systems." Solar Energy 80(12): 1517-1539.

- Nemet, G. F. (2006). "Beyond the learning curve: factors influencing cost reductions in photovoltaics." Energy Policy 34(17): 3218-3232.
- Office of the Deputy Prime Minister, U. K. (2004). Planning Policy Statement 22: Renewable Energy. ISBN 0 11 7539244. t. Crown.
- P. Torcellini, S. P., M. Deru, and D. Crawley (2006). Zero Energy Buildings: A Critical Look at the Definition Conference Paper ACEEE Summer Study Pacific Grove, California
- Randolph, J. and G. M. Masters (2008). Energy for sustainability : technology, planning, policy. Washington, D.C., Island Press.
- Reijenga, T. H. (2003). PV in Architecture. Handbook of Photovoltaic Science and Engineering. H. S. Luque Antonio, John Wiley & Sons.
- REN21 (2010). Renewables 2010 Global Status Report. Paris, REN21 Secretariat.
- R.E.H. Sims, R. N. S., A. Adegbululgbé, J. Fenhann, I. Konstantinaviciute, W. Moomaw, H.B. Nimir, B. Schlamadinger, , C. T. J. Torres-Martínez, Y. Uchiyama, S.J.V. Vuori, N. Wamukonya, X. Zhang, et al. (2007). Energy supply . In Climate Change 2007: Mitigation. . O. R. D. B. Metz, P.R. Bosch, R. Dave, L.A. Meyer Cambridge, United Kingdom and New York, NY, USA. , Cambridge University Press.
- Shawn (2008). Progress Report on Small Wind Energy Development Projects Receiving Funds form the Massachusetts Technology Collaborative (MTC)".
- Solar and Wind Energy Resource Assessment (SIRA, UNEP/ GEF).  
<http://www.geni.org/globalenergy/library/renewable-energy-resources/world/asia/solar-asia/solar-china.shtml>
- Song, F., Q. Zhu, et al. (2005). Meteorological data set for China building thermal environment analysis. Beijing, Architecture & Building Press.
- Trancik, J. (2011) Evaluating energy technologies against climate targets, in review
- Encraft. (2009). "Warwick Wind Trials Final Report." Retrieved June 5th, 2011, from [www.warwickwindtrials.org.uk/resources/Warwick+Wind+Trials+Final+Report+.pdf](http://www.warwickwindtrials.org.uk/resources/Warwick+Wind+Trials+Final+Report+.pdf)
- Stankovic, S., N. Campbell, et al. (2009). Urban wind energy. London ; Sterling,

VA, Earthscan.

Trancik Lab Database. <http://www.mit.edu/~trancik>

Uni-Solar. (2011). "Uni-Solar breaks thin-film efficiency record." Retrieved July 8th, 2011, from <http://www.cleanenergyauthority.com/solar-energy-news/unisolar-breaks-thin-film-pv-efficiency-record-071511/>.

U. S. Environmental Protection Agency (2011). Inventory OF U.S. green house gas emissions and sink:1990 – 2009.

Waldhör, P. (2010/03). ENERGYBASE – THE OFFICE BUILDING OF TOMORROW. FORSCHUNGSFORUM. Vienna, Austrian Federal Ministry of Transport, Innovation and Technology.

Wang, J. (2010). The form of clean energy neighborhoods : how it is guided and how it could be, Massachusetts Institute of Technology: 92 p.

Weisser, D. (2007). "A guide to life-cycle greenhouse gas (GHG) emissions from electric supply technologies." Energy 32(9): 1543-1559.

Wieringa, J. (1993). "Representative Roughness Parameters for Homogeneous Terrain." Boundary-Layer Meteorology 63(4): 323-363.

Wiser, R. and M. Bolinger (2006). Annual Report on U.S. Wind Power Installation, Cost, and Performance Trends: 2006, Energy efficiency and renewable energy U.S. Department of Energy.

Wright, S. H. (2008). "Getting wrapped up in solar textiles." Retrieved March 3rd, 2011, from <http://web.mit.edu/newsoffice/2008/solar-textiles-0609.html>.

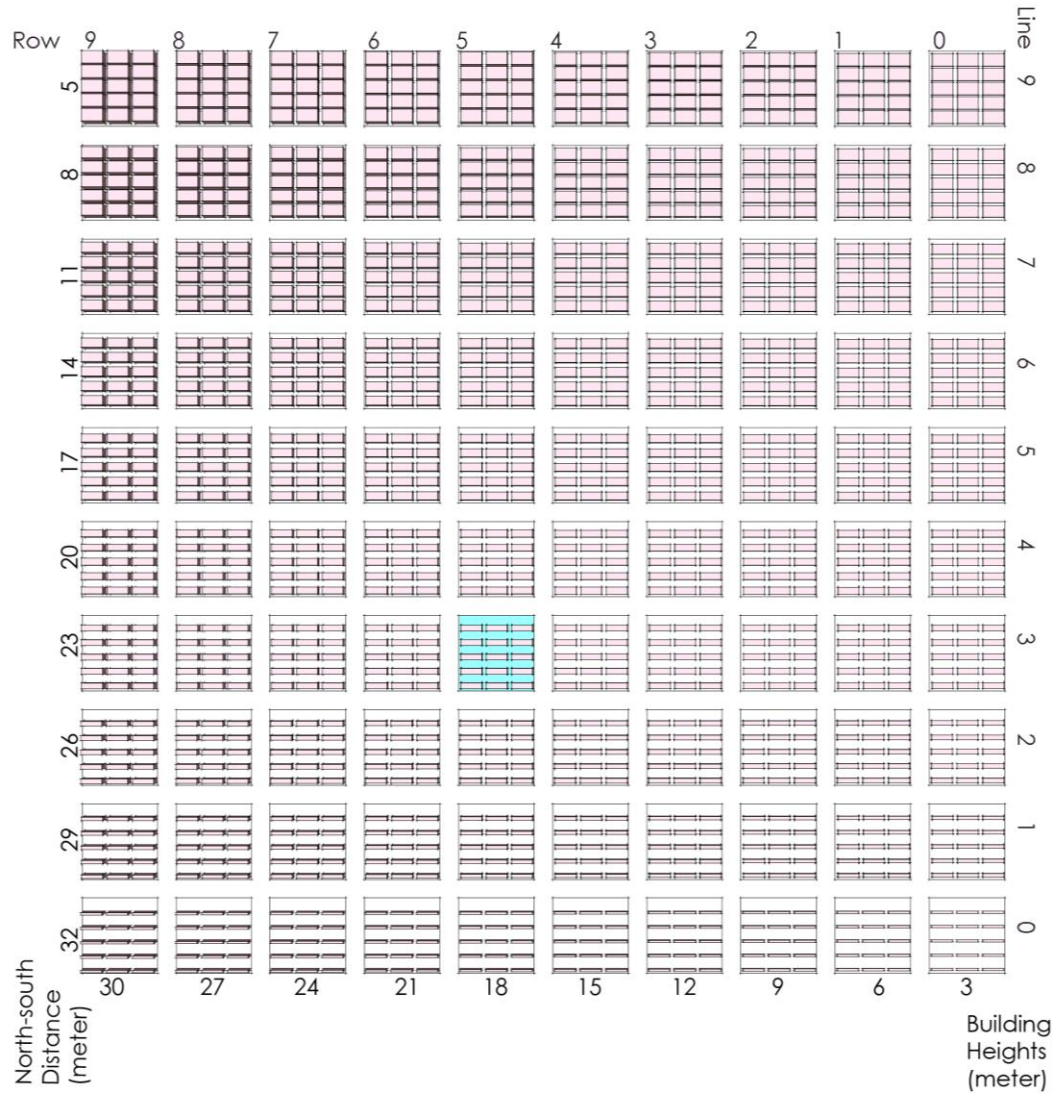
Varis Bokalders, M. B. (2010). The whole building handbook : how to design healthy, efficient and sustainable buildings. London ;, Sterling, VA : Earthscan.

Yamaguchi, Y., Y. Shimoda, et al. (2007). "Proposal of a modeling approach considering urban form for evaluation of city level energy management." Energy and Buildings 39(5): 580-592.

Zhang, J. (2010). Operational energy consumption and GHG emissions in residential sector in urban China : an empirical study in Jinan, Massachusetts Institute of Technology: 138 p.

## Appendix I: The site plans and solar energy potential simulated results of 100 building cluster models

### The Site Plans of 100 building clusters



#### Note

1. The site is 200 meters by 200 meters; the length of each building is 55 meters, and the east-west distance between two closest buildings is 12 meters.
2. Each model is numbered as Model L.R, "L" indicates the Line number and "R" indicates the row number;
3. The Blue model indicates the benchmark model I derived from Dongchang neighborhood (the "slab") in Jinan.

# The renewable solar potential simulated results of 100 modules

## Basic Information

The efficiency of the PV system	0.15
Solar irradiance (tracking)	483 (wh/sq m)
Solar irradiance on the ture-southern face	341.8 (wh/sq m)
Solar Duration	2545.8 hour
The Total Number of the buildings on six	15
Site Area	40000 sq meter

## The simulation results of 100 models

Model No.	Building Information			Form Indicators					Energy*								
	(Line,Row)	length (m)	height (m)	width (m)	Distance between buildings	Roof Area (sq m)	Surface Area (sq m)	Building Volume	Density	Roof Coverage	Spacing Indicator	Building volume ratio	Roof Energy (kwh)	Facade Energy (kwh)	Total Energy (kwh)	Solar Energy Production per site	Solar Energy Production per floor
0.0	55	3	6	6	32	4950	12780	14850	0.12375	12.38%	10.66666667	1.193939394	913352.5	285646.768	1198999	29.974982	242.22208
0.1	55	6	6	6	32	4950	20610	29700	0.2475	12.38%	5.333333333	0.860606061	913352.5	564365.275	1477718	36.942945	149.26442
0.2	55	9	6	6	32	4950	28440	44550	0.37125	12.38%	3.555555556	0.799494949	913352.5	836155.519	1749508	43.737701	117.81199
0.3	55	12	6	6	32	4950	36270	59400	0.495	12.38%	2.666666667	0.693939394	913352.5	1101017.5	2014370	50.35925	101.73586
0.4	55	15	6	6	32	4950	44100	74250	0.61875	12.38%	2.133333333	0.660606061	913352.5	1358951.22	2272304	56.807593	91.810252
0.5	55	18	6	6	32	4950	51930	89100	0.7425	12.38%	1.777777778	0.638383838	913352.5	1609956.68	2523309	63.08273	84.939906
0.6	55	21	6	6	32	4950	59760	103950	0.86625	12.38%	1.52809524	0.6252510823	913352.5	1854033.88	2767386	69.18466	79.866851
0.7	55	24	6	6	32	4950	67590	118800	0.99	12.38%	1.333333333	0.610606061	913352.5	2091182.81	3004335	75.113383	75.8727104
0.8	55	27	6	6	32	4950	75420	133650	1.11375	12.38%	1.185185185	0.601346801	913352.5	2321403.48	3234756	80.8689	72.609562
0.9	55	30	6	6	32	4950	83250	148500	1.2375	12.38%	1.066666667	0.593939394	913352.5	2544695.89	3458048	86.45121	69.839564
1.0	55	3	9	9	29	7425	14985	22775	0.185625	18.56%	9.666666667	1.006060606	1370029	285288.41	165317	41.38293	222.93834
1.1	55	6	9	9	29	7425	22545	44550	0.37125	18.56%	4.833333333	0.672727273	1370029	562931.841	1932961	48.324015	130.1657
1.2	55	9	9	9	29	7425	30105	66825	0.556875	18.56%	3.222222222	0.561616162	1370029	832930.294	2202959	55.073977	98.898275
1.3	55	12	9	9	29	7425	37665	89100	0.7425	18.56%	2.416666667	0.506060606	1370029	1095283.77	2465313	61.632814	83.007156
1.4	55	15	9	9	29	7425	45225	111375	0.928125	18.56%	1.933333333	0.472727273	1370029	1349992.26	2720021	68.000526	73.26556
1.5	55	18	9	9	29	7425	52785	133650	1.11375	18.56%	1.611111111	0.450505051	1370029	1597055.78	2967085	74.177114	66.601225
1.6	55	21	9	9	29	7425	60345	155925	1.299375	18.56%	1.380952381	0.434632035	1370029	1836474.32	3206503	80.162577	61.693181
1.7	55	24	9	9	29	7425	67905	178200	1.485	18.56%	1.208333333	0.422727273	1370029	2068247.87	3438277	85.956916	57.883445
1.8	55	27	9	9	29	7425	75465	200475	1.670625	18.56%	1.074074074	0.413468013	1370029	2292376.45	3662405	91.560131	54.805914
1.9	55	30	9	9	29	7425	83025	222750	1.85625	18.56%	0.966666667	0.406060606	1370029	2508860.06	3878889	96.972221	52.240927
2.0	55	3	12	12	26	9900	17190	29700	0.2475	24.75%	8.666666667	0.912121212	1826705	284847.354	2111152	52.78881	213.28812
2.1	55	6	12	12	26	9900	24480	59400	0.495	24.75%	4.333333333	0.578787879	1826705	58167.615	2287873	59.696816	120.59563
2.2	55	9	12	12	26	9900	31770	89100	0.7425	24.75%	2.888888889	0.467676768	1826705	828950.786	2655566	66.391645	89.416358
2.3	55	12	12	12	26	9900	39060	118800	0.99	24.75%	2.166666667	0.412121212	1826705	1088226.86	2914932	72.873297	73.609391
2.4	55	15	12	12	26	9900	46340	148500	1.2375	24.75%	1.733333333	0.378787879	1826705	138965.85	3165671	79.141777	63.952947
2.5	55	18	12	12	26	9900	53640	178200	1.485	24.75%	1.444444444	0.356565657	1826705	1581177.75	3407583	85.197069	57.371764
2.6	55	21	12	12	26	9900	60930	207900	1.7325	24.75%	1.238095238	0.340692641	1826705	1814862.55	3641568	91.03919	52.547873
2.7	55	24	12	12	26	9900	68220	237600	1.98	24.75%	1.083333333	0.328787879	1826705	2040020.26	38666132	96.666132	48.822289
2.8	55	27	12	12	26	9900	75510	267300	2.2275	24.75%	0.962962963	0.31952862	1826705	225650.88	4083356	102.0839	45.82891
2.9	55	30	12	12	26	9900	82800	297000	2.475	24.75%	0.866666667	0.312121212	1826705	2464754.41	4291459	107.28649	43.348075
3.0	55	3	15	15	23	12375	19395	37125	0.309375	30.94%	7.666666667	0.855757576	2283381	284291.239	2567673	64.191813	207.48869
3.1	55	6	15	15	23	12375	26415	74250	0.61875	30.94%	3.833333333	0.522424242	2283381	558943.157	2842324	71.056111	114.84139
3.2	55	9	15	15	23	12375	33435	111375	0.928125	30.94%	2.555555556	0.411313131	2283381	823955.753	3107337	77.688426	63.699314
3.3	55	12	15	15	23	12375	40455	148500	1.2375	30.94%	1.916666667	0.355757576	2283381	1079329.03	3362710	84.067758	67.933542
3.4	55	15	15	15	23	12375	47475	185625	1.546875	30.94%	1.533333333	0.322424242	2283381	1325062.98	3608444	90.2711107	58.318291



3.1	55	6	15	23	12375	26415	74250	0.61875	30.94%	3.833333333	0.522424242	2283381	538943.157	2842324	71.03811	114.84139
3.2	55	9	15	23	12375	33435	111375	0.928125	30.94%	2.555555556	0.411313131	2283381	823955.753	3107337	77.683426	83.699314
3.3	55	12	15	23	12375	40455	148500	1.2375	30.94%	1.916666667	0.355757576	2283381	1079329.03	3367270	84.067758	67.933542
3.4	55	15	15	23	12375	47475	185625	1.546875	30.94%	1.533333333	0.322424242	2283381	1325063.98	3608444	90.211107	58.318291
3.5	55	18	15	23	12375	54495	222750	1.85625	30.94%	1.277777778	0.30020202	2283381	156157.62	3844539	96.113473	51.778302
3.6	55	21	15	23	12375	61515	259875	2.165625	30.94%	1.095238095	0.272424242	2283381	178612.93	4076994	101.77486	46.995604
3.7	55	24	15	23	12375	68535	297000	2.475	30.94%	0.958333333	0.261424242	2283381	2004428.92	4287810	107.19556	43.311214
3.8	55	27	15	23	12375	75555	334125	2.784375	30.94%	0.815819532	0.24364983	2283381	2211605.59	4494987	112.37467	40.359029
3.9	55	30	15	23	12375	82575	371250	3.09375	30.94%	0.766666667	0.235757576	2283381	2409142.94	4695324	117.31311	37.919388
4.0	55	3	18	20	14850	28350	44550	0.37125	37.13%	6.666666667	0.484848485	2740058	283568.29	3025626	75.596646	203.61117
4.1	55	6	18	20	14850	35300	56100	0.7425	37.13%	3.333333333	0.373737374	2740058	817449.212	3357507	88.937659	82.402773
4.2	55	9	18	20	14850	42350	66850	1.11375	37.13%	2.222222222	0.373737374	2740058	116761.84	3807819	95.195485	64.104704
4.3	55	12	18	20	14850	49400	79600	1.485	37.13%	1.666666667	0.318181818	2740058	153513.45	4275189	106.87973	47.981919
4.4	55	15	18	20	14850	56450	86850	1.85625	37.13%	1.111111111	0.262626263	2740058	1958160.18	4698218	117.45544	39.547287
4.5	55	18	18	20	14850	63500	94050	2.2275	37.13%	0.952380952	0.246753247	2740058	2153046.72	4893104	122.3761	35.61133
4.6	55	21	18	20	14850	70550	101200	2.59875	37.13%	0.740740741	0.22589226	2740058	2336848.03	5076906	126.92264	34.187916
4.7	55	24	18	20	14850	77600	108350	2.97	37.13%	0.666666667	0.218181818	2740058	252138.93	527593.74	86.9831	200.82678
4.8	55	27	18	20	14850	84650	115400	3.34125	37.13%	0.60952381	0.21091342	3196734	552138.93	5478873	93.721818	108.19258
4.9	55	30	18	20	14850	91700	122450	3.7125	37.13%	0.566666667	0.20808658	3196734	808646.244	4005380	100.1345	77.063898
5.0	55	3	21	17	17325	23805	51975	0.43125	43.31%	1.416666667	0.291341991	3196734	1052112.12	4248846	106.22115	61.310908
5.1	55	6	21	17	17325	30855	63900	0.8625	43.31%	1.08952381	0.2808658	3196734	128236.57	4479270	111.98176	51.708749
5.2	55	9	21	17	17325	37905	75950	1.29375	43.31%	0.80952381	0.25786436	3196734	1499916.18	4696563	117.41633	40.412245
5.3	55	12	21	17	17325	44955	87900	1.725	43.31%	0.62962963	0.198749399	3196734	2239037.28	5435371	135.89428	31.375302
5.4	55	15	21	17	17325	51955	94900	2.15625	43.31%	0.555555556	0.171212121	3196734	2729037.38	5683454	143.81794	29.05413
5.5	55	18	21	17	17325	58955	101900	2.5875	43.31%	0.466666667	0.158519529	3196734	3253410	5614049	150.35123	31.504203
5.6	55	21	21	17	17325	65955	108900	3.01875	43.31%	0.415800	0.145800	3196734	3753410	5910794	159.10877	34.468271
5.7	55	24	21	17	17325	72955	115900	3.45	43.31%	0.377777778	0.1341991	3196734	4293410	6195616	167.55535	49.505194
5.8	55	27	21	17	17325	79955	122900	3.88125	43.31%	0.333333333	0.122222222	3196734	4793410	6480104	176.0415	51.03027
5.9	55	30	21	17	17325	86955	129900	4.3125	43.31%	0.291341991	0.11212121	3196734	4981074	6670070	184.81794	52.55535
6.0	55	3	24	14	19800	26010	59400	0.495	49.50%	6.666666667	0.771212121	3653410	1635793.62	5288204	132.23009	38.161643
6.1	55	6	24	14	19800	33060	75600	0.99	49.50%	4.666666667	0.471212121	3653410	1806134.32	5459544	136.4861	34.468271
6.2	55	9	24	14	19800	40110	92700	1.485	49.50%	3.333333333	0.356767677	3653410	1960638.98	5614049	140.35123	31.504203
6.3	55	12	24	14	19800	47160	109800	1.98	49.50%	2.555555556	0.326767677	3653410	2099307.62	5752718	143.81794	29.05413
6.4	55	15	24	14	19800	54210	127500	2.475	49.50%	1.888888889	0.278787878	3653410	2239037.28	5910794	159.10877	34.468271
6.5	55	18	24	14	19800	61260	145200	2.97	49.50%	1.555555556	0.25786436	3653410	238080	5270554	131.76385	33.801852
6.6	55	21	24	14	19800	68310	162900	3.465	49.50%	1.166666667	0.235787878	3653410	252138.93	5478873	93.721818	108.19258
6.7	55	24	24	14	19800	75360	180600	3.96	49.50%	0.952380952	0.22589226	3653410	266280.93	5614049	150.35123	31.504203
6.8	55	27	24	14	19800	82410	198300	4.455	49.50%	0.80952381	0.20808658	3653410	280370.93	5752718	143.81794	29.05413
6.9	55	30	24	14	19800	89460	216000	4.95	49.50%	0.740740741	0.198749399	3653410	294460.93	5893454	148.3532	26.906613
7.0	55	3	27	11	22275	28215	66825	0.556875	55.69%	6.666666667	0.771212121	4110086	1371876.4	5481963	137.04907	41.017304
7.1	55	6	27	11	22275	35265	83625	0.7425	55.69%	4.666666667	0.525555556	4110086	1529980.17	5640066	141.00166	36.171663
7.2	55	9	27	11	22275	42315	101375	0.928125	55.69%	3.333333333	0.411313131	4110086	1676635.45	5868572	122.16804	73.12715
7.3	55	12	27	11	22275	49365	119000	1.2375	55.69%	2.555555556	0.322222222	4110086	1823685.99	6097040.45	117.62226	57.298433
7.4	55	15	27	11	22275	56415	136625	1.546875	55.69%	1.916666667	0.255555556	4110086	1970240.045	6326226	107.19556	43.311214
7.5	55	18	27	11	22275	63465	154250	1.85625	55.69%	1.666666667	0.235757576	4110086	211605.59	4494987	112.37467	40.359029
7.6	55	21	27	11	22275	70515	171875	2.165625	55.69%	1.415800	0.222222222	4110086	226280.93	5614049	150.35123	31.504203
7.7	55	24	27	11	22275	77565	189500	2.475	55.69%	1.222222222	0.21091342	4110086	2409142.94	4695324	117.31311	37.919388
7.8	55	27	27	11	22275	84615	207000	2.784375	55.69%	1.08952381	0.20808658	4110086	254460.93	5752718	143.81794	29.05413
7.9	55	30	27	11	22275	91665	224500	3.09375	55.69%	0.952380952	0.20020202	4110086	268010.18	5893454	148.3532	26.906613
8.0	55	3	30	8	24750	81675	74250	0.56875	61.88%	6.666666667	0.73030303	4566763	275254.375	4842017	121.05042	195.63705
8.1	55	6	30	8	24750	88725	79000	0.61875	61.88%	4.666666667	0.522424242	4566763	299307.62	5076906	126.92264	34.187916
8.2	55	9	30	8	24750	95775	81750	0.66875	61.88%	3.333333333	0.40069697	4566763	313462.982	5305387	132.73466	71.50689



8.3	55	12	30	8	24750	47430	297000	2.475	61.88%	0.666666667	0.243030303	4566763	934739.213	5501502	137.53754	55.570725
8.4	55	15	30	8	24750	53100	371250	3.09375	61.88%	0.533333333	0.209696967	4566763	1099141.4	5665904	141.6476	45.785083
8.5	55	18	30	8	24750	58770	445500	3.7125	61.88%	0.444444444	0.187474747	4566763	1235830.53	5807593	145.06483	39.074701
8.6	55	21	30	8	24750	64440	519750	4.33125	61.88%	0.380952381	0.171601732	4566763	1344806.62	5911569	147.78923	34.121612
8.7	55	24	30	8	24750	70110	594000	4.95	61.88%	0.333333333	0.159696967	4566763	1428069.66	5992832	149.82081	30.26683
8.8	55	27	30	8	24750	75780	668250	5.56875	61.88%	0.296296296	0.15043771	4566763	1479619.65	6046382	151.15956	27.144252
8.9	55	30	30	8	24750	81450	742500	6.1875	61.88%	0.266666667	0.143030303	4566763	1505456.59	6072219	151.80548	24.534219
9.0	55	3	33	5	27725	32625	81675	0.680625	68.06%	1.666666667	0.732782369	5023439	266940.461	5290379	132.25948	194.32064
9.1	55	6	33	5	27725	38025	163350	1.36125	68.06%	0.833333333	0.399449036	5023439	489540.045	5512979	137.82447	101.24846
9.2	55	9	33	5	27725	43425	245025	2.041875	68.06%	0.555555556	0.288337925	5023439	667798.752	5691238	142.28094	69.681513
9.3	55	12	33	5	27725	48825	326700	2.7225	68.06%	0.416666667	0.23787369	5023439	801716.583	5825155	145.62889	53.490867
9.4	55	15	33	5	27725	54225	408375	3.403125	68.06%	0.333333333	0.199449036	5023439	891293.536	5914732	147.86831	43.450743
9.5	55	18	33	5	27725	59625	490050	4.08375	68.06%	0.277777778	0.177226814	5023439	936529.613	5959968	148.99921	36.48588
9.6	55	21	33	5	27725	65025	571725	4.764375	68.06%	0.238095238	0.161353798	5023439	937424.812	5960864	149.02159	31.278309
9.7	55	24	33	5	27725	70425	653400	5.445	68.06%	0.208333333	0.149449036	5023439	893979.135	5917418	147.93545	27.169045
9.8	55	27	33	5	27725	75825	735075	6.125625	68.06%	0.185185185	0.140189777	5023439	806192.581	5829631	145.74079	23.791986
9.9	55	30	33	5	27725	81225	816750	6.80625	68.06%	0.166666667	0.132782369	5023439	674065.15	5697504	142.4376	20.927471

1. For building clusters, we assume each cluster is comprised of fifteen identical cube buildings on the same-area site (200m by 200m), and the building floor height is the same of 3 meters.

2. In the energy simulation, we only calculate the solar energy potential on the roof and vertical southern facade. For the roof mounted PV - we assume the tracking system is adopted to gain the maximum solar energy.

The PV installation area is the same with the roof area - the shading effect caused by PV panels themselves are ignored. For the vertical facade, the PV is assumed to be placed parallel to the surface. The shading effect is considered by the adjusted shading factor

\*. The detail energy calculation formula can be found in Appendix 2

\*\*. The red line is the benchmark cluster in Jinan

## Appendix II: Renewable energy potential simulation methodology

### 1. Solar energy potential simulation methodology

Photovoltaic converts the sunlight into electricity. Its energy potential is related to the average hourly solar irradiation, the total surface area of the PV panels, the effective solar duration and the efficiency of PV system. The formula to estimate the solar energy potential could be written as

$$E_{pv} = \sum_{i=1}^n G_{hy\_i} * A_i * H * \gamma_i * \eta \quad (A)$$

$E_{pv}$  (KWh/year) - the annual electricity generation form solar PV.

$G_{hy\_i}$  (KWh/m<sup>2</sup>)- is average hourly irradiation on surface i, which is the average hourly solar irradiation energy intensity that PV surface i receives over the yearly solar duration.  $G_{hy\_i}$  is an energy intensity unit, the average of a set of momentary solar irradiances in each month over a year. It will be affected by the geographic location, local climate and as the placement of the PV.;

$H$  (unit/year)- is local annual solar duration hour unit. The solar duration is the length of time in which the solar radiation falling on the plane perpendicular to the direction of the sun is greater or equal to 120 W/m<sup>2</sup><sup>34</sup>. This solar duration is determined together by the latitude and the local climate. In our later simulation in Jinan, the solar duration is from the climate database of China Meteorological Administration, which is 2546.8<sup>35</sup>.

$\gamma_i$  - the annual shading adjusting factor on the surface i. It is the ratio of the actual unshaded sunlight hours on PV façade i over its possible sunlight hours. Since the actual solar duration on the PV surfaces in the city could be shorten than local solar duration due to the shading casted by the nearby buildings.

$A_i$  - the total area of the PV surface i;

---

<sup>34</sup> The definition is drawn from European Centre for Medium-Range Weather Forecasts, <http://ecmwf.int/>

<sup>35</sup> China Meteorological Data Sharing System [http://cdc.cma.gov.cn/shuju/search1.jsp?dsid=SURF\\_CLI\\_CHN\\_MUL\\_MYER\\_19712000\\_CES&tpcat=SURF&type=table&pageid=3](http://cdc.cma.gov.cn/shuju/search1.jsp?dsid=SURF_CLI_CHN_MUL_MYER_19712000_CES&tpcat=SURF&type=table&pageid=3)

$\eta$  - the efficiency of PV system. The system efficiency is the product of the module efficiency and the system de-rating rate. In our analysis, we use 17% as the efficiency of the PV system.

To simplify the estimation, I only consider the solar energy potentials from the PV installed on the roof and on the southern facades.

## 1.1 The estimation of $G_{hy\_i}$

### 1.1.1 Disaggregation

The average hourly average irradiation is derived from the average of the hourly irradiation  $G_{hm}$  in each month over a year. The average hourly irradiation in a given month  $G_{hm}$  could be assumed to be equivalent to the average hourly irradiation of a sample day in that month  $G_{hd}$  (A-1). Therefore, I need to estimate the average hourly irradiation in 12 sample days<sup>36</sup>, one day in each month, over a year.

$$G_{hm} = G_{hd} \quad A-1$$

For the annotation of  $G_{xy}$ , the first subscript under the capital symbol indicate the hourly or daily value, the second and third refers to daily, monthly or yearly average value. Furthermore, the slope and orientation of the related surface are referred in the brackets. For example,  $B_{hm}(\alpha, \beta)$  refers to the monthly mean of the daily beam irradiation value on the surface tilted at the angle of  $\beta$  and oriented  $\alpha$  towards the west (positive towards the west and negative towards the east).

This is the method I estimate the average hourly irradiance in a sample day. I assume the effective solar duration for PV energy production is 6 hours a day, which is from 9am to 3pm, when the solar irradiance is the strongest. I estimate the solar irradiance at one temporal point in each hour, which are 9:30 am, 10:30 am, 11:30 am, 0:30 pm, 1:30 pm and 2:30 pm. We assume the hourly solar irradiation value  $G_{hd}$  is equal to the momentary irradiance value  $G_j$  in that corresponding hour  $j$ , and the hourly solar irradiation over that day is the average of the six irradiance values<sup>37</sup> (4). The related functions are

$$G_{hm} = G_{hd} = \frac{1}{6} \sum_{j=1}^6 (G_j * 1) \quad A-2$$

<sup>36</sup> The twelve sample days in energy pro-froma are Jan-17, Feb-14, March-15, April-15, May-15, June-10, Jul-18, Aug-18, Sep-18, Oct-19, Nov-18, Dec-13. This is referred to the cases of Madrid in "Handbook of Photovoltaic Science and Engineering", which uses the above dates to represent their respective month.

<sup>37</sup> A more precise result should be the aggregation of the solar irradiance value in every hour of solar duration, our methodology simply the calculation based on the abovementioned assumptions drawing the average value.

$G_j$  indicates the density of solar power at specific timing point j.

### 1.1.2 The components of $G(\alpha, \beta)$

With these assumptions, the key to estimate the global hourly irradiation is the to calculate solar irradiance on arbitrary orientation  $G(\alpha, \beta)$  at any given moment.

$$G_j = G(\alpha, \beta)$$

A-3

As it shown in Figure II.1,  $\alpha$  is the azimuth of the PV, which is the angle between the projection of the normal of the PV panels and the due south.  $\alpha$  ranges from -90 degree (anticlockwise) to +90 degree (clockwise), and  $\beta$  is the slope of PV.  $G(\alpha, \beta)$  is the sum of three components, so it is also called the global solar irradiance, and the three componets are

$B(\alpha, \beta)$  -Direct or Beam irradiance, which is the power from the beams of light reaching on the surfacing directed from the sun;  $B_j = B(\alpha, \beta)$

$D(\alpha, \beta)$  -Diffuse irradiance, which is the irradiance scattered towards the objects from other part of sky;  $D_j = D(\alpha, \beta)$

$R(\alpha, \beta)$  - Albedo radiation. Rh Albedo irradiance, the radiation reflected on the ground, it is usually very small and can be ignored in some calculation.  $R_j = R(\alpha, \beta)$

$$G(\alpha, \beta) = B(\alpha, \beta) + D(\alpha, \beta) + R(\alpha, \beta) = G_j$$

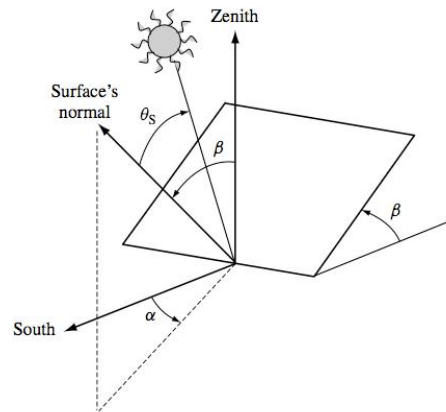


Figure II.1 Receiver position (slope  $\beta$  and azimuth  $\alpha$ ) and sun's rays incidence angle  $\theta_s$

Source: Luque and Hegedus 2003

### 1.1.3 The estimation of $G(\alpha, \beta)$

To estimate  $G(\alpha, \beta)$ , I firstly estimate the extraterrestrial daily irradiation  $B_{0dm}(0)$ ; With this value and the global average daily irradiation  $G_{dm}(0)$  from the climate data, I can estimate the cleanness index  $K_{Tm}$  and identify the weight of the three components in G.

#### 1.1.3.1 The estimation of $B_{0dm}(0)$ based on the location

As the PV panels receive energy from the sun, the power intensity falling on the panel is firstly related to the relative position between the sun and the location of PV panel on the earth.

The monthly average of extraterrestrial irradiation can be calculated as

$$B_{0dm}(0) = \frac{1}{d_{n2} - d_{n1} + 1} \sum_{d_{n1}}^{d_{n2}} B_{0d}(0) \quad \text{A-4}$$

$d_{n1}$  and  $d_{n2}$  are the day number of the first and the last day of the month,  $B_{0d}(0)$  is the integral of the hourly extraterrestrial irradiance over the whole day, and it could be estimated through function A-5, A-6 and A-7.

$$B_{0d}(0) = \sum_{k=1}^m B_{0h-k}(0) \quad \text{A-5}$$

$$B_{0h-k}(0) = B_0 \varepsilon_0 \cos \theta_{ZS-k} \quad \text{A-6}$$

$$\cos \theta_{ZS} = \sin \delta \sin \phi + \cos \delta \cos \phi \cos \omega \quad \text{A-7}$$

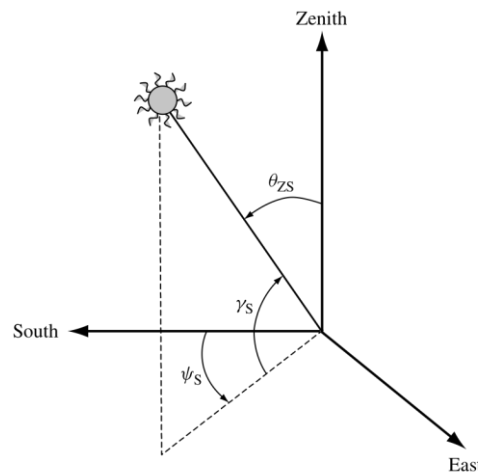


Figure II.2. Position of the sun relative to a fixed point on the earth

Source: Luque and Hegedus 2003

$T$  is the length of the day, which is 24 hours.  $B_0$  is the solar constant 1367w/m<sup>2</sup>,  $\epsilon_0$  is eccentricity correction factor.  $\omega$  is the true solar time, related to the local official time<sup>38</sup>.  $\delta$  is the solar inclination on the given day, and  $\phi$  is geographic latitude.  $\theta_{zs}$  is the the Solar Zenith angle. And  $\theta_{zs}$ ,  $\epsilon_0$  and  $\delta$  all can be calculated based on the day number of the given day. The detail equations used in the energy pro-forma are drawn from “Handbook of Photovoltaic Science and Engineering” (page 907-912).

### 1.1.3.2 The estimation of $G(\alpha, \beta)$ based on $B_{0dm}(0)$

Based on  $B_{0dm}(0)$  and the ground daily irradiation  $G_{dm}(0)$  in each month drawn from the database of Meteorological Administration<sup>39</sup>, I calculate the hourly radiation of a surface with arbitrary orientation at any given time through the following steps.

- 1) Calculate the cleanness index and estimate the direct and diffuse components of horizontal radiation based on the given global radiation. The cleanness index  $K_{Tm}$  is calculated by month – it is the ratio of the recorded global daily irradiation on the horizontal ground  $G_{dm}(0)$  over the extraterrestrial radiation  $B_{0dm}(0)$ . It will determine the composition of the beam irradiation  $B_{dm}(0)$  and the diffuse irradiation  $D_{dm}(0)$  on the ground.

$$K_{Tm} = \frac{G_{dm}(0)}{B_{0dm}(0)} \quad \text{A-8}$$

$$F_{Dm} = \frac{D_{dm}(0)}{G_{dm}(0)} = 1 - 1.13K_{Tm} \quad \text{A-9}$$

$$F_{Dm} = \frac{D_{dm}(0)}{G_{dm}(0)} = 1 - 1.13K_{Tm} \quad \text{A-10}$$

- 2) Estimate the hourly irradiation  $G(0)$  on the horizontal surface from the daily irradiation; The value can be estimated according to the following formulas (Lorenzo,2003).

$$\frac{B_0(0)}{B_{0d}(0)} = \frac{\pi}{T} \times \frac{\cos \omega - \cos \omega_s}{\left( \frac{\pi}{180} \omega_s \cos \omega_s - \sin \omega_s \right)} \quad \text{A-11}$$

<sup>38</sup> The equation is  $\omega = 15 \cdot (TO - AO - 12) - (LL - LH)$ , where TO is the local standard time, AO is usually the time by which clocks are set ahead of the local time zone. LL is the local longitude and LH is the reference longitude of the local time zone. According to the Jinan's time zone and longitude, our analysis uses  $\omega = 15 \cdot (TO - 12) - (117 - 120)$ ,  $\omega = 15TO - 183$ .

<sup>39</sup> In our calculation, the  $G_{dm}(0)$  is based on the data in the book “The special climate dataset for China Building Thermal Environment analysis”. This dataset is derived from the real time climate records of 270 observatories in China Meteorological Administration from 1971 to 2003.

$$\frac{D(0)}{D_d(0)} = \frac{B_0(0)}{B_{0d}(0)} = r_D \quad \text{A-12}$$

$$\frac{G(0)}{G_d(0)} = \frac{B_0(0)}{B_{0d}(0)} (a + b \cos \omega) = r_G \quad \text{A-13}$$

In function A-13 **a** and **b** are two parameters that can be calculated from the following equations:

$$a = 0.409 - 0.5016 \times \sin(\omega_s + 60) \quad \text{A-14}$$

$$b = 0.6609 + 0.4767 \times \sin(\omega_s + 60) \quad \text{A-15}$$

$\omega_s$  is the sunshine angle on that day, it can be calculated based on the day number and the latitude  $\omega_s = -\arccos(-\tan \delta \tan \phi)$ .

- 3) When estimating the irradiance on surface on arbitrary orientation  $G(\alpha, \beta)$  at any given moment, the following equations are used. In equation A-18,  $p$  is the reflectivity of the ground depending on the composition of the ground, which is usually taken as 0.2.  $\theta_s$  The angle of solar incidence between the sun's ray and the normal of the surface, the estimation methods could be found in "Handbook of Photovoltaic Science and Engineering" as well (page 907-912)

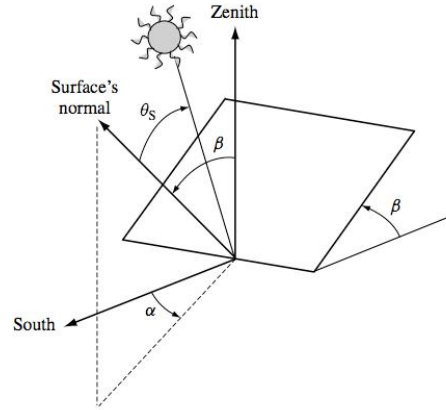


Figure II.2 Receiver position (slope  $\beta$  and azimuth  $\alpha$ ) and sun's rays incidence angle  $\theta_s$

Source: Luque and Hegedus 2003

$$B(\beta, \alpha) = \frac{B(0)}{\cos \theta_{zs}} \bullet \max(0, \cos \theta_s) \quad \text{A-16}$$

$$D(\beta, \alpha) = \frac{D(0)}{\cos \theta_{zs}} \bullet \max(0, \cos \theta_s) \quad \text{A-17}$$

$$R(\beta, \alpha) = \rho G(0) \frac{1 - \cos \beta}{2}$$

A-18

With these formulas, I developed an excel tool that can calculate the  $G(\alpha, \beta)$  of PV at any orientation in Jinan. This tool is used for the average hourly solar irradiance estimation of the roof and surfaces. For the tracking system – in which the surface always stays perpendicular to the sunlight incidents, the result would be generated under the condition that  $\alpha$  is equal to the solar azimuth  $\psi_s$ , and  $\beta$  is the same value as  $\theta_{zs}$ .

## 1.2 The estimation of $\gamma_i$ on the roof and the southern facades

$\gamma_i$  is the ratio of the actual un-shaded sunlight hours over the possible sunlight hours  $H_{tot}$  within the same period on the surface  $i$ . In 100-model energy potential simulation, we assume buildings are of the same height, and the roofs would not be affected by any shades casted by other buildings. Therefore,  $\gamma_{roof}$  is equal to 1. For the southern façade, the actual sunlight hours will be impacted by the spacing of the building and the orientation of the building layout.

### 1.2.1 Spacing

As Appendix I records the spacing indicators and the responded ecotect simulating results of the annual un-shaded sunlight hours on the southern façade of 100 models. We found that the annual sunlight hours would be an inverse function of the spacing indicator. When spacing indicator exceeds certain value, the sunlight hours on the buildings' southern façade will almost level off.

For Jinan, the estimated relationship drawn from the simulation results could be written as

**Error! Objects cannot be created from editing field codes.**

A-19

### 1.2.2 Orientation of building arrays

Even with the same spacing factor, if the building arrays are placed towards different directions, the annual un-shaded sunlight hours on the vertical façade will still differ. As we found in our analysis earlier using the benchmark model facing 19 different orientations, the relationship between the orientation (the azimuth of the normal of vertical southern facade) and the annual sunlight hours fits with a quadric function curve. The simulations results are shown in Table II.1, the highest value of sunlight hours occurs when the angle is zero, i.e the building facing true south.



Table II.1 the simulated results of sunlight hours on the southern facades of the benchmark model at different orientation

<b>Orientati on</b>	<b>Annual sunlight hours</b>	<b>Orientat ion</b>	<b>Annual Sunlight hours</b>
<b>-45</b>	2406.89	<b>5</b>	3003.03
<b>-40</b>	2479.4	<b>10</b>	2948.18
<b>-35</b>	2574.88	<b>15</b>	2935.27
<b>-30</b>	2710.88	<b>20</b>	2859.58
<b>-25</b>	2797.74	<b>25</b>	2755.95
<b>-20</b>	2889.05	<b>30</b>	2669.3
<b>-15</b>	2942.42	<b>35</b>	2566.8
<b>-10</b>	2992.27	<b>40</b>	2442.49
<b>-5</b>	2997.06	<b>45</b>	2444.5
<b>0</b>	2993.6		

The equation between the orientation of the benchmark neighborhood and its annual unshaded hours on the southern façade can be written as

**Error! Objects cannot be created from editing field codes.**

A-20

In the solar energy potential simulation, I will calculate effective sunlight hours on surface I with adjustment of the impact of the spacing and orientation.  $Y_i$  of the southern vertical façade can be calculated as

$$Y_i = (H_{si}/H_{tot}) * (H_{oi}/H_{si}^*). \quad \text{A-21}$$

$H_{si}$  is the effective sunlight hours adjusted by shading caused by spacing, and  $H_{oi}$  is the effective sunlight hours adjusted by the orientation based on the neighborhoods of the same spacing, and  $H_{tot}$  is the total sunlight hours in Jinan over a year. In the 100 model simulation, I assume all building cluster face due south, so only the spacing determines the shading adjusting factor.

### 1.3 $\eta$

$\eta$  refers to the efficiency of PV system. The module efficiency differs from less than 10% to over 20% depending on the PV cell type/products. It is monitored under the standard laboratory condition. The de-rating factor is to adjust the energy loss from system energy conversion, unexpected climate conditions or lower/higher temperature in the real environment. The de-rating factor is usually given as 75%. In our simulation we assume to use the mono crystalline PV panels with module efficiency of 23%, so the system efficiency is about 17%.

## 1.4 Conclusion for the solar PV electricity estimation

For solar PV electricity calculation, there are three types of input variables.

1) Location factors: monthly solar irradiations and the latitude of Jinan;

- The daily global irradiation value on each month:  $G_{dm}(0)$ ;
- Latitude:  $\delta$
- Local longitude: LL

2) Form related factor: the inclination, orientation of PV panels, the corresponding installed area, the average building spacing indicator and etc;

- $\alpha$  the orientation of receiver, which is the angle between the projected vector of the normal of receiver on the ground and the true south.
- $\beta$  is the slope of the receiver
- $d$  is the average south-north distance between two closest buildings
- $h$  is the average building height
- $\sigma$  is the orientation of the building, angle between the projection of the normal of southern surface on the ground and the true south.
- $A_i$  the area of surface  $i$  ;

3) Technology factor: the system type (tracking or fixed) and its efficiency.

- $\eta$ , the efficiency of the system

With these inputs, using the above-mentioned functions, I generated the energy output simulation result recorded in Appendix I. I also used the same methodology in estimating the solar energy potential in four neighborhoods of Jinan.

## 2. Wind energy potential simulation methodology

The wind energy potential estimation only considers the annual electricity energy produced from the roof-mounted wind turbines on the tall buildings, which are over 15storeies in Jinan simulation.

The average power of the wind turbine can be estimated via function B

$$P_w = C_p \frac{1}{2} \rho A v^3 \quad B$$

$P_w$  (W)- the power of the wind turbine

$C_p$  - is the coefficient of performance; It changes with the specific turbines and the wind speed.

$\rho$  (kg/m<sup>3</sup>) - is the air density. Air density will change with the pressure and the temperature. According to ISA (International Standard Atmosphere), at sea level and at 15°C, the air density is approximately 1.225 kg/m<sup>3</sup>. To simplify the calculation, our energy pro-forma keeps the air density constant as 1.225 kg/m<sup>3</sup> for all estimations.

$A$  (m<sup>2</sup>) - is the swept area of the wind turbine, it can be calculated as  $A = \pi \times R^2$ .  $R$  is the radius of the wind turbine.

$v$  (m/s) - the wind speed, the deterministic factor in function B. Our energy pro-forma uses the estimated annual mean wind speed for power estimation. Here,  $v$  is re-adjusted according to its location and form characteristic of the local neighborhood based the recorded annual mean wind speed in Jinan (3m/s)<sup>40</sup>. The estimation of  $V$  is the most complicated part in wind energy output estimation, and the detail description will be presented in the later section.

For the annual energy output, equation B-1 could be used

**Error! Objects cannot be created from editing field codes.**

C

$E_w$  is the annual energy output from the total wind turbines;  $T$  is the time length of the year – which is 8760 (365 times 24 hours); and, 1.91 is the adjustment factor when adopting mean wind speed in energy output estimation under the condition that the Rayleigh distribution<sup>41</sup> is valid (Stankovic, Campbell et al. 2009),  $N$  is the total number of installable wind turbines, which is constrained by the spacing requirement that would be discussed in section 2.2.2

## 2.1 The estimation of the mean wind speed $v$

### 2.1.1 The roughness and the height

The accurate estimation of roughness length requires mathematical calculations involving critical meteorological (Jha). Wieringa (Wieringa 1993) proposed a simply estimating function in measuring the roughness length.  $Z_0 = 0.5 \times A_H \times H$ , where  $A_H$  is building coverage ratio and  $H$  is average building height. Macdonald (MacDonald, Griffiths et al. 1998) refined the methodology by including the explicit appearance of the drag coefficient and the effect of displacement change. Mertens (Mertens 2006) suggested to incorporate the building height variance factor, he argued that the variance of the building should have some impact on the roughness factor. However, no in-depth

<sup>40</sup> This annual mean wind speed is draw from China Metrological Administration recorded climate data between 1971 and 2000.

[http://cdc.cma.gov.cn/shuju/search1.jsp?dsid=SURF\\_CLI\\_CHN\\_MUL\\_MM0N\\_19712000\\_CES&tpcat=SURF&type=table&pageid=3](http://cdc.cma.gov.cn/shuju/search1.jsp?dsid=SURF_CLI_CHN_MUL_MM0N_19712000_CES&tpcat=SURF&type=table&pageid=3)

<sup>41</sup> Weibull is a type of the Rayleigh distribution

analysis on the relationship between the height variance and the roughness length has been conducted. In our estimation, I applied Macdonald's method in calculating the roughness length. The equation is B-2, where the displacement height can be calculated through B-3.

$$\frac{z_0}{H} = (1 - \frac{d}{H}) \exp[-0.5\beta \frac{C_D}{\kappa^2} (1 - \frac{d}{H}) \lambda_f] \quad \text{B-2}$$

$$\frac{d}{H} = 1 + A^{-\lambda_p} (\lambda_p - 1) \quad \text{B-3}$$

In equation B-3, **H** is the average height of the obstacles, **d** is the displacement height,  $\lambda_p$  and  $\lambda_f$  is respectively the frontal area and plan area density – the frontal density is equal to plan density for cube objects (Macdonald 1997). In the pro-forma, I assume they are equal to the building coverage ratio. **C<sub>D</sub>** is the drag coefficient of the buildings, **A** is a constant determined by the arrangement of buildings, and  $\beta$  is a correction factor for the building drag. For a staggered array of cube, **A**=4.4, **C<sub>D</sub>**=1.2 and  $\beta$ =0.55.

With the roughness length and the displacement height, it is possible to estimate a rough wind speed based on the reference wind speed. European researchers have done very substantial works in developing and refining the estimating equation. Since UK NOABL data that widely used in EU was based on the rural environment, their methods usually treat the edge of the urban boundary as a step change in the roughness (Mertens 2005). However, Jinan's mean wind speed data is based on the observatories in the urban area, rather than the rural area<sup>42</sup>. Therefore, our estimation adopts an equation irrespective of the change of the roughness as follows (A.R. Jha, 2011)

$$\frac{V(z)}{V(10)} = \frac{\ln(z / z_0)}{\ln(10 / z_0)} \quad \text{B-4}$$

$$Z=1.25 H_t \quad \text{B-5}$$

In Equation B-4, **V(z)** is the wind speed at operating height **z** (m/sec). **z** is assumed to be 1.25 of the height of the tallest building. **z<sub>0</sub>** is the roughness length, **V(10)** is the wind speed (m/sec) at a reference height 10m from the ground, which is the mean wind speed in Jinan (3m/s).

### 2.1.2 The speed-up effect

When wind passes the sharp-edged building, its high wind speed region will achieve the wind speed increase by 8% - 30%. I take the speed-up effect of the buildings into account. For the wind turbines installed on the top of the shape-edge roof could have

<sup>42</sup> The location of the observatories in Jinan can be found <http://www.jnqx.gov.cn/web/zdzsk.asp>

100% more energy yield in urban area. I hypothesis that the roofs would be sharp-edged, so roof-mounted configuration could increase the wind speed by a coefficient of 1.26<sup>43</sup>.

## 2.2 The estimation of turbine size (swept area) and installable number

### 2.2.1 Size of the wind turbines

The ideal size of wind turbine is correlated to the dimension of the building. The size of the wind turbines, more specific, its swept area is calculated by assuming the diameter of the wind turbine is 0.1 of the building dimension character<sup>44</sup>. The function can be written as equation B-6.  $A_t$ ,  $H_t$  is the floor area and the height of the installed buildings.

**Error! Objects cannot be created from editing field codes.**

B-6

$$A = \frac{1}{2} \pi \left( \frac{D_i}{2} \right)^2 \quad \text{B-7}$$

### 2.2.2 Spacing and the installable number

To avoid the effect from the turbulence caused by the wake of upstream turbines, wind turbines should be placed in certain distance from one another. Since the wind environment in Jinan is between the unidirectional and multidirectional, I assume the distance between two closest turbines are 2 diameters in row and 5 diameters between the rows. The average space required for the wind turbine is  $5D_i \times 2D_i$ , the number of installable wind turbines on a given roof could be calculated through B-8.

$$N = \max\left(1, \frac{A_t}{10D_i^2}\right) \quad \text{B-8}$$

## 2.3 The category of the capacity factor

For urban micro wind turbine, the capacity factor is very low, ranging from 2% to 6.4%(Allen, 2007, Mithraratne, 2009). In my simulation for wind energy potential of the three neighborhoods in Jinan, I used 4% for capacity factor.

## 2.4 Conclusion for the wind electricity estimation

For the estimation on the energy output from the wind turbines, there are three types of input variables as well.

---

<sup>43</sup> For the wind turbines installed on the top of the shape-edge roof could have 100% more energy yield in urban area. If we assume all the energy increase is contributed from the speed-up effect, we can get the coefficient of 1.26.

<sup>44</sup> The cubic root of the building volume

1) Location factors:

- The mean wind speed in Jinan – 3m/s
- The air density – 1.225 kg/m<sup>3</sup>

2) Form related factor: the height, floor area and the number of the tallest buildings, shape of the roof, building coverage and etc;

- Building coverage
- H - The average building height
- A<sub>t</sub> - The floor area of the tallest building
- H<sub>t</sub> - The height of the tallest buildings
- N - The number of the tallest building with wind turbines installed
- The shape type of the roofs

4) Tech-related factor:.

- C<sub>p</sub>, the capacity factor

With these inputs, using the B-series functions, I simulated the wind energy potential in four neighborhoods of Jinan.

Note, this simulation methodology is also applied for the renewable energy potential estimation of Energy Pro-forma. The only difference lays on the efficiency of the system – The energy pro-forma provides three levels of energy system efficiency for PV and wind turbines (the capacity factor for wind) for designers to select, but here I defined the values for both.

The references in this Appendix could be found in the bibliography

## Appendix III: The detailed simulated results of solar energy potential in four geometric prototypes of the neighborhoods in Chapter 5

	Radiance (wh/square meter)	Area (square meter)	Unshaded Hours (units/year)	Total Solar Radiance on the buildings (Kw.h/year)	Proportion of Total Radiance	Average Height	Surface Volume Ratio	Total Construction area (square meter)	Area of the site (square meter)	Roof Area ratio over the total surface area	FAR	Solar energy potential per construction area (kwh/square meter/year)
<b>Model 1 - Jinan Slabs - orientating due south</b>												
ROOF	462.49	825	2546.8	971735.5	62.95%							
FAÇADES				0.0								
South	279.37	990	2067.90227	571932.8	37.05%							
<b>TOTAL</b>				<b>1543668.2</b>	<b>100.00%</b>	<b>18</b>	<b>0.2253</b>	<b>74250</b>	<b>40000</b>	<b>24.70%</b>	<b>1.86</b>	<b>53.01</b>
<b>Model 2 - Jinan Slab - orientating southwest</b>												
ROOF	462.49	825	2546.8	971735.5	66.38%							
FAÇADES				0.0								
Southeast	247.43	990	1660.31079	406701.1	27.78%							
Southwest	244.18	270	1297.378	85534.5	5.84%							
<b>TOTAL</b>				<b>1463971.0</b>	<b>100.00%</b>	<b>18</b>	<b>0.2253</b>	<b>74250</b>	<b>40000</b>	<b>24.70%</b>	<b>1.86</b>	<b>50.28</b>
<b>Model 3 Barcelona Block - orientating due south</b>												
ROOF	462.49	8800	2546.8	10365178.3	93.93%							
FAÇADES				0.0								
South-Outside	279.37	813.6	1945.97042	442310.2	4.01%							
South-Inside	279.37	453.6	1796.92192	227710.0	2.06%							
<b>TOTAL</b>				<b>11035198.4</b>	<b>100.00%</b>	<b>11</b>	<b>0.1433</b>	<b>31680</b>	<b>17689</b>	<b>63.40%</b>	<b>1.79</b>	<b>59.22</b>
<b>Model 4 Barcelona Block - orientating southwest</b>												
ROOF	462.49	8800	2546.8	10365178.3	91.66%							
FAÇADES				0.0								
Southeast outside	247.43	813.6	1547.39484	311503.5	2.75%							
Southeast Inside	247.43	453.6	1593.87463	178886.7	1.58%							
Southwest Outside	244.18	813.6	1456.39434	289334.8	2.56%							
Southwest Inside	244.18	453.6	1470.67353	162892.1	1.44%							
<b>TOTAL</b>				<b>11307795.4</b>	<b>100.00%</b>	<b>11</b>	<b>0.1433</b>	<b>31680</b>	<b>17689</b>	<b>63.40%</b>	<b>1.79</b>	<b>60.68</b>

## Appendix IV: The Metric of Renewable Potential Simulation in the Energy Pro-forma

Logics: Inputs --> Variables in Formula A, B or C --> Renewable Energy Potential

The variables in the formulas are estimated based on the listed three types of inputs. The methodology of estimation is in appendix II.

### Solar PV

$$E_{pv} = \sum_{i=1}^n G_{hy\_i} * A_i * H * \gamma_i * \eta$$

	Inputs of the Proforma	Related Variables in Formula A
LOCATION	The average daily irradiation value on each month: $G_{gm}(0)$	Ghy_i
	The annual solar duration	H
FACTORS	Latitude and longitude	Ghy_i
URBAN FORM	The Orientation of PV receiver*	Ghy_i
	The slope of the PV receiver*	Ghy_i
	The average south-north distance between two closest buildings*	$\Upsilon_i$ (spacing)
	The average building height	$\Upsilon_i$ (spacing)
	The orientation of the building arrays*	$\Upsilon_i$ (orientation)
FACTOR	The area of surface i ;	Ai
TECHNOLOGY FACTOR	$\eta$ , the efficiency of the system	$\eta$

### Urban Micro Wind

$$P_w = C_p \frac{1}{2} \rho A v^3 \quad E_w = 1.91 * P_w * T * N = 1.91 * 8760 * T * N$$

	Inputs of the Proforma	Related Variables in Formula B and C
LOCATION	The mean wind speed in Jinan	v
	The air density – 1.225 kg/m3	$\rho$
FACTORS		
URBAN FORM	Building coverage	v -(roughness height)
	The average building height	v -(roughness height)
	The average floor area of the tallest building*	A, N
	The average height of the tallest buildings*	A, v
	The number of the tallest building with wind turbines installed*	N
FACTOR		
TECHNOLOGY FACTOR	The capacity factor	Cp

### Note

1. \* indicates the new inputs to the Energy Pro-forma.

2. The efficiency of the PV system has three categories: 7.5%, 12.5% and 15%; while the capacity factor of wind turbines could be 3%, 4.5% or 6%.